



Cláudia Sofia Santos Bessa

**Targeted regulation of PKC signaling pathway:
Searching for new therapeutic strategies against
cancer**

Tese do 3^o Ciclo de Estudos Conducente ao Grau de Doutoramento em Ciências Farmacêuticas, especialidade Farmacologia e Farmacoterapia

Trabalho realizado sob a orientação da Professora Doutora Lucília Helena Ataíde Saraiva

Março 2018

DE ACORDO COM A LEGISLAÇÃO EM VIGOR, NÃO É PERMITIDA A REPRODUÇÃO DE QUALQUER PARTE DESTA TESE.

ACKNOWLEDGEMENTS

Firstly, I would like to thank my supervisor Prof Doutora Lucília Saraiva for believing in my abilities and giving me the opportunity to perform my PhD thesis in her research group. Thank you for all the support, patient guidance and dedication over the last five years. Thanks also for sharing your scientific knowledge and experience with me, they were undoubtedly an added value to my personal growth as a researcher. Lastly, thank you for the confidence in my work, for your help, and friendship. Your strength, perseverance and hardworking are remarkable and really inspiring.

I would like to thank Prof Doutora Patrícia Rijo from CBIOS, Universidade Lusófona/iMed, Universidade de Lisboa, responsible of the chemical group that synthesized the compounds to test during my PhD.

I would also like to thank my lab colleagues, in particular to my friends Joana Soares, Sara Gomes, Liliana Raimundo, Ana Sara Gomes, Helena Ramos and Joana Loureiro, for always helping me, for encouraging me, but especially for your friendship, which goes beyond the work and that I hope will continue for many years. A special thanks to Bryan Fernandes, a very committed Master student and that helped me a lot in my lab work. And to all that passed by our lab, namely Clara Pereira, Mariana Leão and Cláudia Maciel, for the support and friendship too.

Many thanks to all the people who showed the willingness to collaborate with us, received me in their labs making me feel so welcome and supported me in everything I needed, namely Doutor Miguel Soares, Doutor António Carlos, Prof Doutor Flávio Reis, Prof Doutora Célia Gomes, Prof Doutor Paulo Oliveira and Doutora Vilma Sardão. I am deeply grateful to Professor Marcelo Kazanietz for believing in the potential of our work, for sharing their vast scientific expertise with us and contributing to the improvement of the quality of the work.

I also acknowledge to Departamento de Ciências do Medicamento, Faculdade de Farmácia, Universidade do Porto, particularly to Prof Doutor Jorge Gonçalves for all the support. Thanks also to the lab technicians Céu and Mónica.

I would also like to acknowledge to the lab technicians, Cristina and Nuno, from Laboratório de Microbiologia for all the support, patient and friendship along the years.

Aos meus pais gostaria de agradecer todos os valores que me transmitiram ao longo destes anos e que me tornaram na pessoa que sou hoje, por apoiarem sempre e incondicionalmente as minhas escolhas e por todo o vosso amor.

Aos meus amigos, obrigada por me acompanharem ao longo deste percurso, sem a vossa amizade seria tudo muito mais difícil. Em especial gostaria de agradecer à Sandra por estar ao meu lado em todos os momentos e por acreditar sempre no meu valor.

I also thank to FCT (Fundação para a Ciência e Tecnologia) for the financial support of my doctoral fellowship (SFRH/BD/87109/2012) and to the Faculty of Pharmacy of University of Porto for provided the logistical support. This work was funded by European Union (FEDER funds POCI/01/0145/FEDER/007728, through Programa Operacional Factores de Competitividade-COMPETE) and National Funds (FCT/MEC, Fundação para a Ciência e Tecnologia and Ministério da Educação e Ciência) under the Partnership Agreement PT2020 UID/MULTI/04378/2013, and the project (3599-PPCDT) PTDC/DTP-FTO/1981/2014-POCI-01-0145-FEDER-016581.



GOVERNO DE
PORTUGAL

MINISTÉRIO DA EDUCAÇÃO
E CIÊNCIA



ABSTRACT

Cancer is a major public health concern with increasing incidence and mortality worldwide. The effectiveness of the current therapeutic options for cancer patients is still limited, mostly due to therapeutic resistance and severe toxic side effects. Additionally, the anticancer alternative drugs approved over the last years have been restricted. As such, the discovery of new therapeutic options against cancer is required.

Compelling evidence have established a key role of protein kinase C (PKC) isozymes in tumor growth and dissemination. However, despite being a promising target in cancer therapy, the lack of PKC isozyme-selective regulators has hampered the clinical translation of PKC-targeting agents.

With the present thesis, it was intended to identify PKC isozyme-selective agents, as well as new anticancer drug candidates by targeting PKC. For such purpose, the effect of a small chemical library of royleanone derivatives on the activity of classical (α and β), novel (δ and ϵ) and atypical (ζ) PKC isozymes was evaluated using a previously developed yeast-based PKC assay. With this cell system, the compound 7 α -acetoxy-6 β -benzoyloxy-12-O-benzoylroyleanone (Roy-Bz) was identified as potential PKC δ -selective activator. Thereafter, *in vitro* PKC assays using recombinant PKC isozymes, molecular docking analysis, and studies in human cancer cells confirmed that Roy-Bz was a PKC δ -selective activator with the C1 domain as putative binding site. Additionally, in human colon cancer cells, Roy-Bz potently inhibited cell proliferation by prompting a mitochondria-mediated apoptotic cell death, and presented an anti-migratory activity, in a PKC δ -dependent manner. Notably, Roy-Bz showed PKC δ -dependent anticancer activity in xenograft mouse models with no apparent toxic side effects. Further supporting its potent anticancer activity, it was also shown that Roy-Bz potentially targets glucose metabolism by dual inhibition of glycolysis and oxidative phosphorylation (OXPHOS). Collectively, these results led to the identification of the first small-molecule PKC δ -selective activator with encouraging application in anticancer therapy, particularly in colon cancer.

In this thesis, it was also shown the growth inhibitory effect of the abietane diterpenoid, 6,7-dehydroroyleanone (DeRoy), as well as of two extracts obtained from *Plectranthus* species, on a panel of human cancer cells. These results reinforced the potential of the *Plectranthus* genus as a promising source of new anticancer drugs.

In conclusion, with the discovery of Roy-Bz, this thesis opens the way to a new era on PKC biology and pharmacology, contributing to the potential redefinition of the structural requirements of PKC isozyme-selective agents, and to the re-establishment of PKC

isozymes as feasible therapeutic targets in cancer. Additionally, it gives rise to new therapeutic opportunities in anticancer therapy.

Keywords: Anticancer drug; Cancer; Isozyme-selective activator; *Plectranthus* genus; PKC

RESUMO

O cancro representa uma das principais preocupações de saúde pública, com um aumento anual da sua incidência e mortalidade no mundo. A eficácia das opções terapêuticas existentes para os doentes oncológicos é ainda limitada, principalmente devido ao aumento da resistência à terapêutica e aos efeitos secundários indesejáveis. Além disso, o número de novos fármacos anticancerígenos aprovados, ao longo dos últimos anos, tem sido reduzido. Desta forma, a descoberta de novas oportunidades terapêuticas para o tratamento do cancro continua a ser uma prioridade.

Diversos estudos têm estabelecido um papel fundamental das isoformas da família da cínase C de proteínas (PKC) no crescimento e disseminação do cancro. No entanto, apesar de ser um alvo promissor na terapia do cancro, a falta de reguladores seletivos das isoformas da PKC tem dificultado a sua translação para a clínica.

A presente tese teve como objetivo identificar agentes seletivos das isoformas da PKC, assim como novos candidatos a fármacos anticancerígenos tendo como alvo a PKC. Para tal, avaliou-se o efeito de uma biblioteca de compostos derivados da roleanona na atividade das isoformas clássicas (α e β I), novel (δ e ϵ) e atípica (ζ) da PKC, utilizando um modelo de levedura previamente desenvolvido em estudos anteriores. Com este sistema celular, identificou-se o composto 7 α -acetoxi-6 β -benzoiloxi-12-O-benzoilroileanona (Roy-Bz) como um potencial ativador seletivo da PKC δ . Posteriormente, realizando-se ensaios *in vitro* com proteínas recombinantes das isoformas da PKC, estudos de 'docking' molecular e ensaios com células tumorais humanas, confirmou-se que o Roy-Bz era um ativador seletivo da PKC δ , tendo como possível local de ligação o domínio C1. Além disso, em células humanas do cancro do cólon, o Roy-Bz inibiu de forma marcada a proliferação celular, através da ativação de uma via apoptótica mediada pela mitocôndria, assim como a migração tumoral, de uma forma dependente da PKC δ . É ainda de realçar que, para além da marcada inibição do crescimento tumoral *in vitro*, o Roy-Bz apresentou atividade anti-tumoral *in vivo*, dependente da PKC δ , sem efeitos tóxicos secundários aparentes. O Roy-Bz demonstrou também atuar ao nível do metabolismo da glucose, através da inibição da glicólise e da fosforilação oxidativa. Tal facto reforçou a potente atividade anticancerígena do composto Roy-Bz. Os resultados obtidos conduziram à identificação da primeira pequena molécula ativadora seletiva da PKC δ com uma aplicação promissora na terapêutica anticancerígena, principalmente no tratamento do cancro do cólon.

Nesta tese, foram ainda identificados o diterpeno de abietano 6,7-dehidroroileanona (DeRoy) e dois extratos obtidos a partir de espécies do género *Plectranthus*, com atividade anti-proliferativa em linhas celulares de tumores humanos. Estes resultados corroboram a

relevância do gênero *Plectranthus* como uma fonte promissora de potenciais fármacos anticancerígenos.

Em conclusão, com a descoberta do composto Roy-Bz, esta tese iniciou uma nova era na biologia e farmacologia da PKC, contribuindo para uma potencial redefinição dos requisitos estruturais dos agentes seletivos das isoformas da PKC, assim como para o restabelecimento das isoformas da PKC como potenciais alvos terapêuticos no cancro.

Palavras-chave: Agente anticancerígeno, Cancro, Ativador isoforma seletivo, Género *Plectranthus*, PKC

INDEX

ACKNOWLEDGEMENTS	iii
ABSTRACT	v
RESUMO	vii
INDEX	ix
INDEX OF FIGURES	xii
INDEX OF TABLES	xiii
ABBREVIATIONS	xiv
CHAPTER 1 - Introduction	17
1.1. Cancer	19
1.1.1. Cancer epidemiology	19
1.1.2. Cancer hallmarks	20
1.1.3. Anticancer therapeutic strategies	22
1.2. Protein kinase C.....	25
1.2.1. PKC family	26
1.2.1.1. <i>Regulation of PKC activity</i>	28
1.2.2. Biological functions of PKC	30
1.2.2.1. <i>Dual role of PKC isozymes in cancer</i>	32
1.2.3. PKC mutation in cancer.....	35
1.2.4. Targeting PKC activity.....	36
1.2.5. Screening strategies	40
1.2.5.1. <i>Genetically encoded fluorescent reporters</i>	40
1.2.5.2. <i>Yeast-based assays</i>	40
1.3. Natural products.....	42
1.4. Scope of the thesis.....	44
CHAPTER 2 - Material and Methods	45
2.1. Compounds.....	47
2.2. Construction of pESC-(<i>LEU2</i>)-PKC $\delta\Delta$ C1 plasmid	47
2.3. Yeast transformation	48
2.4. Yeast-based screening assay	48
2.5. Yeast cell cycle analysis.....	49
2.6. Analysis of yeast plasma membrane integrity and DNA fragmentation.....	49
2.7. <i>In vitro</i> PKC assay.....	49
2.8. Molecular docking	50
2.9. Human cancer cell lines and culture conditions.....	50

2.10.	Immunofluorescence and confocal microscopy	51
2.11.	Sulforhodamine B (SRB) assay	51
2.12.	Trypan blue assay	51
2.13.	Colony formation assay	52
2.14.	Analysis of cell cycle and apoptosis in human cell lines	52
2.15.	Western blot analysis	52
2.16.	Analysis of reactive oxygen species (ROS) generation	53
2.17.	Analysis of mitochondrial membrane potential ($\Delta\Psi_m$)	53
2.18.	Generation of colon cancer spheroids (colonosphere assay)	54
2.19.	Extraction and purification of plasmid DNA.....	54
2.20.	Generation of stable PKC δ -knockdown cell line	54
2.21.	<i>In vitro</i> migration assays.....	55
2.22.	Comet assay	55
2.23.	Micronucleus assay.....	56
2.24.	<i>In vivo</i> antitumor and toxicity assays	56
2.25.	Immunohistochemistry assay	57
2.26.	TUNEL assay	57
2.27.	Tandem resazurin/SRB assay	57
2.28.	Cellular oxygen consumption measurements	58
2.29.	Flow cytometric data acquisition and analysis	59
2.30.	Statistical analysis.....	59
CHAPTER 3 – Results		61
CHAPTER 3.1 - Discovery of a small-molecule protein kinase Cδ-selective activator with promising application in colon cancer therapy		63
3.1.1.	Effect of compounds on yeast growth	65
3.1.2.	Roy-Bz is a selective activator of PKC δ that binds to the C1-domain.....	66
3.1.3.	Roy-Bz inhibits the proliferation of colon cancer cells	71
3.1.4.	Roy-Bz pro-apoptotic and anti-migratory activity in HCT116 cancer cells is mediated by PKC δ -selective activation	73
3.1.5.	Roy-Bz is non-genotoxic in human cancer and normal cells and has <i>in vivo</i> PKC δ -dependent antitumor activity with no apparent toxic side effects	76
3.1.6.	Discussion	82
CHAPTER 3.2 - Roy-Bz: a potential dual inhibitor of glycolysis and oxidative phosphorylation in colon cancer		85
3.2.1.	Roy-Bz induces mitochondrial dysfunction with inhibition of cellular respiration in colon cancer cells.....	87

3.2.2.	Roy-Bz inhibits glycolysis in tumor tissues of human HCT116 xenografts ..	89
3.2.3.	Discussion.....	91
CHAPTER 3.3 - Exploring the anticancer potential of <i>Plectranthus</i> genus ..		93
3.3.1.	Anti-proliferative activity of DeRoy and synthetic derivatives in human cancer cells	95
3.3.2.	Anti-proliferative activity of <i>Plectranthus</i> spp. extracts in human cancer cells	96
3.3.3.	Discussion.....	97
CHAPTER 4 - General Discussion.....		99
CHAPTER 5 - References.....		105
Appendix.....		139

INDEX OF FIGURES

Figure 1.1. Estimated incidence and mortality for	20
Figure 1.2. Cancer hallmarks	22
Figure 1.3. Schematic representation of the domain structure of PKC isozymes grouped by subfamilies.....	27
Figure 1.4. Proposed model for the regulation of cPKC isozymes	29
Figure 1.5. Yeast PKC phenotypic assay developed to screen PKC isozyme-selective activators	42
Figure 3.1.1. Schematic representation of royleanone structures	65
Figure 3.1.2. Roy-Bz selectively activates PKC δ in yeast and induces an apoptotic cell death.....	67
Figure 3.1.3. Roy-Bz selectively activates PKC δ through binding to the C1-domain.....	69
Figure 3.1.4. Roy-Bz selectively translocates PKC δ to the perinuclear region in human tumor cells	70
Figure 3.1.5. Roy-Bz inhibits the growth of colon cancer cells	72
Figure 3.1.6. Roy-Bz inhibits the growth of colonospheres	74
Figure 3.1.7. Roy-Bz pro-apoptotic activity is mediated by PKC δ -selective activation in HCT116 cancer cells.....	75
Figure 3.1.8. Roy-Bz anti-migratory activity is mediated by PKC δ -selective activation in HCT116 cancer cells.....	77
Figure 3.1.9. Roy-Bz is non-genotoxic in human cancer and normal cells.....	78
Figure 3.1.10. Roy-Bz has <i>in vivo</i> PKC δ -dependent antitumor activity with no apparent toxic side effects.....	80
Figure 3.1.11. Roy-Bz inhibits proliferation and angiogenesis, and induces apoptosis in tumor tissues of human HCT116 xenograft mouse models	81
Figure 3.2.1. Roy-Bz has cytotoxic effect in colon cancer cells.....	87
Figure 3.2.2. Roy-Bz induces mitochondrial dysfunction in colon cancer cells.....	88
Figure 3.2.3. Roy-Bz inhibits cellular respiration in colon cancer cells	89
Figure 3.2.4. Roy-Bz has anti-glycolytic activity in tumor tissues of human HCT116 xenograft mouse models.....	90
Figure 3.3.1. Chemical structure of abietane diterpenoid DeRoy.....	95
Figure 5.1. Putative molecular mechanism of action of Roy-Bz-induced apoptosis.	102

INDEX OF TABLES

Table 1.1: PKC modulators under clinical trials as anticancer agents.	39
Table 3.1.1. EC ₅₀ values of compounds tested on individual PKC isozymes.	66
Table 3.1.2. Toxicity studies of Roy-Bz in Wistar rats.....	79
Table 3.3.1. IC ₅₀ values of DeRoy and derivative compounds in human cancer cells.....	96
Table 3.3.2. IC ₅₀ values of <i>Plectranthus</i> spp. extracts in human cancer cells	97

ABBREVIATIONS

a.a.	Amino acids
ARA	Arachidonic acid
ATM	Aurothiomalate
BAK	Bcl-2-antagonist/killer
BAX	Bcl-2 associated X protein
Bcl-2	B cell lymphoma 2
Ca²⁺	Calcium
CF	Catalytic fragment
CKAR	C-kinase activity reporter
CP	Cyclophosphamide
CRC	Colorectal cancer
CSC	Cancer stem cell
Cyt c	Cytochrome c
DAB	3,3'-diaminobenzidine
DAG	Diacylglycerol
DAPI	4',6-diamidino-2-phenylindole
DCA	Dichloroacetate
DGK	Diacylglycerol kinase
DiOC₆(3)	3,3'-dihexyloxacarbocyanine iodide
DISC	Death-inducing signaling complex
DMEM	Dulbecco's Modified Eagle's Medium
DMSO	Dimethyl sulfoxide
EDTA	Ethylenediaminetetraacetic acid
EGFR	Epidermal growth factor receptor
ER	Endoplasmic reticulum
ETC	Electron transfer chain
ETOP	Etoposide
FBS	Fetal bovine serum
FCCP	Carbonyl cyanide-4-(trifluoromethoxy)phenylhydrazone
FDA	Food and Drug Administration
FRET	Förster/fluorescence resonance energy transfer
GFP	Green fluorescent protein
GOF	Gain-of-function
HDI	Human development index
HK2	Hexokinase 2

HRP	Horseradish-peroxidase
HSP90	Heat shock protein 90
H&E	Hematoxylin and eosin
IP₃	Inositol 1,4,5-trisphosphate
LOF	Loss-of-function
MCT4	Monocarboxylate transporter 4
MMP	Mitochondrial membrane potential
MMP-2/-9	Matrix metalloprotease-2/-9
MN	Micronucleus
MOM	Mitochondrial outer membrane
MOMP	Mitochondrial outer membrane permeabilization
NSCLC	Non-small cell lung cancer
OCR	Oxygen consumption rate
OD	Optical density
Par6	Partitioning-defective 6
PB1	Phox/Bem1
PBS	Phosphate buffer saline
PCR	Polymerase chain reaction
PDK1	Phosphoinositide-dependent kinase 1
PI	Propidium iodide
PIP₂	Phosphatidylinositol-4,5-biphosphate
PKC	Protein Kinase C
PMA	Phorbol 12-myristate 13-acetate
PRB	13-acetylphorbol
PS	Pseudosubstrate
RACK	Receptor for activated C kinases
ROS	Reactive oxygen species
SDS	Sodium dodecyl sulfate
Ser	Serine
SRB	Sulforhodamine B
TCA	Trichloroacetic acid
TIGAR	<i>TP53</i> -induced glycolysis and apoptosis regulator
Thr	Threonine
VEGF	Vascular endothelial growth factor
Wt	Wild-type
YNB	Yeast nitrogen base

CHAPTER 1

Introduction

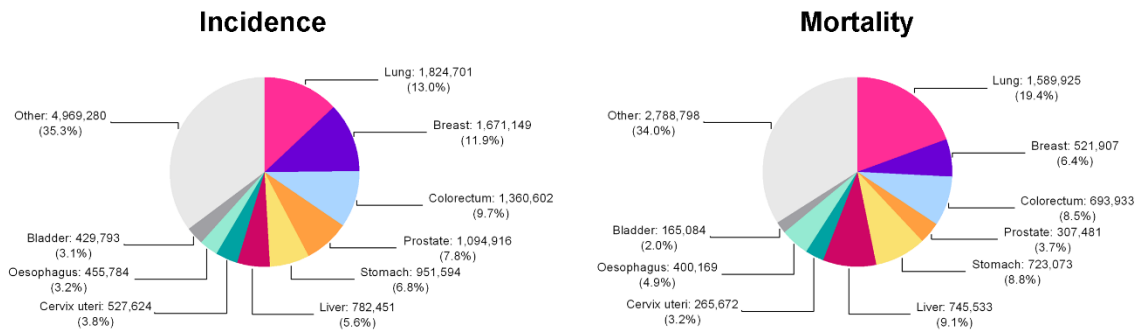
1.1. Cancer

1.1.1. Cancer epidemiology

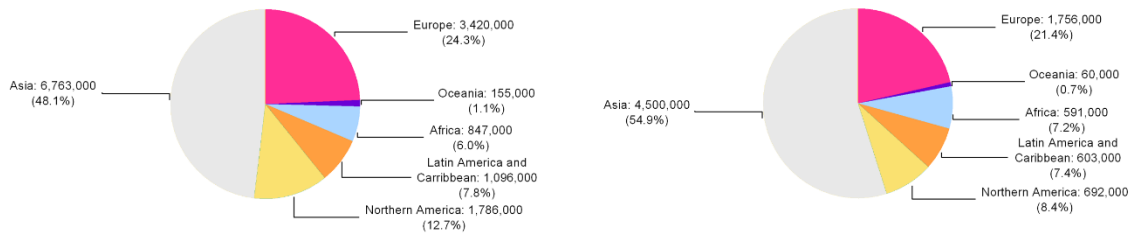
Cancer is a major public health concern worldwide, causing even more deaths than all coronary heart disease or stroke according to World Health Organization (WHO) estimates (1). For 2012, the GLOBOCAN predicted approximately 14 million new cancer cases and 8.2 million deaths in the world (2). These data tend to increase over the next few years, being expected that 20 million people develop cancer annually and 11 million die by 2025. As indicated in Figure 1.1A, lung (1.82 million cases), breast (1.67 million cases) and colorectal (1.36 million cases) cancers exhibit the highest incidence rates, followed by prostate, stomach and liver cancers. However, lung (1.6 million deaths), liver (745,533 deaths) and stomach (723,073 deaths) cancers are the most deadly (Fig. 1.1A). The highest incidence of cancer is observed in Asian (6.76 million cases), with a mortality rate higher than 50% (4.5 million cases) (Fig. 1.1B). Europe and Northern America have the second highest incidence and mortality rates, in opposition to Oceania with the lowest rates (Fig. 1.1B). In Portugal, cancer is the second cause of death (<https://www.ine.pt>) and, following the worldwide trend, it is expected an increase in the new cancer cases, mainly due to the population ageing, human lifestyle, and infections. Contrary to global trends, in Portugal, colorectal cancer (CRC) has the highest incidence rate, followed by prostate and breast cancers, and it is also the most lethal (Fig. 1.1C).

As referred, CRC is the third most commonly diagnosed malignancy and the fourth leading cause of cancer-related deaths in the world (Fig. 1.1A). CRC is characterized by a significant variation in incidence and mortality rates across the different human development index (HDI) levels of countries. Accordingly, a study from Arnold and co-workers (2016) concluded that in numerous medium-to-high HDI-indexed countries, such as Latvia, Estonia, Lithuania, Russia, China and Brazil, the CRC incidence and mortality rates tend to rapidly increase (3). Conversely, in some of the highest HDI-indexed countries, including USA, Japan and France, both CRC incidence and mortality have decreased. An intermediate pattern was also described for very high HDI-indexed countries, such as Canada, United Kingdom, Denmark and Singapore, with an increase of incidence and a decrease of mortality.

A



B



C

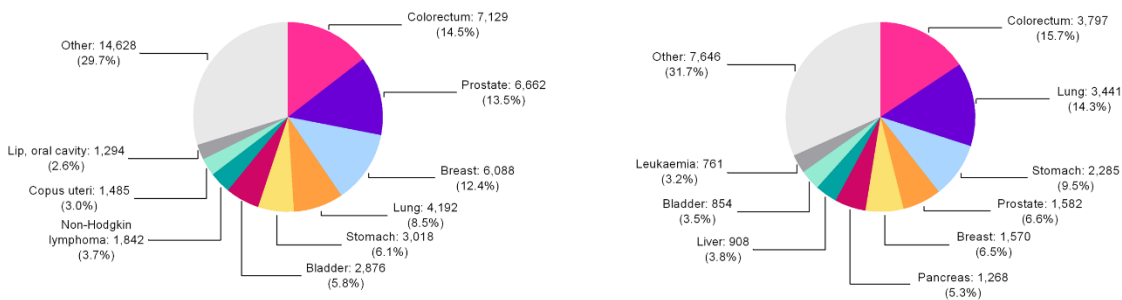


Figure 1.1: Estimated incidence and mortality for: (A) different types of cancer; (B) cancer worldwide; (C) cancer in Portugal. [Graphs from GLOBOCAN 2012: Estimated cancer Incidence Mortality and Prevalence Worldwide in 2012 (<http://globocan.iarc.fr/Default.aspx>)].

1.1.2. Cancer hallmarks

Over the last years, the extensive research around cancer clearly indicated that tumorigenesis is a multistep process elicited by genome mutations that progressively drive the malignant transformation of normal cells into cancer cells. Currently, it is well-established that tumors are more than masses of proliferating cancer cells. Instead, they comprise heterogeneous subclonal populations involved in heterotypic interactions between them, thus forming a complex tissue (4). In addition, beyond tumor biology, the tumor microenvironment has proved to be crucial for tumor progression and maintenance. In fact, the role of microenvironment reinforces the idea that tumors are complex organs,

resulting from the process of human tumor pathogenesis, encompassing multiple cells, molecules and blood vessels that surround and feed the tumor (4).

In 2000, Hanahan and Weinberg described, for the first time, the major hallmarks (or physiologic alterations) of cancer cells involved in tumor growth and metastatic dissemination (5). The abilities acquired by cancer cells during tumor development included self-sufficiency in growth signals, insensitivity to growth inhibitory signals, evasion of apoptosis, limitless replicative potential, sustained angiogenesis, and tissue invasion and metastasis (Fig. 1.2) (5). Contrary to normal cells that strictly depend on exogenous growth-promoting factors to proliferate, cancer cells are able to produce their own growth signals, and consequently sustaining a chronic proliferation. Besides of inducing pro-proliferative factors, the signaling pathways of cancer cells that negatively regulate proliferation, through activation of senescence or apoptosis, are also deregulated. Actually, several evidence indicate that numerous tumor suppressor genes, such as *Rb* (retinoblastoma-associated) and *TP53*, have mutations that lead to their inactivation. The resistance to cell death is another characteristic of tumors, where apoptosis is limited or circumvented, favoring the progression of tumors to states of high-grade malignancy and resistance to therapy (6, 7). However, the hallmarks mentioned above are not sufficient by themselves to generate macroscopic tumors. Indeed, contrasting to the behavior of normal cells that enter into senescence or crisis/apoptosis after a limited number of cell divisions, cancer cells have an unlimited replicative potential, being able to overcome these barriers. On the other hand, in order to supply all the needs both in terms of nutrients and oxygen during tumor growth, angiogenesis is permanently 'switch on', including in early development stages of invasive cancers (8, 9). Additionally, also invasion and metastasis have been intimately associated with highly aggressive carcinomas. This is a multistep process that begins with local invasion of cancer cells, intravasation into blood and lymphatic vessels, transport to distant tissues, and subsequent growth of tumor metastasis. These carcinomas have been mainly characterized by alterations in genes encoding cell-to-cell and cell-to-extracellular matrix adhesion molecules. In 2011, two other emerging hallmarks were described, namely the reprogramming of energy metabolism that ensures the neoplastic proliferation, and the evading immune destruction by tumor cells (Fig. 1.2) (4). At the same time, it was reported that all the functions acquired during the multistep process of tumorigenesis are dependent on two enabling characteristics of cancer cells, specifically the genome instability and mutation, and the tumor-promoting inflammation (Fig. 1.2) (4).

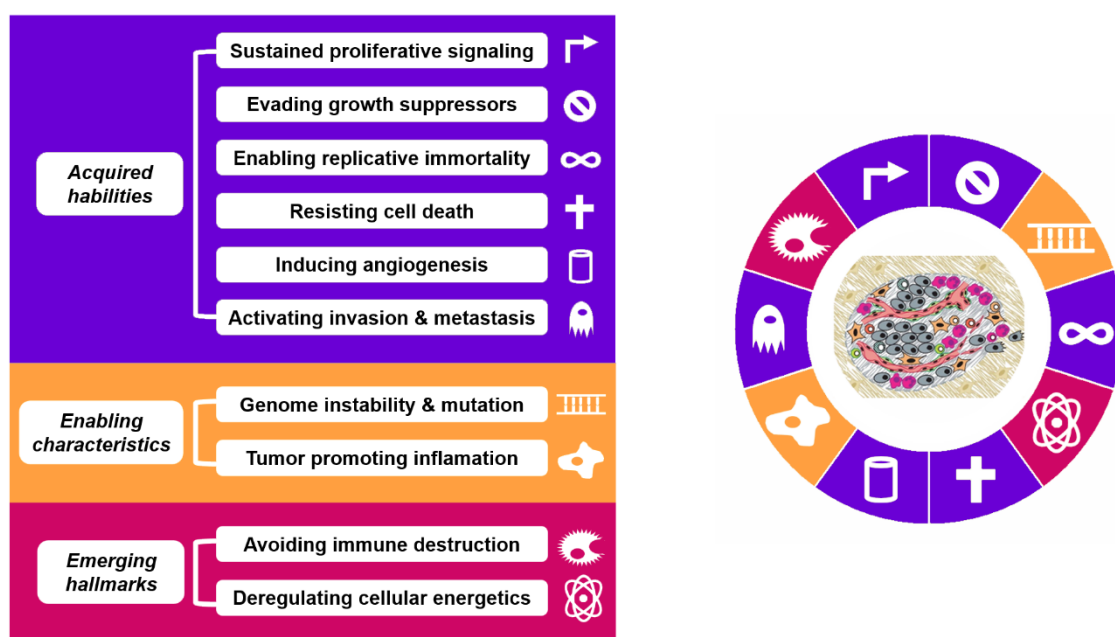


Figure 1.2: Cancer hallmarks. Schematic representation of the six hallmarks originally proposed in 2000, and of four additional hallmarks and/or characteristics later described for cancer cells. [Adapted from (4)].

1.1.3. Anticancer therapeutic strategies

Over the past few decades, surgical resection, radiotherapy and conventional chemotherapy have been the major approaches in cancer treatment. However, there are several inherent limitations in these therapeutic options, particularly secondary toxic side effects and therapeutic resistance, which have compromised their efficiency against cancer. Despite great advances in cancer research, with a deeper understanding of its pathobiology, the availability of effective anticancer agents remains unsatisfactory. Actually, even though anticancer drugs represent a substantial proportion of total new drug approvals, their success rates in clinical trials have been disappointing (7% in phase I and less than 50% in phase III) (10).

The conventional chemotherapy acts on rapidly replicating cells, being unable to discriminate between cancer and normal cells. Therefore, it is often associated with various undesirable toxic side effects, as fatigue, nausea, vomiting, diarrhea, weight changes, hair loss, anemia, easy bruising and bleeding, fertility problems, among others (www.cancer.org). In order to minimize this high toxicity, these drugs have been often administrated in regimens of single doses, or in short-term therapeutic cycles at higher concentrations (11).

In the last years, the interest of the pharmaceutical companies has moved from conventional non-specific cytotoxic agents to targeted therapy (12, 13). In fact, targeted therapies are currently the focus of anticancer drug development, being the basis of precision medicine, an emerging approach that takes into account individual genetic variability, environment, and lifestyle for each patient to prevent and treat disease. The major goal of targeted cancer therapy is to kill cancer cells without affecting the healthy ones, therefore minimizing undesirable toxic side effects and improving the quality of life of patients. Consistently, targeted therapies are designed to interfere with specific molecular targets involved in cancer growth and dissemination (14, 15). Currently, there are different types of targeted therapies approved for cancer treatment (either small-molecules or monoclonal antibodies), including hormones, immunotherapies, signal transduction inhibitors, gene expression modulators, apoptosis inducers, and angiogenesis inhibitors. However, although targeted therapies have proved to be a valuable alternative for cancer treatment, exhibiting less severe side effects and more effective results, they are closely associated with the acquisition of drug resistance, particularly due to the occurrence of mutations on the molecular target and/or to the recruitment of alternative compensatory growth pathways independent of the target (16).

Although the current cancer therapies can induce partial or even a complete cancer regression in some patients, the relapse is the most common scenario, with recurrent cancers becoming more aggressive and resistant to therapy (17). For long, the genetic and epigenetic alterations in malignant cells have been the main focus of study in cancer biology and in the development of new therapies (18). However, over the last years, it has become clear that tumor growth and progression are not only driven by cumulative gene mutations, but are highly affected by the heterogeneous tumor cell population and surrounded microenvironment. In fact, currently the development of novel anticancer therapeutic alternatives have been based on the emergent concept that tumors consist of heterogeneous cell populations mainly characterized by a high phenotypic diversity, which seems to be the major driver of cancer recurrence. Among these populations, the discovery of cancer stem cells (CSCs), also termed as tumor-initiating cells (TICs), have attracted increasing interest due to their capacity to self-renew and drive tumorigenesis (19, 20). Actually, it was demonstrated that only a small fraction of cells, namely CSCs, are able to form colonies *in vitro* or seed new tumors in mice (21). In addition, several works have shown that CSCs are involved in tumor initiation (22), maintenance (23, 24), metastasis (25), and recurrence (26-28). Accordingly, the limited efficacy of anticancer therapies may be attributed to the inability of targeting CSCs within the tumor. Indeed, cumulating data have shown that CSCs are more resistant than non-CSCs (29-31). Based on this, many

efforts have been made to better understand the epigenetic mechanisms that allow to differentiate between non-CSCs and CSCs, and to design novel therapeutic strategies able to target CSCs for complete cancer eradication. Moreover, the tumor microenvironment is a dynamic structure that, besides cancer cells, comprises the extracellular matrix and stromal, endothelial, and immune cells that are recruited from nearby tissues and bone marrow (32, 33). Accordingly, tumor microenvironment is continuously changing, both at molecular and cellular levels, as a result of the interaction between incipient cancer cells and non-transformed cells, leading to phenotypic alterations, and consequently to tumor growth and metastatic dissemination (34). The interplay between tumor cells and tumor microenvironment may occur through cell-to-cell and cell-to-extracellular matrix adhesion molecules interactions, or through regulation of the secretion of soluble molecules, such as growth factors, chemokines and cytokines, which are implicated in the activation/inhibition of the main tumor signaling pathways. As such, the identification and modulation of relevant targets in tumor microenvironment prove to be a valuable approach in the prevention and treatment of cancer. Indeed, a dramatic increase in the pre-clinical development and clinical testing of agents that target tumor microenvironment has been observed, being a large number of these drugs approved by the Food and Drug Administration (FDA). Currently, one of the most representative examples are the angiogenic inhibitors, that impact on vascular endothelial growth factor (VEGF) or other pro-angiogenic signaling pathways, which have been successfully tested in clinical trials and consequently approved for clinical use in a variety of cancers (35, 36).

Additionally, in response to genetic mutations and/or to the stressful and fluctuating microenvironment conditions, cancer cells are able to reprogram the entire metabolic pathway to sustain their high proliferation rates (4). Accordingly, almost a century ago, metabolic alterations, characterized by the enhancement of the glycolytic capacity, with increased glucose uptake and lactate production, and the absence of respiration even in aerobic conditions, were described in cancer cells, being termed as 'Warburg effect' (37). These alterations were in fact recognized as distinctive features of cancer cell metabolism, since in normal cells ATP is mainly produced through oxidative phosphorylation (OXPHOS) in mitochondria. Based on this, glucose metabolism has also received much attention in an attempt to better understand the cancer physiology, and to improve the pharmacology of anticancer agents. The extensive research around this issue has allowed establishing a close correlation between glucose metabolism and tumor heterogeneity, which in turn critically affect the resistance to anticancer therapy (38). Therefore, the use of glycolytic inhibitors was established as a promising therapeutic strategy against cancer. However, taking into account the tumor cell metabolic heterogeneity, the application of a single

metabolic therapeutic strategy, based on glycolysis inhibition, revealed to be ineffective, not leading to a complete tumor eradication. In fact, the combined use of glycolytic inhibitors, which act on highly proliferative cells eliminating the ATP produced via 'Warburg effect', with OXPHOS inhibitors that sensitize cancer cells with low proliferative rates and oxidative metabolism (including CSCs), has represented the most attractive approach to effectively kill heterogeneous cell populations, avoiding tumor cell relapse and therapeutic resistance (38, 39). One example is the widely used antidiabetic drug metformin, which is an inhibitor of glycolysis (by HK2 inhibition) and OXPHOS (by mitochondrial complex I inhibition) (40, 41). Based on this, metformin has been tested either alone or in combination therapy, namely with dichloroacetate (DCA; an inhibitor of pyruvate dehydrogenase kinase) (39). Nevertheless, its use in combination with other metabolic drugs has shown to be the most effective strategy against tumor relapse (42-44). The combination of metabolic modulators with other chemotherapeutic agents has also shown great potential against the ever-increasing resistance to conventional chemotherapy. Consistently, in paclitaxel-resistant human lung (45) and oral (46) cancer cells, with overexpression of pyruvate dehydrogenase kinase 1/2, the combination with DCA sensitized these cells to paclitaxel.

Collectively, cancer must be understood and treated as a whole. In fact, cancer medicine has changed drastically and currently encompasses a panel of integrative approaches ranging from personalized diagnostics to therapeutics (47). The combination of targeted therapies with other strategies that hit different parts of the cell signaling pathway, or with conventional chemotherapeutic drugs, has proven to be the most embracing approach, which has already shown successful results in clinical trials (15). However, the search for selective regulators of key molecular targets in cancer has been one of the major challenges in targeted therapy.

1.2. Protein kinase C

In 1977, Nishizuka and co-workers identified for the first time a new protein kinase, originally called PKM (48-50). Two years later, using a purified holoenzyme, it was found that this protein was a calcium (Ca^{2+})-activated and phospholipid-dependent kinase (51, 52). Based on this Ca^{2+} -dependent kinase activity, it was renamed protein kinase C (PKC). The continuous efforts to characterize PKC led to the identification of the lipid second messenger diacylglycerol (DAG) as an endogenous activator of this kinase (52, 53). Afterwards, several studies established PKC as a cellular receptor for the natural occurring

phorbol esters (54-56). Since then, an extensive research has been done in the PKC field, giving rise to over 60,000 citations in PubMed, making PKC one of the most studied kinases.

Early it was demonstrated the involvement of PKC isozymes in key cellular processes that regulate cell survival and cell death (57). This has supported the crucial role of PKC isozymes in numerous human pathologies, including diabetes (58, 59), heart failure (60, 61), Alzheimer and Parkinson (62, 63), autoimmune diseases (64-67), and cancer (57, 68). However, despite all the efforts to unravel the function of individual PKC isozymes in different cellular processes, discrepant outcomes have frequently been achieved. This has been mainly attributed to the high complexity of the PKC-signaling pathway, particularly the existence of several structurally-related isozymes in the same cellular environment, and the pronounced expression heterogeneity of PKCs in different cell types (57). The lack of isozyme-selective PKC modulators has also greatly contributed to the conflicting data. Nonetheless, despite this limitation, PKC has remained an appealing therapeutic target in the treatment of several human diseases.

1.2.1. PKC family

PKC belongs to the AGC family of kinases (also including PKA and PKG) (69), consisting of at least ten serine/threonine kinases encoded by nine different genes (70, 71). Briefly, PKC isozymes are grouped, according to their regulatory domain structure and co-factors required for activation, into three subfamilies: classical/conventional (cPKC; α , alternatively spliced β I and β II, and γ), novel (nPKC; δ , ϵ , η and θ), and atypical (aPKC; ζ and λ). Besides the most representative members, it has also been described the brain-specific alternative transcript PKM ζ , which only encodes the catalytic domain of PKC ζ (72), and spliced PKC δ variants (73-75). Structurally, PKC isozymes share a highly conserved carboxy-terminal region (C-terminus), comprising an ATP-binding domain and a catalytic domain, linked through a flexible hinge region (V3) to the membrane-targeting amino-terminal regulatory domain (N-terminus) (Fig. 1.3) (76, 77). The regulatory domain encompasses two membrane targeting regulatory elements, C1 and C2 (or C2-like) regions, as well as the pseudosubstrate (PS) segment, which retains the kinase in an autoinhibited conformation, through engagement in the substrate-binding cleft of the catalytic domain. The C1 domain of cPKCs and nPKCs contains two tandem cysteine-rich zinc finger motifs (C1A and C1B) that bind to DAG or phorbol esters in membranes. The C2 domain differs from cPKCs to nPKCs. In fact, whereas in cPKCs the C2 domain binds anionic phospholipids in a Ca²⁺-dependent manner, nPKCs do not bind Ca²⁺ due to the loss of functionality of the C2 domain (termed as C2-like) caused by the absence of key aspartate

residues required to coordinate Ca^{2+} (77). Contrary, aPKC isozymes bind neither DAG nor Ca^{2+} , but they contain a modified C1 domain that retains the binding ability to anionic phospholipids (although with lower affinity), and a Phox/Bem1 (PB1) domain that mediates protein–protein interactions on protein scaffolds. In particular, it was reported that PB1 domain of aPKCs specifically interact with the PB1 domain of scaffold proteins p62 and Partitioning-defective 6 (Par6) (78-82). Besides the PB1 domain of aPKCs, also the C2 domain of cPKCs and nPKCs is involved in protein-protein interactions, mediating the relocation of PKCs upon activation to specific subcellular compartments. Indeed, several data suggested that activated PKCs may bind to specific anchoring proteins, termed as receptors for activated C kinases (RACKs), localized at specific membrane microdomains in the cytoskeleton, through the C2 domain (83). This interaction of PKC with these proteins allows a higher proximity of its allosteric activators and substrates. Another PKC binding partner is the heat shock protein 90 (HSP90) chaperone that interacts with PKC ϵ C2 domain, promoting the shuttling of PKC ϵ into the mitochondria (84).

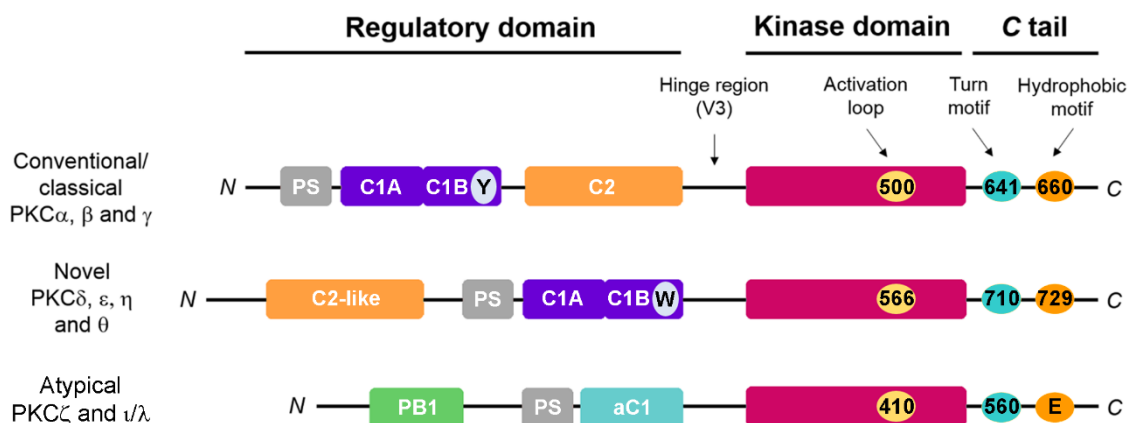


Figure 1.3: Schematic representation of the domain structure of PKC isozymes grouped by subfamilies. PKC isozymes share a common architecture, with a *N*-terminal regulatory moiety that regulates the catalytic activity of the *C*-terminal kinase domain. The regulatory domain comprises the autoinhibitory PS segment, C1, or atypical C1 (aC1; for atypical PKCs), C2 and PB1 domains. Concerning to C1 domain, cPKCs differs from nPKCs in a single amino acid, tyrosine (Y) in classical vs tryptophan (W) in novel isozymes in C1B domain, which increases the affinity of nPKCs to DAG in two order of magnitude compared to cPKCs. The *C*-terminal kinase moiety contains the catalytic domain (red rectangles) that is prime phosphorylated on the activation loop (yellow circle), and a *C*-terminal tail that is phosphorylated at the turn (cyan circle) and hydrophobic motifs (orange circles). Atypical isozymes have a glutamic acid (E) at the phosphoacceptor site on the hydrophobic motif.

1.2.1.1. Regulation of PKC activity

Newly synthesized PKCs are bind to plasma membrane in an open and degradation-sensitive conformation, in which its membrane targeting motifs and PS segment are exposed. Subsequently, PKCs are retained in an inhibitory conformation in the cytoplasm by a series of ordered, tightly coupled, and constitutive phosphorylations, designated as 'maturation' process, which ensures the stability and the catalytic competence of these enzymes (Fig. 1.4) (85, 86). The initiation of PKC processing is dependent on the binding of a conserved PXXP motif in the kinase domain to the molecular chaperone Hsp90 with Cdc37 (87). Thereafter, PKC is first phosphorylated on a conserved threonine in the activation loop (localized at the catalytic domain) by phosphoinositide-dependent kinase 1 (PDK1), in which it is also involved the kinase complex mTORC2 (Fig. 1.4) (85). The conformational change induced by this phosphorylation leads to the exposure of the turn and the hydrophobic motifs at the C-terminus, and to their subsequent autophosphorylation. These post-translational modifications render PKC resistant to proteases and phosphatases, preventing its degradation, as well as catalytically competent. The mature PKC is released into the cytosol in an autoinhibited conformation achieved by intramolecular interactions between the N-terminal PS region and the C-terminal catalytic domain, in which the substrate binding pocket is occupied by the PS sequence (Fig. 1.4) (57).

Under physiological conditions, the activation of PKC is regulated by extracellular agonists, which increase the intracellular levels of the second messengers DAG and Ca^{2+} in response to the stimulation of receptor tyrosine kinases (RTKs) or other cell surface receptors. In fact, the stimulation of these receptors induces the activation of effector molecules, including membrane-associated phospholipase C (PLC), which catalyze the hydrolysis of phosphatidylinositol-4,5-biphosphate (PIP_2) into DAG and inositol 1,4,5-trisphosphate (IP_3). Additionally, the increase of cytoplasmic free Ca^{2+} results from the interaction of IP_3 with the inositol trisphosphate receptors (InsP3R), promoting the rapid release of Ca^{2+} from the endoplasmic reticulum (ER). In cPKCs, the activation occurs in two steps that begin with the induction of cytosol-to-membrane translocation, through binding of the C2 domain to membrane phospholipids in a Ca^{2+} -dependent manner, allowing the engagement of PKC to plasma membrane (88, 89). Thereafter, PKC binds its membrane-embedded ligand DAG, primarily via C1B domain, an event that prompts the release of the catalytic domain from the PS-binding cavity, enabling the substrate binding and phosphorylation, and the subsequent activation of downstream signaling cascades (Fig. 1.4) (77). Regarding nPKCs, these kinases are able to translocate to membranes in response to agonists, even in the absence of high intracellular Ca^{2+} levels. Actually, it was demonstrated that PKC δ compensates this gap on membrane recruitment since its C1

domain binds membranes with a two-fold higher affinity than the C1 domain of cPKCs (90, 91).

The inactivation of PKC may occur by two distinct processes, namely by the metabolism of DAG (92) and by a process termed as downregulation (93). The reduction in membrane DAG levels is catalyzed by diacylglycerol kinase (DGK), which phosphorylates DAG leading to its conversion into phosphatidic acid (PA). This event stimulates the redistribution of PKC to the cytosol, and the subsequent acquisition of an autoinhibited conformation (Fig. 1.4). On the other hand, when PKCs undergo prolonged activation, due to the exposition to extracellular ligands not readily metabolized like phorbol esters, they lose activity. Indeed, the long-term residency of PKC in an open and membrane-bound conformation leads to its dephosphorylation due to a higher sensitivity of PKC to phosphatases (94). This mechanism is initiated by the okadaic acid-insensitive PH domain Leucine-rich repeat Protein Phosphatase (PHLPP), which catalyzes the dephosphorylation of the hydrophobic motif of cPKCs and nPKCs (95) followed by dephosphorylation of the turn motif and activation loop by okadaic acid-sensitive PP2A phosphatases (96). Upon dephosphorylation, PKC is ubiquitinated and degraded by the proteasome (97).

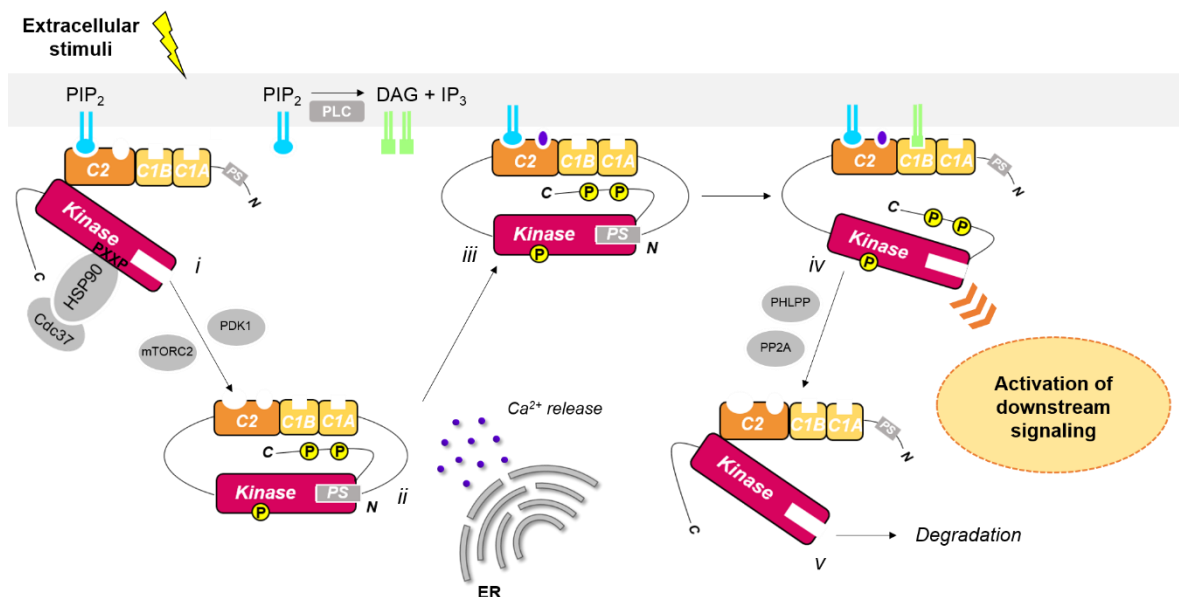


Figure 1.4: Proposed model for the regulation of cPKC isozymes. Following its biosynthesis, PKC exhibits an open and degradation-sensitive conformation, in which its regulatory modules are unmasked (*i*). Then, it is processed by a series of ordered phosphorylations at three priming sites, which leads to the acquisition of an autoinhibited conformation (*ii*). The hydrolysis of PIP₂ results in Ca²⁺-dependent recruitment of PKC to the plasma membrane via engagement of the C2 domain (*iii*), and subsequently to DAG via C1B domain (*iv*). Once activated, PKC phosphorylates downstream

substrates, which in turn prompts the activation of signaling cascades. The membrane-bound conformation of PKC is sensitive to dephosphorylation, leading to its degradation by the proteasome (v).

1.2.2. Biological functions of PKC

The increasing interest in understanding the biology of PKC isozymes led to the development of alternative isozyme-specific tools, including dominant inhibitory kinases, transgenic and knock-out mouse models, antisense/small-interfering (si)RNA, and clustered regularly interspaced short palindromic repeats-associated protein-9 nuclease (CRISPR/CAS9), besides the use of standard PKC modulators (98). The extensive work performed in this area has greatly contributed to our deeper knowledge about the role of PKCs in various cellular responses, including proliferation, survival, apoptosis, cell migration and metabolism (99, 100).

Amongst the numerous cellular processes regulated by PKC, cell death is one of the most studied, underlying the development of many pathologies, such as cancer (101). Particularly, apoptosis, also known as type I programmed cell death, is a genetically controlled mechanism, triggered by intra- or extracellular signaling, that ensures the removal of damaged cells from the organism (102). The apoptotic-signaling cascade is divided into two major pathways, the extrinsic or death receptor pathway and the intrinsic or mitochondrial pathway. However, both pathways converge on the activation of cysteine aspartate proteases, also called caspases, the key executors of apoptosis (103). The extrinsic pathway is activated by binding of secreted ligands, such as Fas ligand (FasL) to the cell-surface death receptor of the tumor necrosis factor receptor (TNFR) family, Fas (also called CD95/Apo-1). The oligomerization of death receptor is induced upon ligand binding, which in turn leads to the recruitment of the adaptor protein Fas-associated death-domain protein (FADD) and of pro-caspase-8, forming the death-inducing signaling complex (DISC). Consequently, DISC cleaves pro-caspase-8, resulting in the activation of downstream effectors caspase-3 and caspase-7, amplifying the death signal that triggers apoptotic events (102). In contrast, the intrinsic mitochondrial pathway is initiated in response to intracellular stimuli, including oxidative stress, DNA damage, hypoxia or growth-factor deprivation, which prompt the mitochondrial outer membrane permeabilization (MOMP) (104). However, the mitochondrial integrity is tightly regulated by the interaction between pro- and anti-apoptotic proteins of the B cell lymphoma 2 (Bcl-2) family. Thus, under stress conditions, the pro-apoptotic Bcl-2 associated X protein (BAX) and Bcl-2-antagonist/killer (BAK) proteins undergo dimerization, and insert into the

mitochondrial outer membrane (MOM) forming pores that disrupt the membrane's integrity (105). Following MOMP, cytochrome *c* (cyt *c*) is released into the cytosol, where it binds to the apoptotic protein activating factor-1 (Apaf-1) driving the formation of a caspase activation structure, termed apoptosome (105). The apoptosome recruits and activates the initiator caspase-9, which in turn cleaves the executioner caspase-3 and-7, thereby promoting apoptosis.

The first studies confirming the involvement of PKC isozymes in the regulation of apoptosis used phorbol esters as PKC activators (106, 107). Despite the attempt to clarify the role of specific PKC isozymes in the apoptotic process by several studies, this has proved to be a challenging task, since their impact on apoptosis showed to be highly dependent on cellular background and stimuli applied (108). In fact, distinct stimuli dictate the PKC translocation to distinct subcellular compartments, determining the phosphorylation of different substrates, and subsequently different cellular responses (108). PKC δ has been one of the most studied PKC isozymes, being intimately implicated in the apoptotic response to DNA damage and cytotoxic stress (99, 109-111). Actually, both *in vitro* and *in vivo* studies sustained the pro-apoptotic role of PKC δ . For instance, it was shown that cells isolated from PKC $\delta^{-/-}$ mice were resistant to apoptosis, and the irradiation-induced damage was lower in PKC $\delta^{-/-}$ mice (112, 113). Importantly, upon DNA damage, PKC δ is activated through phosphorylation on specific tyrosine residues, inducing its nuclear accumulation, which is considered a critical event for the execution of apoptosis by PKC δ in response to genotoxic stress (114). In the nucleus, activated caspase-3 proteolytically cleaves PKC δ in the hinge region, resulting in the release of a constitutively active PKC δ catalytic fragment (PKC δ -CF), recognized as a potent apoptotic inducer (115, 116). Accordingly, cumulating evidence have indicated that, during the apoptotic process, the majority of PKC δ substrates are nuclear proteins. Particularly, it was reported that PKC δ phosphorylates the DNA-dependent protein kinase catalytic subunit (DNA-PK), stimulating DNA-damage induced apoptosis (117). However, also mitochondria is described as a translocation site of PKC δ in response to oxidative stress, ischemia and phorbol esters (109, 118, 119). At mitochondria, it is suggested that PKC δ directly interferes with the regulation of the apoptotic machinery, namely through the induction of post-translational modifications that control the activity of Bcl-2 family proteins. For instance, it was demonstrated that PKC δ triggers apoptosis by suppressing the phosphorylation of the pro-apoptotic protein, Bcl-2-associated death promoter (BAD), or by stimulating BAX and BAK activity (119, 120). The regulation of p53 activity by PKC δ , both at transcriptional and post-translational levels, has also been suggested (121, 122). Nonetheless, despite numerous studies have corroborated

its pro-apoptotic activity, there are also reports describing a pro-survival function of PKC δ , which is generally preceded by its translocation to the ER (111).

Despite the great advances in the knowledge of PKC cellular functions, the full understanding of the role of individual PKC isozymes in human diseases, including cancer, is still far from being achieved.

1.2.2.1. Dual role of PKC isozymes in cancer

Phorbol esters, a family of natural occurring diterpenoids isolated from the seed oil of the plant *Croton tiglium* of the *Euphorbiaceae* family (123), established the first connection between PKC and cancer. The carcinogenic activity of the croton oil was first described in the early 40's, based on the development of papillomas in mouse skin after exposure to a single application of a sub-effective dose of a carcinogen followed by chronic application of phorbol 12-myristate 13-acetate (PMA) (124, 125). Later, it was reported that phorbol esters bind with high affinity to PKC, competing with the physiological ligand DAG for the same binding site, with subsequent PKC activation (54, 56, 126). Particularly, like with DAG, phorbol esters retain the C1 domain of PKC on membranes through a contiguous hydrophobic surface, which is assembled by their insertion into the hydrophilic cleft on C1 domain (127, 128). Collectively, these findings allowed to recognize PKC as a major kinase in tumorigenesis, and contributed to the dogma that PKC acts as an oncoprotein (57). However, besides the induction of an acute activation of PKC, phorbol esters also trigger a PKC downregulation process. As such, currently, it is still controversial if the tumor-promoting properties of phorbol esters are due to PKC activation or to its loss by downregulation. Nevertheless, phorbol esters have represented crucial tools in PKC research field, greatly contributing to the elucidation of PKC cellular functions in cancer.

PKC α has been frequently associated with increased proliferation and survival, being commonly recognized as tumor promoter (129-132). Yet, several evidence have indicated that PKC α has tissue-specific functions, acting either as tumor promoter or tumor repressor depending on cell type. Consistently, it is known that the levels of PKC α differ with the type of cancer, being overexpressed in bladder, endometrial and breast cancers, and downregulated in colorectal and malignant renal cell carcinomas (68). Accordingly with its pro-survival role, the overexpression of PKC α in U87 glioblastoma cells stimulated proliferation, and increased the resistance to apoptosis in response to radiation and chemotherapy (129, 133, 134). Moreover, the ectopic expression of PKC α in MCF-7 breast cancer cells increased proliferation, anchorage-independent growth, and tumorigenic potential in nude mice (135). Nevertheless, in LNCaP prostate cells, PKC α behaved as

tumor suppressor, inducing apoptosis upon treatment with PMA and radiation, an effect abrogated by the expression of a PKC α kinase-dead mutant (136). Additionally, activation of PKC α in non-small cell lung cancer (NSCLC) inhibited cell growth and senescence with p21 upregulation (137). PKC α was also implicated in the regulation of invasion and metastasis. Actually, in breast cancer cells, cell invasion was promoted by ErbB2-dependent activation of PKC α (138). Additionally, the overexpression of PKC α in MCF-7 cells increased motility, which was associated with a decrease in the expression levels of E-cadherin and β -catenin, and an increase of matrix metalloprotease-2 and -9 (MMP-2 and -9) (139, 140). Consistently, the number of metastasis in lung was significantly reduced by the treatment with a PKC α antagonist peptide (141).

Regarding PKC δ , compelling evidence have shown that it mostly acts as an anti-proliferative and pro-apoptotic kinase. Accordingly, the overexpression of PKC δ in ovary (CHO) cells induced a G2/M-phase arrest, with inhibition of cell division upon PMA treatment (142). PKC δ also caused a G1-phase arrest, with upregulation of p21, in lung adenocarcinoma cell lines (143). In addition, PKC δ mediated apoptosis in response to genotoxic agents in C5 rat parotid salivary acinar cells, with translocation from cytosol to nucleus, through proteolytic activation by caspase-3 cleavage (114). Of note that, PKC δ -mediated apoptosis may only require an allosteric activation, without the generation of the PKC δ -CF, as demonstrated in androgen-dependent prostate cancer cells (144). In an additional work, it was shown that the tumor promoting effect of phorbol esters was abrogated by the transgenic overexpression of PKC δ in mouse skin (145). Moreover, clinical data have revealed reduced protein levels of PKC δ in colon cancer tissues compared to normal ones (146). Consistently, overexpression of PKC δ in Caco-2 colorectal adenocarcinoma cells inhibited anchorage-dependent and independent growth, increasing apoptosis and inducing differentiation (146). Similarly, its overexpression also inhibited the transformed phenotype of *src*-overexpressing rat colonic epithelial cells (147). In fact, several studies are consistent with a tumor-suppressive function of PKC δ in colon cancer (146-150). On the other hand, it was reported that the ectopic expression of PKC δ promoted anchorage-independent growth and developed resistance to apoptotic stimuli in mammary cells (151). Also in PC-3 human prostate xenograft model, the activation of PKC δ stimulated tumor growth and angiogenesis (152). Concerning to migration and invasiveness, there are many contradictory results. For example, it was shown that overexpression of PKC δ in highly motile BT-549 breast cancer cells reduced migration, while its downregulation enhanced motility and MMP-9 secretion in MCF-7 cells (153). Conversely, downregulation of PKC δ in murine MTLn3 mammary breast cancer model suppressed the metastatic

process to lung (154). More recently, it was reported that PKC δ phosphorylates BAG3, which in turn regulates epithelial-mesenchymal transition (EMT) in thyroid cancer cells (155).

Conversely, PKC ϵ has been widely recognized by its oncogenic properties (156-158). In fact, in mouse NIH3T3 embryonic fibroblasts, the overexpression of PKC ϵ induced a transforming phenotype, increasing cell proliferation and anchorage-independent growth (156). Additionally, PKC ϵ -overexpressing NIH3T3 cells were able to grow and form solid tumors into nude mice, an effect not observed with non-transfected cells (156). Interestingly, some reports have established a correlation between the proliferative and pro-survival role of PKC ϵ and its ability to regulate caspases and Bcl-2 family proteins. In particular, it was shown that PKC ϵ inhibited apoptosis in breast cancer cells by preventing BAX activation through inhibition of its translocation to mitochondria (159). Several works have also demonstrated that overexpression of PKC ϵ induced tumor cell invasion and metastasis in different cell models, such as human breast, glioma and renal cell carcinoma (160-162). On the other hand, inoculation of PKC ϵ -depleted cells into nude mice resulted in tumor growth inhibition and decreased incidence of lung metastases (160). Also corroborating its oncogenic role, overexpression of PKC ϵ has been observed in numerous cancers, including in majority of primary tumors from invasive ductal breast cancer and NSCLC patients (160, 163). A correlation between increased PKC ϵ levels and enhanced cancer recurrence, as well as decreased overall survival, was also found in head and neck squamous cell carcinoma (HNSCC) patients (164).

Concerning to atypical PKCs, it is interesting to note that while PKC ι is overexpressed in the majority of cancers, PKC ζ can be either up- or downregulated in different human cancers (68). Despite conflicting results, it is widely accepted that PKC ζ mainly exerts tumor suppressor functions, whereas PKC ι promotes tumor growth (68). Actually, a pro-apoptotic role of PKC ζ has been described in various cancer models, including colon (149) and ovarian cancer (165). Additionally, PKC ζ -deficient mice exhibited increased Ras-induced lung carcinogenesis, arguing for a tumor suppressor function of PKC ζ . Interestingly, although little is known about the involvement of PKCs in metabolism, PKC ζ was also reported as a critical regulator of tumor metabolic pathways. Particularly, under starvation conditions, PKC ζ -deficient cancer cells are able to reprogram their metabolism, to consume glutamine through the serine biosynthetic pathway, in order to supply the energetic cellular needs, which further reinforces the a tumor suppressor function of PKC ζ (166). However, there are also some reports highlighting a pro-survival role of PKC ζ (167, 168). Regarding PKC ι , it was shown that it is an essential mediator of oncogenic K-Ras, being essential for

the maintenance of the tumor-initiating properties (169, 170). Moreover, in ovarian cancer, disruption of PKC α inhibited the clonal expansion, anchorage-independent growth, and tumorigenic potential of tumor initiating cells (171, 172).

1.2.3. PKC mutation in cancer

To date, in diverse cancer types, over 1,000 cancer-associated somatic mutations were identified in the structural domains of PKC isozymes (173). The results of the analysis of approximately 50 of these mutations showed that about two-thirds of them led to inactivation/loss-of-function (LOF), without the identification of any gain-of-function (GOF) mutation (100). Additionally, it is possible to predict the existence of many other LOF mutations in PKC family members localized in highly conserved motifs required for catalysis (174). These inactivating mutations may interfere with crucial processes involved in PKC activation, namely by preventing their processing phosphorylation and the binding of second messengers, or even their catalytic activity (77). Indeed, it was reported that mutant PKC can impair the processing phosphorylation of PKC isozymes through inhibition of effectors of this mechanism, thus avoiding the accumulation of other PKC isozymes (175). They can also disrupt normal PKC signaling, redirecting PKC to other substrates, and potentially activating other signaling pathways involved in tumor development (176).

The majority of PKC LOF mutations are heterozygous, acting in a dominant negative manner with respect to the wild-type (wt) counterpart, and even to other PKC isozymes, which contributes to their malignancy (77). Consistently, the correction of the mutant allele (A509T) of *PRKCB* to wt by genome editing in DLD1 colon cancer cells, not only led to the suppression of anchorage-independent growth, but also reduced the tumor growth in xenograft models (100). Contrary, its deletion only partially decreased anchorage-independent growth, revealing that PKC β is haploinsufficient with respect to this outcome (100).

Accumulated data have also supported that PKC prevents oncogenesis, through inhibitory phosphorylation of oncoproteins. Particularly, phosphorylation of epidermal growth factor receptor (EGFR), which is one of the main PKC substrates, on threonine (Thr)654 leads to the reduction of EGFR tyrosine kinase activity, decreasing ligand binding capacity, and promoting its internalization (177-180). Besides transmembrane receptors, other PKC substrates were also identified, including K-Ras oncogene. Actually, it was recently reported that PKC phosphorylates K-Ras on serine (Ser)181, preventing tumor growth in mouse models by inhibiting its interaction with calmodulin, an effect promoted by the PKC activator, prostratin (181). Therefore, it is expected that LOF PKC mutations

stimulate tumor cell growth and survival by abolishing the inhibitory activity of PKC in these signaling pathways.

As a whole, based on the evidence that PKC activity is often compromised in cancer due to LOF mutations, it is currently claimed that PKC isozymes function as tumor suppressors rather than tumor promoters.

1.2.4. Targeting PKC activity

As promising targets in cancer, amazing efforts have been made in an attempt to develop PKC isozymes-targeting agents for anticancer therapy. However, this has proved to be a challenging task, mainly due to the high degree of sequence homology and structural resemblance among PKC isozymes. This is particularly evident for the catalytic domain, since the similarity extends to other kinases, (76). The complexity of this targeting process is increased by the co-expression of multiple PKC isozymes in cells, some of which exhibiting antagonistic functions (182). Therefore, for long, the modulation of PKC isozymes has been associated with off-target effects, and subsequently with unwanted toxic side effects.

In general, approaches to target PKC can be classified according to their specific site of action. Agents that interfere with the PKC catalytic activity can competitively bind either to the ATP- or substrate-binding site. The most common and potent kinase inhibitors are the ATP-competitive small-molecules, although in most cases they have little or no selectivity for PKC isozymes. Among these, staurosporine, a natural indolocarbazole produced by *Streptomyces staurosporeus*, inhibits all PKC isozymes, as well as other kinases, including PDK1, with high binding affinity (183-186). The synthesis of semi-synthetic derivatives of staurosporine led to the identification of *N*-benzoyl-staurosporine, also known as midostaurin or PKC412, as a potent inhibitor of all PKCs (187, 188). This compound has been tested in clinical trials of patients with different cancers (<https://clinicaltrials.gov/ct2/results?term=Midostaurin>), either as monotherapy or in combination therapy, and recent data revealed improved results in terms of patients survival (189, 190). Enzastaurin (also known as LY317615) is another synthetic compound initially reported as selective for PKC β (191). However, later studies demonstrated that it also targets other PKC isozymes, as well as other kinases. Despite the promising results obtained in phase I and II clinical trials (<https://clinicaltrials.gov/ct2/results?term=LY317615>), the use of enzastaurin hydrochloride alone in patients with diffuse large B-cell lymphoma (DLBCL) did not improve patient survival (192). Currently, enzastaurin is under clinical trials as monotherapy and in combination with conventional chemotherapies for pediatric brain tumors and malignant

gliomas (193, 194). Rottlerin (also termed mallotoxin), a natural product isolated from the Asian tree *Mallotus philippensis*, was originally described as PKC δ -selective inhibitor (195). Nevertheless, the selectivity of rottlerin for PKC δ has also been questioned by several studies. In fact, it has been demonstrated that rottlerin could also inhibit multiple kinases, including a potassium channel opener regulator of mitochondrial membrane potential (MMP) (196). Interestingly, using computational pharmacophore modeling, novel PKC δ -selective inhibitors were developed, particularly the chimeric hybrid BJE106, which targets PKC δ with high selectivity (IC₅₀ of 50 nM), inhibiting the growth of NRAS-mutant melanoma cells and inducing cell death in BRAF-mutant melanomas (197).

Bryostatin-1 is a macrocyclic lactone isolated from the marine bryozoan *Bugula neritina* (198), which binds with high affinity to the C1 domain. However, in contrast to phorbol esters, it has low pro-tumorigenic activity, antagonizing the tumor-promoting effects of phorbol esters (199, 200). Additionally, bryostatin-1 inhibits tumor growth both *in vitro* and *in vivo*. Based on these results, bryostatin-1 was tested in several clinical trials (<https://clinicaltrials.gov/ct2/results?term=bryostatin>), and despite the promising anticancer activity obtained in phase I, the results of phase II trials as monotherapy were disappointing (201-203). However, in combination therapy with other cytotoxic agents, it has shown improved efficacy, particularly in advanced esophageal, gastric, and gastroesophageal cancers (203-205), and in B-cell non-Hodgkin lymphoma (205). Yet, the complexity of its synthesis have made unfeasible the large-scale production of bryostatin-1, restricting its use in other studies. As such, several efforts have been made to synthesize structural-related analogs with similar activity for clinical use (206). Picolog is an example of a synthetic bryostatin analogue with picomolar affinity for PKC, which induces apoptosis in mantle lymphoma cells with inhibition of tumor growth in xenograft mouse models (207, 208). However, Picolog and other bryostatin derivatives, such as Merle 23 and neristatin-1, have still not been tested in patients. Moreover, following the rational design of C1 domain ligands, a set of five-membered ring DAG lactones were generated based on the 3D structure of the PKC δ C1B domain in complex with PMA. These novel synthetic DAG analogues bind to PKC C1 domain with an affinity three- to four-fold higher than DAG. Among these compounds, HK434 and HK654 induced apoptosis in human prostate LNCaP cancer cells (209). However, the high degree of identity in the C1 domain of cPKC and nPKC, particularly in the DAG binding motif, continue to be the major obstacle to the development of isozyme-selective compounds.

Ingenols are another group of C1 domain ligands with clinical application, which bind to PKC isozymes with similar *in vitro* affinity, but differentially activate PKCs in distinct cell models (210). Particularly, ingenol mebutate (Picato[®]) is in the market since 2012 for the

treatment of actinic keratosis, and seems to be effective for the treatment of basal cell carcinomas (211).

Another strategy to target specific PKC isozymes has been focused on intra- and intermolecular interactions established by PKCs. Actually, the C2 domain (in cPKCs and nPKCs) and the PB1 domain (in aPKCs) are involved in the recruitment of activated PKC isozymes to distinct subcellular compartments, through interaction with unique isozyme-specific anchoring proteins (83). As such, peptides have been generated to selectively inhibit PKC isozymes by preventing the PKC interaction with anchoring proteins, as RACKs (212). In fact, several peptides derived from different regions of PKC, as C2 domain, have been developed, which can prevent scaffolding interactions with subsequent inhibition of PKC activity (213, 214). Although these peptides have been initially designed to elucidate the cellular function of these protein-protein interactions, they quickly reached therapeutic relevance. Actually, the ϵ V1-2 peptide, which targets PKC ϵ , showed anticancer activity in xenograft models of NSCLC and impaired lung cancer cell motility signaling (215, 216). Beyond the peptides, the small-molecule PKC inhibitor aurothiomalate (ATM) was also identified as disruptor of the PB1-PB1 domain-mediated binding of PKC ι to Par6, inhibiting the transformed growth of NSCLC models (217, 218).

The antisense therapy, based on the inhibition of expression of PKC isozymes using oligonucleotides with complementary sequences to mRNA of genes of interest, has been also used. Aprinocarsen (ISIS-3521) is a 20-base antisense oligonucleotide that induces PKC α downregulation, markedly reduces cancer cell proliferation and invasion, and inhibits xenograft tumor growth (219, 220). Although it has been tested in clinical trials for patients with prostate, breast, ovarian, colon, lung, glioblastoma, melanoma, and other cancers (221), the results obtained were not encouraging.

The PKC modulators under clinical trials as anticancer agents, and their clinical status, are presented in Table 1.1.

Table 1.1: PKC modulators under clinical trials as anticancer agents.

Agents	Clinical status	References
ATP-competitive inhibitors		
UCN-01 <i>Non-selective</i>	Phase II in metastatic TNBC (NCT00031681)	(222)
	Phase II in metastatic melanoma (NCT00072189)	(223)
	Phase II in ovarian cancer (NCT00072267)	(224)
Midostaurin (PKC412) <i>Non-selective</i>	Phase III in AML (NCT03379727)	(225)
	Phase IIa in metastatic melanoma	(226)
	Phase I in NSCLC	(188)
Sotrastaurin (AEB071) <i>Selectivity for cPKCs and nPKCs</i>	Phase II in CLL (NCT02285244)	(227)
Enzastaurin (LY317615) <i>Some selectivity for PKCβ</i>	Phase III in diffuse large B-cell lymphoma (NCT03263026)	(192)
	Phase II in pancreatic cancer (NCT00267020)	(228)
	Phase II in lung cancer (NCT00414960)	(229)
	Phase I in pediatric brain tumor (NCT00503724)	(193)
	Phase II in recurrent malignant gliomas (NCT00586508)	(194)
C1 domain ligands		
Bryostatins-1 <i>Selectivity for cPKCs and nPKCs</i>	Phase II in ovarian cancer (NCT00006942)	(230)
	Phase II in pancreatic cancer (NCT00031694)	(231)
	Phase II in esophageal cancer (NCT00005599)	(204)
	Phase II in renal cell carcinoma (NCT00003968)	(232)
Ingenol mebutate (PEP005) <i>Non-selective</i>	Phase IIa, IIb and III in actinic keratosis (NCT0010796; NCT00742391; NCT00916006; NCT00915551; NCT00942604; NCT01541553)	(233-236)
	Phase I/II in Non-melanoma skin cancer	(237)
Inhibitors of the protein-protein interactions		
Aurothiomalate (ATM) <i>Selectivity for PKCι</i>	Phase I in NSCLC (NCT00575393)	(238)
	Phase I in ovarian cancer	(238)
	Phase I in pancreatic cancer	(238)
Antisense oligonucleotides inhibitors		
Aprinocarsen (ISIS-3521) <i>Selectivity for PKCα</i>	Phase II in ovarian cancer	(239)
	Phase II in high-grade gliomas	(240)
	Phase II and III in NSCLC (NCT00042679; NCT00034268)	(241-243)
	Phase II in Non-Hodgkin's lymphoma	(244)
	Phase II in colorectal cancer	(245, 246)

TNBC, triple negative breast cancer; AML, acute myeloid leukemia; NSCLC, non-small cell lung cancer; CLL chronic lymphocytic leukemia.

1.2.5. Screening strategies

1.2.5.1. *Genetically encoded fluorescent reporters*

Traditionally, the most used strategy to demonstrate the phosphorylation of residues that activate protein kinases has been the immunoblotting, using phospho-specific antibodies (247). Nonetheless, this can be an ineffective measure of prior cell activation since PKCs are constitutively phosphorylated during the maturation process. To overcome this limitation, the analysis of PKC translocation to membranes, by immunoblotting or immunofluorescence using PKC-specific antibodies, became the most reliable activation measure, as a result of allosteric alterations (248-250). Additionally, the cellular activity of PKC has also been studied by immunoblotting using phospho-specific antibodies against PKC substrates. However, although *in vitro* kinase activity assays are still the basis for the analysis of PKC activity, they do not provide a complete spatiotemporal picture of all signaling events (251). In turn, the use of fluorescently-tagged PKC in live cells has allowed to monitor membrane translocation as a readout of activation. Actually, this approach has been used to study the translocation kinetics of PKC over time in response to natural agonists (252, 253), or phorbol esters (254). On the other hand, a live-cell imaging system with genetically encoded biosensors based on Förster/fluorescence resonance energy transfer (FRET) has also been extensively used. Particularly, this technique allows to visualize dynamic conformational changes of macro-biomolecules (255-257), the binding between two molecules (258, 259), and it is also applied to the high-throughput screening (260, 261). Regarding PKC, C-kinase activity reporter (CKAR) is the most used tool to directly measure PKC activity, and employs the modular architecture of activity reporter originally developed for tyrosine kinases (262) and protein kinase A (PKA) (263). Briefly, once activated, PKC phosphorylates the substrate, resulting in a conformational change in the reporter that produces a FRET change, thus enabling the readout of PKC activity in real time. Besides the preservation of the physiological cellular context and spatiotemporal information, FRET reporters also demonstrated great sensitivity for low affinity or transient interactions.

1.2.5.2. *Yeast-based assays*

In 1993, a yeast model system was established by Riedel and colleagues to separately analyse the function of each PKC isozyme (264). Particularly, they demonstrated that the expression of mammalian cPKC α and β I in yeast induced biological responses similar to those obtained in mammalian cells. In fact, the activation of these isozymes by phorbol esters triggered a specific phenotype characterized by a delay in yeast growth,

which was proportional to the degree of enzymatic activation (Fig. 1.5) (264, 265). On the other hand, PKC inhibitors, such as chelerythrine, reverted the growth inhibitory effect of PKC activators (266). Based on this, the yeast PKC phenotypic assay became a valuable tool to screen for PKC isozyme-specific modulators (267). It was also used to establish a PKC structure-activity relationship, namely using PKC α mutants lacking certain amino acid sequences within the regulatory and catalytic domains (265). Additionally, using a PKC α β I chimera, in which the C-terminal of PKC α was replaced by the corresponding PKC β I sequence, it was demonstrated that these two isozymes were complementary, exhibiting a similar phenotype (268). Furthermore, with deletions in PKC α , it was identified a novel regulatory segment in C2 domain that retains the enzyme in an inactive conformation and simultaneously regulates the PKC catalytic activity (269). This finding led other authors to identify other regions in the regulatory domain that, like PS segment, were also implicated in the PKC α auto-inhibition (270). In fact, with these studies, it was demonstrated the existence of intramolecular interactions between the regulatory and catalytic regions of PKC α , which contribute to the maintenance of the enzyme in an inactive conformation. Altogether, these works validated yeast as a promising cell system to study individual mammalian PKCs, in a simplified eukaryotic cellular environment without the interference of other isozymes.

In particular, the yeast PKC phenotypic assay was extensively used in the characterization of the potency and isozyme-selectivity of well-known PKC activators and inhibitors. Notably, it has also contributed to the discovery of new PKC isozyme-selective activators (271, 272) and inhibitors (273, 274) from the screening of a chemical library of xanthenes. A new selective activator of nPKC δ and ϵ , the diterpene compound 6,11,12,14-tetrahydroxy-abieta-5,8,11,13-tetraene-7-one (coleon U), with potent antiproliferative effects against several human tumors cells was also discovered using the yeast approach (275). In that work, it was verified that while PMA activated nPKCs, inducing their translocation from the cytosol to the plasma membrane and a G2/M-phase cell cycle arrest, coleon U induced the translocation of nPKCs to the nucleus and a metacaspase- and mitochondria-dependent apoptosis. Interestingly, these results were in accordance with those described for mammalian cells (276), confirming that also in yeast distinct stimuli prompted the translocation of PKCs to different cellular compartments with the subsequent induction of distinct cellular responses.

Collectively, with these works, it was shown that several functional features of mammalian PKC isozymes are conserved in yeast. Most importantly, yeast proved to be a valuable and reliable drug screening tool, providing relevant clues about the molecular mechanism of action of several drugs. Moreover, due to its easy manipulation and reduced

doubling time, yeast allows simple and fast screenings well-adaptable to HTS methodologies in a cost-effective manner. As a whole, the yeast-cell model revealed to be useful as a first-line targeted screening strategy for a preliminary selection of compounds to be tested in more complex cell systems (277, 278).

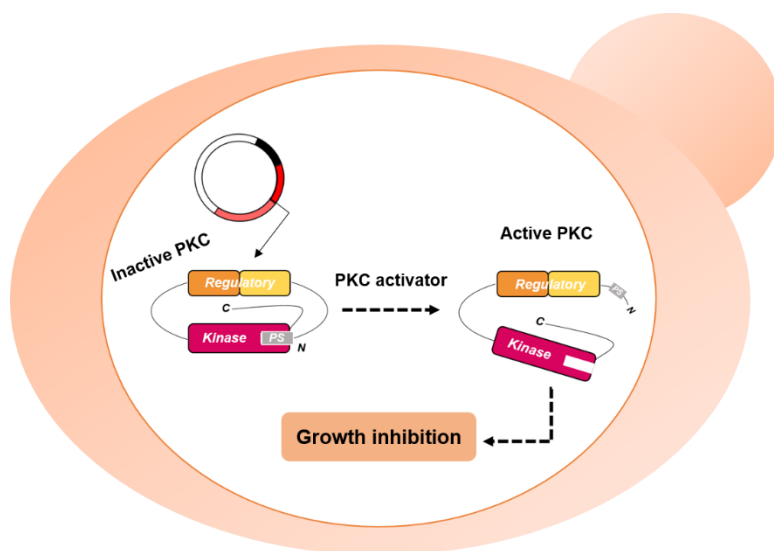


Figure 1.5: Yeast PKC phenotypic assay developed to screen PKC isozyme-selective activators. This system is based on the heterologous expression of individual mammalian PKC isozymes, and on the subsequent evaluation of the impact of small-molecules on yeast cell growth. The activation of mammalian PKC induces yeast growth inhibition, not observed in control yeast (yeast transformed with the empty vector), which is proportional to the degree of PKC activation.

1.3. Natural products

Over the years, compounds derived from natural sources such as plants, have been the most profitable source of new therapeutic agents. Although the pharmaceutical industry has tried to redirect its focus to the production of synthetic compounds, this strategy was not well-succeeded, with an evident decrease of the new drugs that reached the market (279). Indeed, recent data showed that from 1,135 new drugs approved by FDA, from 1981 to 2010, over 50% were from natural sources (280). This led the research groups to reconsider the natural products as a major source of promising therapeutic agents. Natural compounds from plants are derived from the secondary metabolism, and are themselves, in the unmodified state, a source of new bioactive agents. In addition, they can be used as

scaffolds for the development of semi-synthetic analogues with improved pharmacological properties. The selection of species for the isolation of bioactive compounds has been supported by references from traditional medicine and by chemotaxonomic studies (281). Particularly, chemotaxonomic studies with the Lamiaceae family led to an increasing interest for *Plectranthus* L'Her genus, which comprises more than 300 species mainly distributed by Africa, Asia and Australia (282). Actually, these species have been used for many years in traditional medicine, and are recognized by the wide range of biological activities of their extracts or isolated compounds, including anti-infectious, antioxidant, anti-inflammatory and anticancer (283-286). The *Plectranthus* genus is chemotaxonomically characterized by the presence of caffeic acid esters, rosmarinic acid and nepetoidins A and B (287). However, the most commonly studied compounds from this genus are diterpenoids, a structurally diverse class of compounds consisting of four isoprene units forming a 20-carbon backbone (288). Particularly, abietanes such as royleanones, which have been widely associated with antimicrobial, antimycobacterial and anticancer activities, are among the most frequently reported diterpenic structures (283, 284, 286, 289).

Concerning to anticancer properties, over half of the compounds with this biological activity are natural products or their derivatives (290). Several studies have validated the cytotoxic potential of both extracts and isolated compounds from *Plectranthus* genus against cancer cells. This is the case of the nPKC δ and ϵ selective activator coleon U, and of 7 α -acetoxy-6 β -hydroxyroyleanone, obtained from *P. grandidentatus* (283), and their semi-synthetic derivatives (283, 284). These works have reinforced the potential of abietane diterpenes, as promising anticancer drug candidates particularly by targeting PKC.

1.4. Scope of the thesis

Compelling data have established PKC isozymes as major regulators of tumor growth and dissemination. However, we are still far from a complete understanding of the function of each PKC isozyme in cancer (76). The lack of isozyme-selective modulators has hampered the achievement of such a goal, as well as the translation of PKC modulators into the clinic. Therefore, for long, it became imperative the development of PKC isozyme-selective targeting agents. These compounds would greatly contribute to the advance of the biology and pharmacology of PKCs and would have promising applications in anticancer therapy. With the present thesis, we aimed to identify:

- i) PKC isozyme-selective agents;
- ii) New anticancer drug candidates by targeting PKC.

To this end, it was screened a small chemical library of royleanone derivatives from the *Plectranthus* genus. The drug discovery strategy used, in this thesis, encompassed the identification of potential PKC isozyme-selective agents using a yeast-based PKC assay, followed by validation of their molecular mechanism of action and anticancer activity in human cancer cells and animal models (Chapter 3.1 and 3.2). Additionally, other species of *Plectranthus* genus were studied as potential sources of new anticancer agents (Chapter 3.3).

The major outcomes achieved in this thesis, particularly its contribution to anticancer drug development by targeting PKC, are discussed in Chapter 4.

CHAPTER 2

Material and Methods

2.1. Compounds

PMA and arachidonic acid (ARA) were purchased from Enzo Life Science (Grupo Taper SA, Sintra, Portugal); etoposide (ETOP) from Calbiochem (VWR, Carnaxide, Portugal); hydroxyurea and cyclophosphamide (CP) from Sigma-Aldrich (Sintra, Portugal). All natural and semi-synthetic compounds, as well as plant extracts were provided by Prof Doutora Patrícia Rijo (CBIOS, Universidade Lusófona, Lisboa, Portugal). Natural diterpene 7α -acetoxy- 6β -hydroxyroyleanone (Roy) was extracted from *Plectranthus grandidentatus* as described (286). Subsequently, the semi-synthetic derivatives 7α -acetoxy- 6β -propionyloxy-12-O-propionyroyleanone (Roy-Pr2) and 7α -acetoxy- 6β -benzoyloxy-12-O-benzoylroyleanone (Roy-Bz) were synthesized following procedures formerly described (289). Natural diterpene 6,7-dehydroroyleanone (DeRoy) was isolated from essential oil of *P. madagascariensis* plant as described (291). Their synthetic derivatives, 6,7-dehydro-12-O-pro-2-yn-1-yloxy-royleanone (FRP19) and 6,7-dehydro-12-O-(1R,2S,5R)-2-isopropyl-5-methylcyclohexyl(oxy)-royleanone (FRP20), were prepared according to procedures described (292). The extracts were prepared from sixteen different *Plectranthus* spp. plants cultivated in Instituto Superior de Agronomia do Campus da Universidade de Lisboa, Portugal. Briefly, the extractions were prepared with the organic solvent, acetone, in a concentration of approximately 10% (w/v), according to the procedure described in (293). All tested compounds and extracts were dissolved in dimethyl sulfoxide (DMSO; Sigma-Aldrich), except hydroxyurea and CP that were dissolved in water.

2.2. Construction of pESC-(LEU2)-PKC δ Δ C1 plasmid

The wt *PRKCD* gene was amplified from the original clone provided by Dr. Nigel Goode (The Royal Veterinary College, Hawkshead Lane, Hertfordshire, UK) using the gene specific primers Xho1 PKC δ forward (F) (5'-CCGCTCGAGATGGCCCCGTTCTGCGCATC-3') and NheI PKC δ reverse (R) (5'-CTAGCTAGCCTATTCCAGGAATTGCTC-3'). After verifying the fragment by sequencing, it was cloned into the XhoI /NheI sites of pESC-(LEU2) plasmid (Agilent Technologies, Chandigarh, India) under control of the *GAL1* promoter. According to manufacturer's instructions, open reading frame (ORF) cloned in this vector will be expressed as a tagged protein with an N-terminal Myc-tag. Positive clones (pESC-(LEU2)-PKC δ) were further confirmed by sequencing and maintained in *Escherichia coli* strain NovaBlue cells. The deletion of C1 domain in the wt *PRKCD* gene was carried out by standard protocol of overlap primer extension using polymerase chain reaction (PCR) as described (294), and

with the help of the outer gene specific primers Xho1 PKC δ F and NheI PKC δ R, and the inner primers PKC δ C1 del F (5'-AACATCGACATGCCTCAAAAGCTCTTAGCTG-3') and PKC δ C1 del R (5'-CAGCTAAGAGCTTTTGAGGCATGTTCGATGTT-3'). First, the region upstream and downstream to the C1 domain was amplified using outer and inner primer pair followed by overlapping PCR to obtain the final product lacking C1 domain. The final product was digested with XhoI and NheI enzymes and ligated with similarly digested pESC-(*LEU2*). Positive clones were sequenced in their entirety to confirm the desired modification at the corresponding position and maintained in *E. coli* NovaBlue cells.

2.3. Yeast transformation

The pESC-(*LEU2*) plasmid (empty vector) and the plasmid obtained in 2.2 (pESC-(*LEU2*)-PKC $\delta\Delta$ C1) used in the yeast transformation process were firstly amplified in *E. coli* DH5 α strain (Lucigen, Frilabo, Porto, Portugal), and thereafter extracted using the *GenEluteTM HP Plasmid Miniprep Kit* (Sigma-Aldrich). After extraction, *Saccharomyces cerevisiae* CG379 strain was transformed using the lithium acetate/single-stranded carrier/polyethylene glycol (DNA LiAc/SS Carrier DNA/PEG) method as described (295). For selection of transformed yeast, cells were routinely grown in selective minimal medium with 2% (w/w) glucose (Sigma-Aldrich), 0.7% (w/w) yeast nitrogen base (YNB) without amino acids (a.a.) (Difco, Quilaban, Sintra, Portugal), and all the a.a. required for yeast growth (50 μ g/mL), except leucine, and incubated at 30°C, under continuous orbital shaking (200 rpm).

2.4. Yeast-based screening assay

Yeast cells expressing PKC α , β I, δ , ϵ , ζ and control yeast (transformed with empty vector) obtained in previous works (275), and PKC $\delta\Delta$ C1 obtained in 2.3, were used. The expression of PKC $\delta\Delta$ C1 in yeast was previously confirmed by immunoblotting (see Appendix; Fig. 1). For expression of mammalian proteins, cells (routinely grown in minimal selective medium) were diluted to an optical density (OD) at 600 nm (OD₆₀₀) of 0.05 in induction selective medium containing 2% (w/w) galactose (Sigma-Aldrich), 1% (w/w) raffinose (Acros Organics, VWR), 0.7% (w/w) YNB without a.a., and a mixture of all the a.a. required for yeast growth (50 μ g/mL), except leucine. Yeast cells were incubated at 30°C under continuous orbital shaking (200 rpm), in the presence of 0.1 - 30 μ M of compounds (or 0.1% DMSO) only for approximately 42 h (time required by control yeast, incubated with DMSO

only, to achieve 0.4 OD₆₀₀). Yeast growth was analyzed by counting the number of colony-forming units (CFU), after 2 days incubation at 30°C, on Sabouraud Dextrose Agar (Liofilchem, Frilabo).

2.5. Yeast cell cycle analysis

Yeast cell cycle progression was analyzed basically as described (275). Briefly, about 1×10^7 cells (incubated in galactose selective medium with 10 μ M PMA, 10 μ M Roy-Bz (or DMSO only) for 42 h) were fixed in 70% (v/v) ethanol overnight at 4°C, followed by incubation with 250 μ g/mL RNase A (DNase-free; Sigma-Aldrich) for 3 h at 50°C, and thereafter with 1 mg/mL Proteinase K (Sigma-Aldrich) for 3 h at 37°C. Afterwards, cells were stained with 10 μ M Sytox Green Nucleic Acid (Invitrogen, Alfacel, Carcavelos, Portugal) overnight at 4°C, followed by flow cytometry analysis. Fluorescence from at least 30,000 cells was analyzed.

2.6. Analysis of yeast plasma membrane integrity and DNA fragmentation

Propidium iodide (PI) and TUNEL staining, to monitor plasma membrane integrity and DNA fragmentation respectively, were carried out as described (275). Briefly, about 1×10^7 cells (incubated in galactose selective medium with 10 μ M PMA, 10 μ M Roy-Bz, or DMSO only, for 42 h) were collected and incubated with 5 μ g/mL PI (Sigma-Aldrich) for 10 min at room temperature. TUNEL was performed using the *In Situ* Cell Death Detection Kit Fluorescein (Roche Diagnostics, Sigma-Aldrich) and according to the manufacturer's instructions. Approximately 500 cells were counted in five random microscope fields using an Eclipse E400 fluorescence microscope (Nikon).

2.7. *In vitro* PKC assay

To measure *in vitro* PKC activation, the non-radioactive PKC kinase activity kit (ADI-EKS-420A; Enzo Life Sciences), and purified recombinant human PKC proteins, cPKCs (mix of PKC α , β and γ), PKC δ , PKC ϵ , and PKC ζ (Merck Millipore, Grupo Taper), were used according to the manufacturer's instructions. Briefly, 10 ng of recombinant PKC was incubated with 10^{-7} - 10^{-3} μ M PMA/ARA or Roy-Bz (or DMSO only) for 1 h, and then transferred to a 96-well plate pre-coated with a synthetic peptide. A phosphospecific substrate antibody that recognizes the phosphorylated form of the substrate was added and

detected using a peroxidase-conjugated antibody. The degree of PKC activation was directly proportional to the amount of phosphorylated substrate determined by measuring the OD₄₅₀ using a microplate reader (Biotek Instruments Inc., Synergy MX, USA). The EC₅₀ (concentration required to induce 50% of the maximal response achieved with the positive control (constitutively activated PKC) of the kit) values were then calculated.

2.8. Molecular docking

The crystallographic structure of PKC δ with protein data bank (PDB) code 1PTR having 13-acetylphorbol (PRB) as co-crystallized ligand as described (127) was used to test the binding mode of Roy-Bz. First, the co-crystallized PRB molecule was re-docked to test the efficiency of the docking procedure in reproducing the experimental binding pose. The binding pose was reproduced with autodock 4.2 with a root-mean-square deviation (RMSD) of 0.47Å. The exact same conformation was reproduced with the molecule being slightly less inserted into the protein. All autodock docking parameters were produced with Autodock Tools and were kept at the default. The docking box was centered on the crystallographic position of the PRB molecule having 42, 62 and 36 grid points in x, y and z with a grid spacing of 0.375.

2.9. Human cancer cell lines and culture conditions

Human colon (HCT116 and HT-29) and colorectal (SW-837) adenocarcinoma, human breast adenocarcinoma (MCF-7), and human NSCLC (NCI-H460) cell lines were purchased from ATCC (LGC Standards S.L.U., Barcelona, Spain, 2013). Cell lines were frozen down at early passages (<5), routinely tested for mycoplasma contamination using *MycoAlert Plus Mycoplasma Detection Kit* (Lonza, VWR), and used between 2 to 8 passages after thawing. All tumor cells were routinely cultured in RPMI-1640 medium with ultraglutamine (Lonza), and supplemented with 10% fetal bovine serum (FBS; Gibco, Alfacene). For metabolism assays, HCT116 cells were routinely cultured in Dulbecco's Modified Eagle's Medium (DMEM) glucose-free (D5030; Sigma-Aldrich), with 5 mM glucose (Sigma-Aldrich), 4 mM L-glutamine (Sigma-Aldrich), 1 mM sodium pyruvate (Sigma-Aldrich), 21 mM sodium bicarbonate (Sigma-Aldrich), and supplemented with 10% FBS (pH 7.4). Cell lines were maintained at 37°C in a humidified atmosphere of 5% CO₂.

2.10. Immunofluorescence and confocal microscopy

For localization studies of green fluorescent protein (GFP)-fused PKCs, HCT116 cells (at a final density of 1×10^5 cells/well) were transfected with 2 μg of pEGFP-N1-PKC α , pEGFP-N1-PKC δ or pEGFP-N1-PKC ϵ using lipofectamine 3000 (Invitrogen), plated on coverslides in 12-well plates, and incubated for 48 h. Thereafter, cells were treated with 0.01 - 100 μM Roy-Bz, 100 nM PMA (positive control) (or DMSO only) for 1 h, washed with phosphate buffer saline (PBS; Sigma-Aldrich), and fixed with ice-cold methanol. Samples were stained with 1 $\mu\text{g}/\text{mL}$ 4',6-diamidino-2-phenylindole (DAPI) for 10 min at 4°C, mounted on a glass slide, and the cellular localization of GFP-fused PKCs was visualized using a Nikon TE2000-U microscope.

2.11. Sulforhodamine B (SRB) assay

For analysis of *in vitro* proliferation, human cell lines were seeded in 96-well plates at a final density of 5.0×10^3 (for HCT116, HT-29, MCF-7 and NCI-H460) and 7.5×10^3 (for SW-837) cells/well, and incubated for 24 h. Cells were thereafter treated with 0.1 - 10 μM PMA, 0.11 - 2.84 μM Roy-Bz, 1.56 - 50 μM 6,7-dehydroroyleanone and derivatives, or 1.56 - 50 $\mu\text{g}/\text{mL}$ plant extracts, for 48 h. For the SRB assay, following fixation with 10% trichloroacetic acid (TCA), plates were stained with 0.4% SRB (Sigma-Aldrich) and washed with 1% acetic acid (VWR). The bound dye was solubilized in 10 mM Tris Base (Sigma-Aldrich), and the absorbance was measured at 510 nm in a microplate reader (Biotek Instruments Inc.). The maximum concentration of solvent used in this assay (0.25% DMSO) was included as control, and the growth obtained was set as 100%. The IC₅₀ (concentration that causes 50% of growth inhibition) values were determined from the concentration-response curves.

2.12. Trypan blue assay

For analysis of cell viability, HCT116 cells were seeded in 24-well plates at a final density of 6×10^4 cells/well for 24 h, followed by treatment with 0.1 - 6 μM Roy-Bz for 24 h. For trypan blue exclusion assay, cells (non-adherent and adherent) were harvested and resuspend in PBS. An equal volume (1:1) of cell suspension was mixed with 0.4% Trypan Blue (Sigma-Aldrich), and then the number of viable/dead cells was determined on a hemocytometer and normalized to a drug-free control (DMSO; correspondent to the maximum concentration used). Cell viability was calculated as the number of viable cells

divided by the total number of cells. The IC_{50} values were determined from the concentration-response curves.

2.13. Colony formation assay

Human cell lines were seeded in 6-well plates at a final density of 5.0×10^2 (for HCT116 and SW-837) and 1.0×10^3 (for HT-29) cells/well, and incubated with 0.07 - 0.3 μ M Roy-Bz (or DMSO only, correspondent to the maximum concentration used) for 11 days. Thereafter, colonies were fixed using 10% methanol and 10% acetic acid for 10 min and stained with 0.5% crystal violet (Sigma-Aldrich) in methanol/H₂O (1:1) for 15 min. Colonies containing more than 20 cells were counted.

2.14. Analysis of cell cycle and apoptosis in human cell lines

Human cell lines were seeded in 6-well plates at a final density of 1.5×10^5 (for HCT116 and HT-29) or 2.25×10^5 (for SW-837) cells/well, and incubated for 24 h. Cells were thereafter treated with 8 μ M PMA, 1 μ M Roy-Bz, or DMSO only for 24 h. For cell cycle analysis, cells were fixed in ice-cold 70% ethanol, incubated with RNase A at a final concentration of 20 μ g/mL for 15 min at 37°C, and further incubated with 50 μ g/mL PI for 30 min at room temperature, followed by flow cytometry analysis. Apoptosis analysis was performed by flow cytometry using the *Annexin V-FITC Apoptosis Detection Kit I* (BD Biosciences, Enzifarma, Porto, Portugal), according to the manufacturer's instructions.

2.15. Western blot analysis

For analysis of protein expression in human tumor cell lines, cells were seeded in 6-well plates at a final density of 1.5×10^5 (for HCT116 and HT-29) or 2.25×10^5 (for SW-837) cells/well, and incubated for 24 h, and thereafter treated with 0.5 - 3.5 μ M Roy-Bz (or DMSO only) between 0 - 96 h. Whole cell lysates were prepared by lysing the cells with RIPA buffer (150 mM NaCl, 1.0% IGEPAL CA-630, 0.5% sodium deoxycholate, 0.1% sodium dodecyl sulfate (SDS), and 50 mM Tris, pH 8.0; Sigma-Aldrich) in the presence of ethylenediaminetetraacetic acid (EDTA)-free protease inhibitor cocktail (Sigma-Aldrich) for 1 h at 4°C. Soluble fractions of cell lysates were then isolated by centrifugation at 8000 rpm for 10 min. For mitochondrial and cytosolic fractions of human tumor cells, the *Mitochondrial Fractionation Kit* (Active Motif, Frilabo) was used according to the manufacturer's

instructions. For analysis of yeast protein expression, samples were lysed with Cellytic™ Y Cell Lysis Reagent (Sigma-Aldrich) in the presence of EDTA-free protease inhibitor cocktail (Sigma-Aldrich). Protein extracts were quantified using the Coomassie staining, Bradford (Sigma-Aldrich).

Proteins (40 µg) were denatured by boiling in Laemmli Sample Buffer (4x; Bio-Rad, Life Science, Amadora, Portugal) containing 10% β-mercaptoethanol (National Diagnostics, Frilabo) for 5 min, electrophoresed in 10% sodium dodecyl sulfate polyacrylamide gel electrophoresis (SDS-PAGE), and then transferred to a Whatman nitrocellulose membrane (Protan, VWR). Membranes were blocked with 5% milk or 5% bovine serum albumin (BSA; Sigma-Aldrich) in Tris Buffered Saline with Tween 20 (TBST; Sigma-Aldrich), and probed overnight with a primary antibody (see Appendix; Table 1) followed by 2 h incubation with a horseradish-peroxidase (HRP)-conjugated secondary antibody (see Appendix; Table 1). For analysis of cytosolic and mitochondrial fractions, membranes were stripped (Abcam protocol), and reprobated with the primary antibodies for the loading controls GAPDH and COX IV, respectively. The signal was detected using the *ECL Amersham Kit* (GE Healthcare, VWR) and the Kodak GBX developer and fixer (Sigma-Aldrich). Band intensities were quantified using the Bio-Profil Bio-1D++ software (Vilber-Lourmat, Marne La Vallée, France), and were normalized against the control sample (DMSO; set as 1). Western blots presented in this thesis are representative of three independent experiments.

2.16. Analysis of reactive oxygen species (ROS) generation

HCT116 cells were seeded in 6-well plates, at a final density of 1.5×10^5 cells/well for 24 h, and then treated with 0.5 µM Roy-Bz (or DMSO only) for 24 h. Afterwards, cells were harvested and stained with 3 µM MitoSOX (Invitrogen) for 30 min at 37°C, followed by flow cytometry analysis.

2.17. Analysis of mitochondrial membrane potential ($\Delta\Psi_m$)

HCT116 cells were seeded in 6-well plates, at a final density of 1.5×10^5 cells/well for 24 h, and then treated with 0.5 µM Roy-Bz or DMSO only for 16 h. Thereafter, cells were harvested and incubated with 1 nM 3,3'-dihexyloxacarbocyanine iodide (DiOC₆(3)) (Alfagene) for 30 min, at 37°C, followed by flow cytometry analysis.

2.18. Generation of colon cancer spheroids (colonsphere assay)

HCT116 cells were resuspended in serum-free stem cell culture media consisting of DMEM (Lonza) supplemented with 10 ng/mL bFGF and 20ng/mL EGF (Bio-techne, Citomed Lda, Lisboa, Portugal), 1× B27 (Life Technologies, Porto, Portugal), and 5 µg/mL insulin (Sigma-Aldrich). Cells were plated in 24-well ultra-low attachment plates (Corning Inc.; one spheroid/well) at 1×10^3 cells/well. Treatments with 2 - 3.5 µM Roy-Bz (or DMSO only) were performed 3 days after spheroid formation for up to 96 h, or with 0.25 - 1 µM Roy-Bz (or DMSO only) were performed at the seeding time for 48 h. Spheroid formation was monitored using an inverted Nikon TE 2000-U microscope at 100× magnification with a DXM1200F digital camera and using Nikon ACT-1 software. Spheroid diameters were quantified using the ImageJ software.

2.19. Extraction and purification of plasmid DNA

E. coli bacterial cell cultures transformed with control pSuper plasmid or pSuperPKCδ.RNAi [Addgene plasmid #10819; (296)] were inoculated in Luria-Bertani (LB) medium (Liofilchem), containing 1 µg/mL ampicillin (Sigma-Aldrich), and grown overnight at 37 °C. Bacterial cells were pelleted by centrifugation, and highly purified plasmid DNA was obtained using the *PureYield™ Plasmid Midiprep System* (Promega, VWR) according to the manufacturer's instructions. The amount of plasmid DNA was quantified using NanoDrop™ 1000 Spectrophotometer (Thermo Fisher Scientific).

2.20. Generation of stable PKCδ-knockdown cell line

HCT116 cells were seeded in 24-well plates at a final density of 6×10^4 cells/well for 24 h. For the generation of stable cell lines, cells were co-transfected with 1 µg of control pSuper plasmid (control; mock) or 900 ng of pSuperPKCδ.RNAi [Addgene plasmid #10819;(296)] and 100 ng of pSUPERpuro plasmids, and 2 µg/mL Lipofectamine 2000 (Invitrogen) for 72 h. Stable transfectants were selected with 3 µg/mL puromycin (Sigma-Aldrich) for 4 weeks. Clones were screened for PKCδ expression silencing by Western blot using an anti-PKCδ antibody (see Appendix; Fig. 2).

2.21. *In vitro* migration assays

Cell migration was analyzed using the Wound Healing Scratch assay as described (297), and the *QCM 24-Well Fluorimetric Chemotaxis Cell Migration Kit* (8 μm ; Merck Millipore). In the Wound Healing Scratch assay, PKC δ -knockdown and control HCT116 cells were seeded at a density of about 5×10^5 cells/well and grown to confluence in 6-well plates. After reaching the confluence, a fixed-width wound was created in the cell monolayer using a sterile 200 μL tip, and then cells were treated with 0.25 μM Roy-Bz (or DMSO only) for 48 h. Cells were thereafter photographed, using the Moticam 5.0MP camera with Motic's AE2000 inverted microscope (VWR) with 100 \times magnification, at different time-points of treatment until complete closure of the wound. Wound closure was calculated by subtracting the 'wound' area (measured using Image J software) at the indicated time-point of treatment from the 'wound' area at the starting point. In the *QCM 24-Well Fluorimetric Chemotaxis Cell Migration Kit*, about 5×10^5 cells/mL of PKC δ -knockdown and control HCT116 cells were prepared in serum free RPMI 1640 medium and treated with 0.25 μM Roy-Bz or DMSO only, followed by incubation for up to 24 h. Cell suspensions were distributed into 24-well plates (300 μL /insert), followed by addition of 500 μL medium containing 10% FBS to the lower chamber. Cells that migrated through the 8 μm pore membranes were eluted, lysed and stained with a green-fluorescence dye that binds to nucleic acids. The number of migrated cells is proportional to the fluorescence signal measured using a microplate reader (Biotek Instruments Inc.) at 480/520 nm (ex/em).

2.22. Comet assay

HCT116 cells were seeded in 6-well plates at a final density of 1.5×10^5 cells/well for 24 h, followed by treatment with ETOP, Roy-Bz (or DMSO only) for 48 h. To evaluate DNA damage, *OxiSelect Comet Assay Kit* (Cell Biolabs, MEDITECNO, Carcavelos, Portugal) was used according to the manufacturer's instructions, with Tris/borate/EDTA (TBE) for electrophoresis. Tail DNA quantification considers the percentage of cells with more than 5% of DNA in the tail (assessed by Open Comet/ImageJ); tail moment corresponds to the product of the tail length and the % of DNA in the tail. Cells were photographed using a Nikon DS-5Mc camera and a Nikon Eclipse E400 fluorescence microscope, and images processed using a Nikon ACT-2U software (Izasa).

2.23. Micronucleus assay

Genotoxicity was analyzed by cytokinesis-block micronucleus assay in lymphocytes as described (298). Fresh peripheral blood samples were collected from healthy volunteers into heparinized vacutainers. Blood samples, suspended in RPMI 1640 medium and supplemented with 10% FBS, were treated with 0.5 - 1.5 μ M Roy-Bz, 1 μ g/mL CP (positive control; Sigma-Aldrich) (or DMSO only) for 44 h. Cells were thereafter treated with 3 μ g/mL cytochalasin B (Sigma-Aldrich) for 28 h. Lymphocytes were isolated by density gradient separation (Histopaque-1077 and -1119; Sigma-Aldrich), fixed in methanol/glacial acetic acid (3:1), and stained with Wright stain (Sigma-Aldrich). For each sample, 1000 binucleated lymphocytes were blindly scored using a Nikon AlphaPhotoF2 YS2 light optical microscope; the number of micronuclei per 1000 binucleated lymphocytes was recorded.

2.24. *In vivo* antitumor and toxicity assays

Animal experiments were conducted according to the EU Directive 2010/63/EU and the National Authorities. Female BALB/c nude mice with about 14 weeks of age and 20 g of body weight, and male Wistar rats with about 12 weeks of age and 300 g of body weight were purchased from Charles-River Laboratories. All mice were randomly housed (3 mice per cage) under pathogen free conditions in individual ventilated cages (standard 12 h light/12 h dark cycle at 22°C). Mice were given ad libitum water and food for 7 days prior to experimentation. For the toxicity assays, Wistar rats were treated with 10 mg/kg Roy-Bz, vehicle, or saline solution (control) by intraperitoneal injection, twice a week during two weeks. Samples of blood and organs (heart, liver, kidney and spleen) were then collected for toxicological analysis. Each group was composed of four animals. Xenograft tumor assays were performed with HCT116 cells stably transfected with control pSUPER plasmid or pSuperPKC δ -RNAi. Briefly, 1×10^6 cells (in PBS) were inoculated subcutaneously in the dorsal flank of mice. Tumor dimensions were assessed by caliper measurement and their volumes were calculated [tumor volume=(L \times W²)/2; L and W represent the longest and shortest axis of the tumor, respectively]. Treatment was started when tumors reached a volume of about 100 mm³ (which occurred 14 days after the grafts). Mice were treated twice a week for two weeks with 10 mg/kg Roy-Bz or vehicle by intraperitoneal injection. Tumor volumes and body weights were monitored twice a week until the end of the treatment. Animals were sacrificed by cervical dislocation at the end of the study, when tumors reached about 1500 mm³, or the animals present any signs of morbidity. Each group was composed of six animals.

2.25. Immunohistochemistry assay

Tumor tissues were fixed in 10% formalin, embedded in paraffin, sectioned at 4 μm , and stained with hematoxylin and eosin (H&E) or antibodies, following standard methodologies. Briefly, after deparaffination and rehydration, antigen retrieval was performed by boiling the sections, for 20 min, in 10 mM citrate buffer (pH 6.0) for all antibody's staining, with the exception of anti-VEGF, for which the tissue was treated with 10 mM EDTA buffer (pH 8.0). Slices were then held for 20 min at room temperature. After dewaxing, and blocking the endogenous peroxidases with UltraVision Hydrogen Peroxide Block, sections were treated with UltraVision Protein Block solution, both from Lab Vision Thermo Scientific (Grupo Taper SA). Incubation with primary antibodies for Ki-67, VEGF, and GLUT1 (see Appendix, Table 2) was performed for 2 h at room temperature, and for BAX, caspase-3, HK2, MCT4 and TIGAR (see Appendix, Table 2) overnight at 4°C. Immunostaining was carried out using the *UltraVision Quanto Detection System HRP DAB Kit* (Lab Vision Thermo Scientific), according to the manufacturer's instructions. Tissue sections were counterstained with Gill's heamatoxylin (Lab Vision Thermo Scientific), dehydrated, clarified and mounted. The primary antibody was replaced by 10% non-immune serum for negative controls. Images were obtained using an Eclipse E400 fluorescence microscope (Nikon) with 200 \times magnification, with Digital Sight camera system (Nikon DS-5Mc) and software Nikon ACT-2U.

2.26. TUNEL assay

The analysis of DNA fragmentation was performed using the *In Situ Cell Death Detection Kit Fluorescein* (Roche Diagnostics), according to the manufacturer's instructions. Briefly, after deparaffination and rehydration, tissues sections were treated for 20 min in 10 mM citrate buffer (pH 6.0), and incubated with TUNEL Reaction Mixture for 60 min at 37°C in the dark. Tissues were counterstained with 0.1 $\mu\text{g}/\text{mL}$ DAPI. Images were obtained using an Eclipse E400 fluorescence microscope (Nikon) with 200 \times magnification, with Digital Sight camera system (Nikon DS-5Mc) and software Nikon ACT-2U.

2.27. Tandem resazurin/SRB assay

HCT116 cells were seeded in 96-well plates, at a final density of 4.5×10^3 cells/well, for 24 h. Cells were thereafter treated with 1.5 - 4 μM Roy-Bz (or DMSO only) for 48 h, in normoxic conditions (99% O_2). Briefly, after treatments, the medium was removed and cells

were incubated with 1 $\mu\text{g}/\text{mL}$ resazurin solution for 30 min as described (299). Metabolic activity was determined based on the reduction of resazurin to resorufin by the dehydrogenases present in viable cells, and subsequent resorufin fluorescence measurement at 540/590 nm (ex/em) in a microplate reader at 30, 60, 240 and 360 min, and expressed in relative fluorescence units (rfu's). After resazurin assay, the solution was removed, cells were fixed with 10% TCA, and the cell mass was determined by the SRB assay as described in 2.11. The maximum concentration of solvent used in this assay (0.25% DMSO) was included as control, and the values obtained were set as 100%. Data were expressed as percentage of vehicle.

2.28. Cellular oxygen consumption measurements

The oxygen consumption rate (OCR) was analysed by the Agilent Seahorse XF Cell Mito Stress Test (Agilent Technologies, Soquímica, Lisboa, Portugal) using a Seahorse XF[®]96 Extracellular Flux Analyzer (Seahorse Bioscience, Germany), and according to the manufacturer's instructions. Briefly, HCT116 cells were seeded in Seahorse XF cell culture microplate, at a final density of 2.5×10^4 cells/well in D5030 medium with 5 mM glucose, 4 mM L-glutamine, 1 mM sodium pyruvate, 21 mM sodium bicarbonate, and supplemented with 10% FBS (pH 7.4), for 24 h. Thereafter, cells were treated with 1.5 - 4 μM Roy-Bz, for 48 h in normoxic conditions. XF[®]96 sensor cartridge for each cell plate was placed in a 96-well calibration plate containing 200 μL /well calibration buffer and left to hydrate overnight at 37°C. After treatments, the culture medium was removed, replaced by pre-warmed XF Cell Mito Stress Test Assay medium, consisting of D5030 with 5 mM glucose, 4 mM L-glutamine, 1 mM sodium pyruvate, and without FBS (adjusted pH to 7.4 with 1N NaOH), and incubated at 37°C for 1h. The compounds (oligomycin, carbonyl cyanide-4-(trifluoromethoxy)phenylhydrazone (FCCP), and the mix of rotenone and antimycin A) provided by the Seahorse XF Cell Mito Stress Test Kit were reconstituted with the previously prepared assay medium. For OCR measurements, XF[®]96 sensor cartridge was pre-loaded with 1 μM oligomycin into reagent delivery port A, 0.5 μM FCCP into port B, and 1 μM rotenone/1 μM antimycin A mix into reagent delivery port C. Oligomycin, FCCP, and the mix of rotenone and antimycin A, were then pneumatically injected by the XF[®]96 Analyzer into each well, with measurement of OCR using a 3 min mix, 5 min measure cycle. Results were analyzed using the Software Version Wave Desktop 2.2.

2.29. Flow cytometric data acquisition and analysis

The Accuri™ C6 flow cytometer and the CellQuest software from BD Biosciences (Enzifarma, Porto, Portugal) were used. The FlowJo software was used to identify and quantify cell cycle phases.

2.30. Statistical analysis

Data are presented as mean \pm SEM of 'n' samples, where 'n' refers to independent experiments, not replicates. Data analyses were carried out using GraphPad Prism Software version 6.0. For comparison of two groups, unpaired student's *t*-test was used; statistical significance was set as * $p < 0.05$; ** $p < 0.01$; *** $p < 0.001$. For comparison of multiple groups statistical analysis relative to controls was performed using the two-way analysis of variance (ANOVA).

CHAPTER 3

Results

Identification of PKC isozyme-selective agents and anticancer drugs

CHAPTER 3.1

Discovery of a small-molecule protein kinase C δ -selective activator with promising application in colon cancer therapy

Bessa, C., Soares, J., Raimundo, L., Loureiro, J.B., Gomes, C., Reis, F., Soares, M.L., Santos, D., Dureja, C., Chaudhuri, S.R., Lopez-Haber, C., Kazanietz, M.G., Gonçalves, J., Simões, M.F., Rijo, P., Saraiva, L.

***Cell Death Dis.* 2018 Jan; 9:23**

Doi: 10.1038/s41419-017-0154-9

Based on the previous identification of coleon U (an abietane diterpene compound isolated from *P. grandidentatus*), described as selective activator of nPKC δ and ϵ (275), it was obtained a small library of royleanone derivatives. This library was composed by the natural diterpenoid, 7 α -acetoxy-6 β -hydroxyroyleanone (Roy; Fig. 3.1.1A), and the semi-synthetic derivatives, 7 α -acetoxy-6 β -propionyloxy-12-O-propionyroyleanone (Roy-Pr2; Fig. 3.1.1B), and 7 α -acetoxy-6 β -benzoyloxy-12-O-benzoylroyleanone (Roy-Bz; Fig. 3.1.1C). The ability of these compounds to activate PKC isoforms from classical (α and β I), novel (δ and ϵ) and atypical (ζ) subfamilies was studied using a previously developed yeast PKC screening assay (275). In this assay, PKC activators induce a significant growth inhibition in mammalian PKC-expressing yeast, which is proportional to the degree of PKC activation, having no effect on control yeast (empty vector) (275).

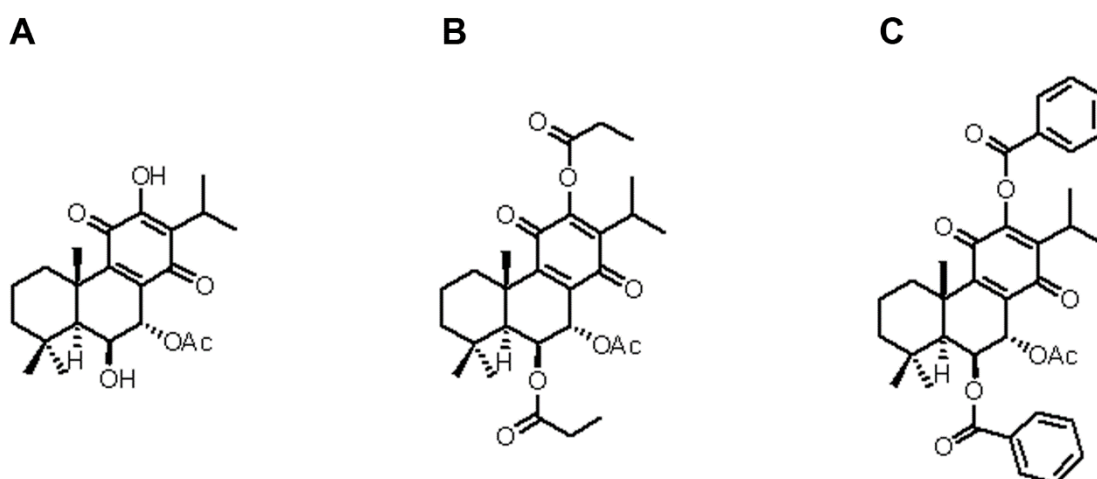


Figure 3.1.1: Schematic representation of royleanone structures. (A) 7 α -acetoxy-6 β -hydroxyroyleanone; **(B)** 7 α -acetoxy-6 β -propionyloxy-12-O-propionyroyleanone; **(C)** 7 α -acetoxy-6 β -benzoyloxy-12-O-benzoylroyleanone.

3.1.1. Effect of compounds on yeast growth

Using the yeast PKC assay, the inhibitory effect of 0.1 - 30 μ M PMA (an established activator of cPKCs and nPKCs), ARA (activator of cPKCs, nPKCs and aPKC ζ), Roy, Roy-Pr2 or Roy-Bz on the growth of yeast expressing individual PKC isoforms was analyzed. From the dose-response curves obtained, they were determined the EC₅₀ values for the tested compounds (Table 3.1.1) and their selectivity for the different PKC isoforms was evaluated. The results obtained showed that the natural diterpene Roy activated all PKC

isozymes with the exception of PKC δ , the derivative Roy-Pr2 activated cPKCs and nPKCs with a similar pharmacological profile to PMA, and the compound Roy-Bz selectively activated PKC δ with a higher potency than the standard activator, PMA (Table 3.1.1). Altogether, these results indicate that promising modulators of PKC with high potency and isozyme-selectivity may emerge from the exploitation of this family of compounds.

Table 3.1.1. EC₅₀ values of compounds tested on individual PKC isozymes.

Compounds	EC ₅₀ (nM)				
	PKC α	PKC β I	PKC δ	PKC ϵ	PKC ζ
PMA	111,6 \pm 18,4	243,2 \pm 69,1	573,8 \pm 36,7	1678 \pm 46,48	-
ARA	-	-	-	-	205,4 \pm 32.6
Roy	350 \pm 42	423 \pm 67	<i>ND</i>	994 \pm 63	4113 \pm 159
Roy-Pr2	195 \pm 16	229 \pm 21	325 \pm 49	770 \pm 46	<i>ND</i>
Roy-Bz	<i>ND</i>	<i>ND</i>	107 \pm 53	<i>ND</i>	<i>ND</i>

EC₅₀ values were considered the concentration of compound that caused 50% of the maximal growth inhibition caused by the positive controls (PMA, for cPKCs and nPKCs; ARA, for PKC ζ), which was set as 100%. Data are mean \pm SEM of four independent experiments. -, not tested; *ND*, non-determinable (when the maximal response achieved was lower than 50% growth inhibition).

Based on the results obtained in yeast, the compound Roy-Bz was selected for further studies in order to confirm its selectivity for PKC δ and to study its anticancer activity.

3.1.2. Roy-Bz is a selective activator of PKC δ that binds to the C1-domain

As previously referred, using the yeast PKC assay, it was observed that whereas 0.1 - 30 μ M PMA inhibited the growth of yeast expressing cPKCs (α and β I) and nPKCs (δ and ϵ), 0.1 - 30 μ M Roy-Bz only inhibited the growth of PKC δ -expressing yeast without significant effects on yeast expressing other PKCs (Fig. 3.1.2A). Interestingly, in PKC δ -expressing yeast, while PMA-induced growth inhibition was associated with G2/M-phase cell cycle arrest, Roy-Bz-induced growth inhibition was mediated by apoptotic cell death, as demonstrated by the increase in DNA fragmentation with preservation of plasma membrane integrity (Fig. 3.1.2C, D). Additionally, Roy-Bz-induced growth inhibition was completely

abolished in yeast expressing a PKC δ in which the C1-domain has been deleted (Δ C1-PKC δ ; Fig. 3.1.2B) (Fig. 3.1.2A). In fact, a similar result was obtained with PMA, which is known to bind PKCs at the C1-domain (Fig. 3.1.2A). These results indicate that Roy-Bz is a PKC δ -selective activator and, like PMA, it should have the C1-domain as the predicted binding site.

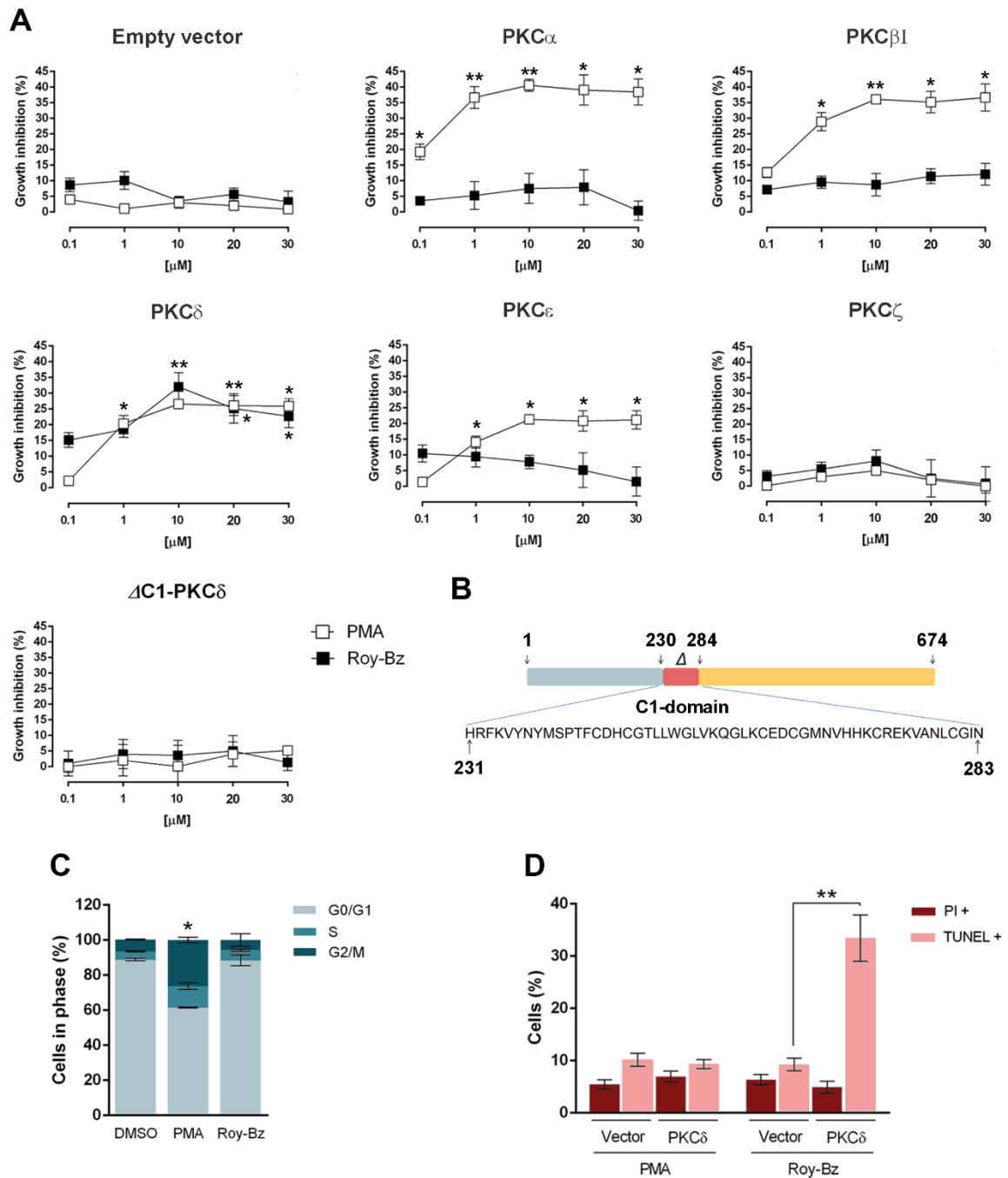


Figure 3.1.2: Roy-Bz selectively activates PKC δ in yeast and induces an apoptotic cell death.

(A) Dose-response curves for the inhibitory effect of PMA and Roy-Bz on the growth of yeast

expressing mammalian PKC isozymes and control yeast (empty vector), for 42 h treatment; growth of yeast incubated with vehicle was set as 100%. **(B)** Schematic representation of deletion of C1-domain at amino acids 231-283 in the *PRKCD* gene. **(C,D)** Effect of 10 μ M PMA and Roy-Bz on **(C)** cell cycle progression, and **(D)** DNA fragmentation (TUNEL+)/loss of plasma membrane integrity (PI+) of PKC δ -expressing yeast (and control yeast in **D**), for 42 h treatment. In **A**, **C** and **D**, data are mean \pm SEM of five independent experiments; values significantly different from control yeast **(A,D)** or vehicle **(C)**: * p <0.05, ** p <0.01, unpaired Student's *t*-test.

To confirm the PKC isozyme selectivity observed in the yeast assay, we next performed an *in vitro* kinase assay using recombinant human cPKCs (a mix of PKC α , β and γ), nPKC δ , nPKC ϵ , and aPKC ζ . All recombinant PKCs were effectively activated at 10^{-4} μ M PMA/ARA (positive controls: PMA for cPKCs and nPKCs; ARA for aPKC ζ) (Fig. 3.1.3A). Remarkably, 10^{-7} - 10^{-3} μ M Roy-Bz only increased the activity of PKC δ (Fig. 3.1.3B). Roy-Bz activated PKC δ with an EC $_{50}$ (concentration required to induce 50% effect) value of 58.8 ± 3.6 nM ($n=5$), similar to that of PMA (61.9 ± 4.3 nM, $n=5$). Thus, the *in vitro* kinase assays, in accordance with the yeast assays, revealed a remarkable selectivity of Roy-Bz for PKC δ . Besides, these results show that Roy-Bz is as effective as PMA to activate PKC δ .

Next, the potential binding mode of Roy-Bz to PKC δ was explored by molecular docking studies (Fig. 3.1.3C, D). Like PRB (positive control), which establishes direct strong hydrogen bond interactions with *Gly253* and *Thr242* (hydrogen bond donors), and *Leu251* (hydrogen bond acceptor) in the C1-domain of PKC δ , Roy-Bz also interacted with *Gly253* and *Thr242*, but exchanged *Leu251* with *Gln257*, all acting as hydrogen donors to carbonyl oxygen functional groups. It is interesting to note that like in the case of PRB, these interactions also stabilized the molecule from both sides of the cleft. The estimated autodock free energy of binding for PRB was -7.54 kcal/mol and for Roy-Bz was -7.87 kcal/mol, and a clustering analysis of the molecular docking results showed other three poses similar to the top-ranked (the most populated one; in a total of 10 poses and 6 different clusters). These predicted binding models support the Roy-Bz binding to the PKC δ -C1-domain.

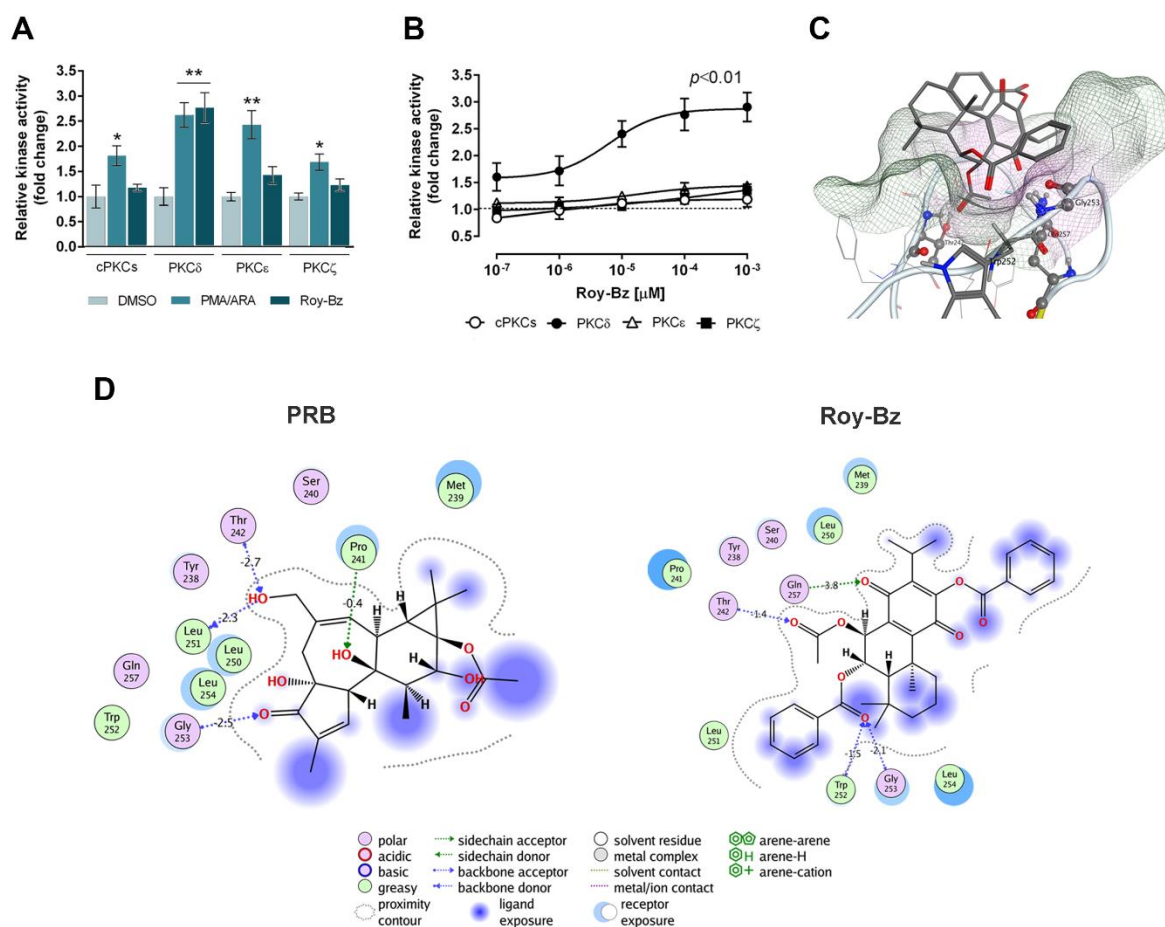


Figure 3.1.3: Roy-Bz selectively activates PKC δ through binding to the C1-domain. (A,B) *In vitro* kinase assay with recombinant PKCs; **(A)** increase of PKC activity by 10^{-4} μ M PMA/ARA and 10^{-4} μ M Roy-Bz; **(B)** dose-response curves for the increase of PKC activity by Roy-Bz; kinase activity of endogenous PKC activator phosphatidylserine was set as 1. In **A**, data are mean \pm SEM of five independent experiments; values significantly different from vehicle: * p <0.05, ** p <0.01, unpaired Student's *t*-test; in **B** two-way analysis of variance (ANOVA) (p <0.01). **(C,D)** Molecular docking studies for Roy-Bz interaction with the C1-domain of PKC δ . **(C)** Top ranked docking pose of Roy-Bz with *Gly253*, *Thr242* and *Gln257* highlighted through a CPK representation. The hydrogen bonds between Roy-Bz and these residues are also displayed through a dotted blue line. The interaction between the alpha-hydrogen of *Trp252* and the carbonyl (CH \cdots O) is also represented and the residue is highlighted in licorice. All residues within 4.5 Å of Roy-Bz are represented and the molecular surface of the pocket is displayed through a mesh that changes from green in lipophilic regions to pink (hydrophilic). **(D)** Scheme of PRB and Roy-Bz interactions. The pocket proximity contour is represented by grey dotted lines, the ligand exposure is depicted in violet and the receptor exposure in blue. Direct interactions are represented by a dotted or green line along with the interaction energy (kcal/mol) estimated by MOE.

The translocation of PKC from the cytosol to membranes, either plasma membrane or internal membranes, is a well-known hallmark of PKC activation (83, 212). As such, we evaluated the impact of Roy-Bz on the translocation of PKC α , PKC δ and PKC ϵ in human HCT116 colon cancer cells using GFP-fused PKCs (Fig. 3.1.4A, B). As previously reported in LNCaP prostate cancer cells (300), also in HCT116 cells the treatment with PMA triggered the subcellular redistribution of the three PKC isozymes. There was a clear translocation to the plasma membrane for PKC α , PKC δ and PKC ϵ , and as reported in other models (300), PKC δ also translocated to a perinuclear compartment. When we assessed the ability of Roy-Bz to translocate PKCs, there were obvious differences with regard to PMA. Indeed, Roy-Bz was unable to translocate PKC α or PKC ϵ , while it selectively translocated PKC δ to the perinuclear region (Fig. 3.1.4A, B). A dose-dependent analysis of PKC δ translocation in HCT116 cells revealed an EC₅₀ value of $0.19 \pm 0.07 \mu\text{M}$ ($n=3$). Thus, these results reinforce those previously obtained and further demonstrate the selectivity of Roy-Bz for PKC δ .

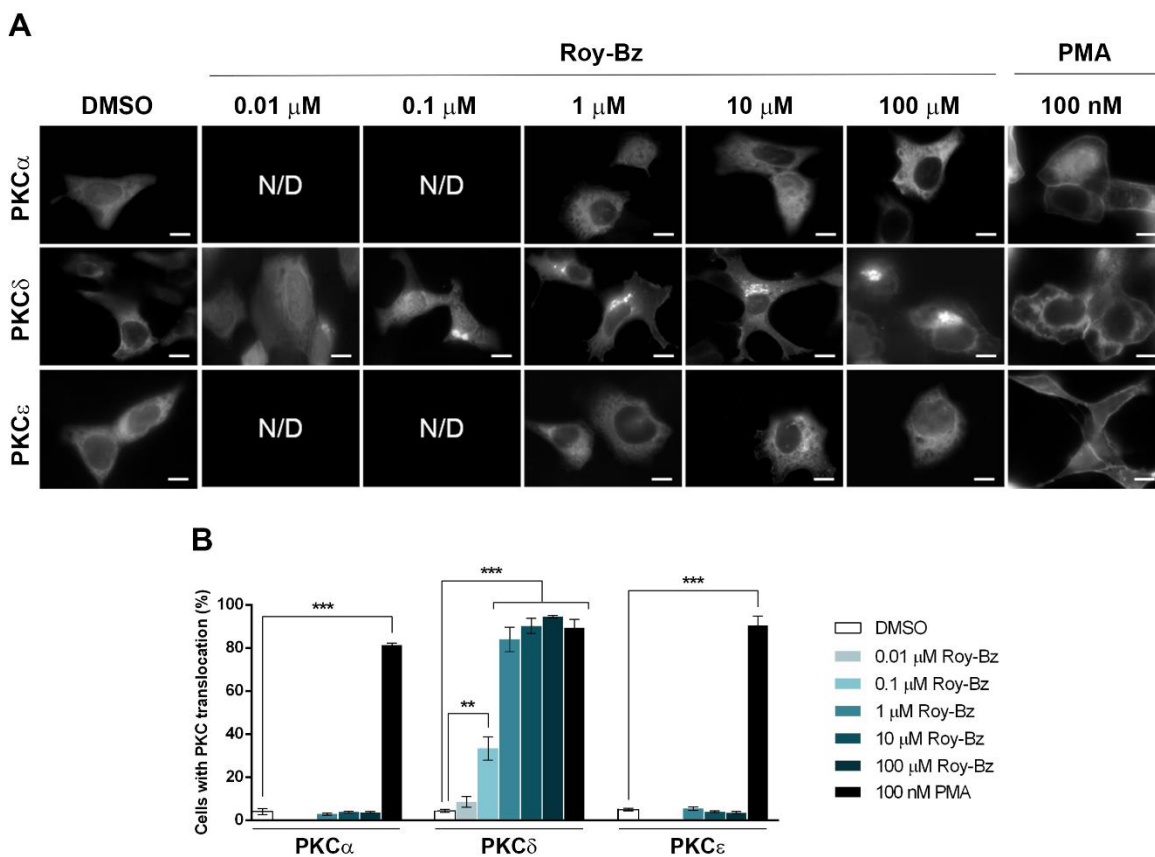


Figure 3.1.4: Roy-Bz selectively translocates PKC δ to the perinuclear region in human tumor cells. HCT116 cells transfected with pEGFP-N1-PKC α , pEGFP-N1-PKC δ , or pEGFP-N1-PKC ϵ were

treated with PMA, Roy-Bz, or vehicle for 1 h; PKC localization was determined by confocal microscopy. **(A)** Images are representative of three independent experiments; scale bar=10 μm and magnification=100 \times . **(B)** Quantification of cells with PKC translocation; data are mean \pm SEM of three independent experiments; values significantly different are indicated (** $p < 0.001$), unpaired Student's *t*-test.

3.1.3. Roy-Bz inhibits the proliferation of colon cancer cells

The effect of Roy-Bz on proliferation of human colorectal cancer cells was evaluated using the SRB assay (Fig. 3.1.5A, B). Treatment of HCT116, HT-29 and SW-837 cells (with similar PKC δ expression levels; see Appendix, Fig. 3) with Roy-Bz for 48 h resulted in a dose-dependent inhibition of cell growth (IC_{50} values of $0.58 \pm 0.05 \mu\text{M}$ for HCT116, $1.50 \pm 0.06 \mu\text{M}$ for HT-29, and $1.08 \pm 0.03 \mu\text{M}$ for SW-837; $n=5$). The pronounced inhibitory effect of Roy-Bz on cell proliferation/viability of colorectal cancer cells was further demonstrated by assessing the colony forming ability (Fig. 3.1.5C). In fact, even in the most resistant SW-837 cells, $0.3 \mu\text{M}$ Roy-Bz reduced the colony forming ability $\sim 75\%$ relative to vehicle.

Interestingly, while in HT-29 and SW-837 cells the Roy-Bz growth inhibitory effect was associated with G2/M-phase cell cycle arrest (Fig. 3.1.5D; particularly pronounced in HT-29) and apoptosis (Fig. 3.1.5E), in HCT116 cells the Roy-Bz-induced growth inhibition was only mediated by apoptosis. In fact, Roy-Bz had no effect on cell cycle progression (Fig. 3.1.5D; similar results were obtained for 8, 16 and 48 h treatment, data not shown) and markedly increased Annexin V-positive cells (Fig. 3.1.5E). Conversely, in HCT116 cells, PMA, with an IC_{50} value about 14-fold higher than that of Roy-Bz ($7.83 \pm 1.67 \mu\text{M}$, $n=5$; Fig. 3.1.5A), inhibited cell growth through induction of S-phase cell cycle arrest and apoptosis (see Appendix; Fig. 4). Additionally, in HCT116 cells, the induction of apoptosis by Roy-Bz was further reinforced by the occurrence of caspase-3 and PARP cleavage, an increase in pro-apoptotic p53 and BAX levels, and a reduction in the levels of anti-apoptotic proteins Bcl-2 and survivin (Fig. 3.1.5F, G).

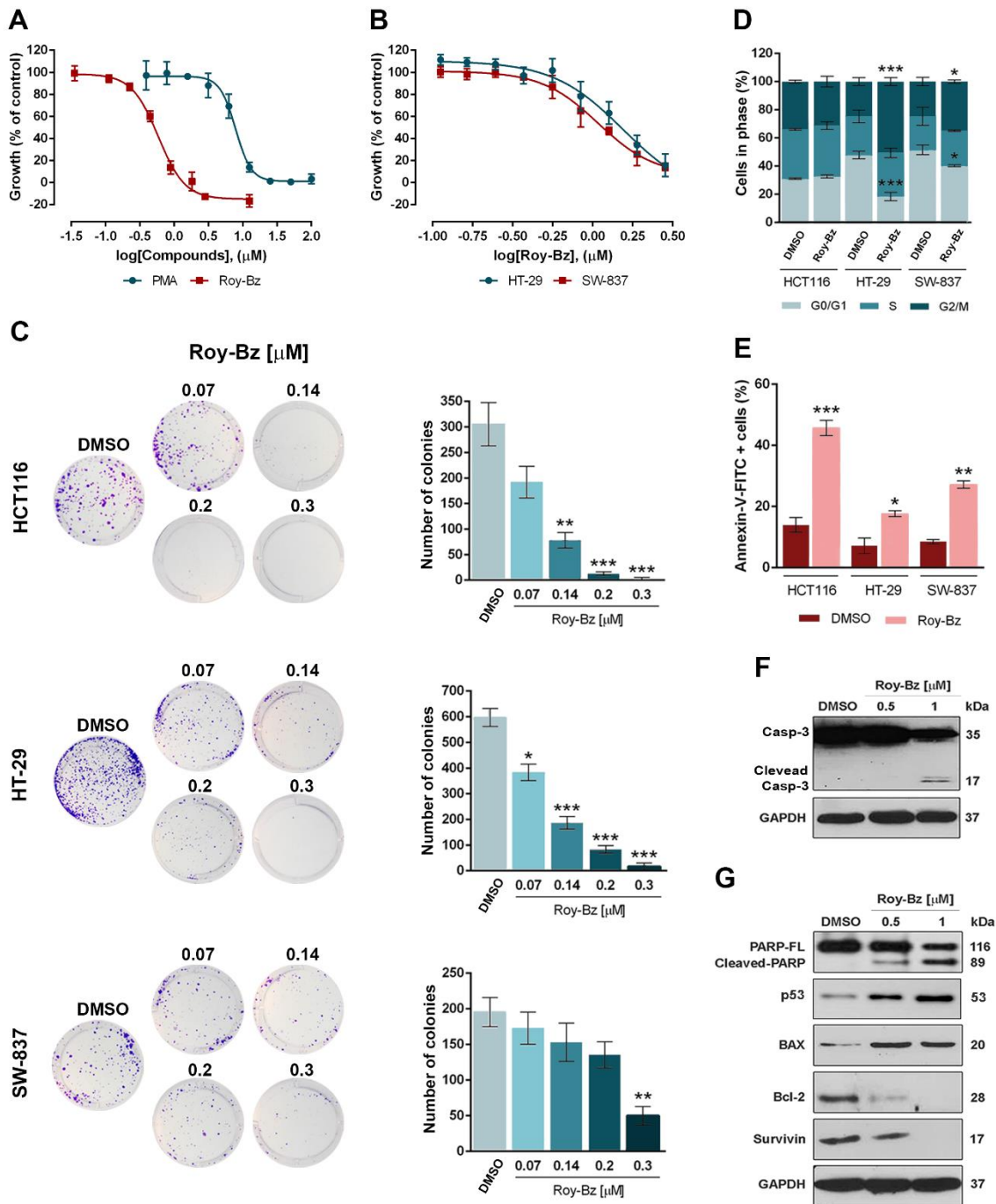


Figure 3.1.5: Roy-Bz inhibits the growth of colon cancer cells. (A,B) Dose-response curves for the growth of (A) HCT116, (B) HT-29 and SW-837 cells treated with 0.11 - 10 μM Roy-Bz or PMA for 48 h; data are mean \pm SEM of five independent experiments; growth obtained with vehicle was set as 100%. (C) Colony formation assay for HCT116, HT-29 and SW-837 cells treated with Roy-Bz; images correspond to a representative experiment of four; graphs represent mean \pm SEM of four independent experiments. (D) Cell cycle arrest, and (E) Annexin V-positive cells were determined for 24 h treatment with 1 μM Roy-Bz; data are mean \pm SEM of four independent experiments. (F,G) Western blot analysis of (F) caspase-3 and (G) PARP cleavage, BAX, p53, Bcl-2, and survivin expression levels, for 24 h treatment with Roy-Bz in HCT116 cells. In F and G immunoblots represent

one of three independent experiments; GAPDH was used as loading control. In **C**, **D** and **E**, values significantly different from vehicle ($*p<0.05$, $**p<0.01$, $***p<0.001$), unpaired Student's *t*-test.

In an attempt to explore the antitumor activity of Roy-Bz in a system that more closely resembles the *in vivo* features of the tumor microenvironment and is highly enriched in a small population of CSCs, a colonosphere culture model was generated from HCT116 cells. In fact, the spheroid-formation (colonosphere) assay is recognized as a valuable tool for assessment and expansion of stem cells in colon cancer (301). In addition, according to several studies, colon CSCs can mainly be identified by the expression of cell biomarkers, such as CD44 and ALDH (302-305). Actually, a positive correlation between the CD44 decrease and the therapeutic response of patients with colorectal cancer has been recently identified (304, 305). To test the effect of Roy-Bz in colonosphere growth, 3-day-old spheroids were treated with Roy-Bz for up to 96 h (Fig. 3.1.6A). A significant reduction in colonosphere diameter by Roy-Bz relative to vehicle was observed both at 72 h (at 3 and 3.5 μM) and 96 h (at 2 - 3.5 μM). Accordingly, 3.5 μM Roy-Bz markedly reduced the expression levels of the stemness markers CD44 and ALDH2 after 96 h treatment (Fig. 3.1.6B). Of note, a pronounced reduction of matrix metalloproteinase-9 (MMP-9) and increase of E-cadherin, prominent players in extracellular matrix homeostasis and metastasis (73), were also observed under these treatment conditions (Fig. 3.1.6B). The effectiveness of Roy-Bz in colonosphere formation was also checked by evaluating the colonosphere diameter after 48 h treatment with Roy-Bz added at the seeding time of HCT116 cell suspension (Fig. 3.1.6C). The results showed a notable dose-dependent reduction in colonosphere formation ability by Roy-Bz, with an abolishment of colonosphere formation at 1 μM Roy-Bz. Altogether, these results evidence a potent inhibitory activity of Roy-Bz in the growth of colon cancer cells, including in CSCs, suggesting a potential effect of the drug against cancer chemoresistance, dissemination and recurrence.

3.1.4. Roy-Bz pro-apoptotic and anti-migratory activity in HCT116 cancer cells is mediated by PKC δ -selective activation

To evaluate the involvement of PKC δ in Roy-Bz-induced apoptosis, a PKC δ stable knockdown model was generated upon transfection of the metastatic colon cancer HCT116 cells with a PKC δ RNAi plasmid. As control, we used HCT116 cells transfected with non-target control RNAi. PKC δ silencing was confirmed by Western blot (see Appendix, Fig. 2). The impact of 0.1 - 6 μM Roy-Bz on the viability of PKC δ -depleted and control HCT116 cells

was thereafter evaluated by a trypan blue assay. As shown in Fig. 3.1.7A, silencing PKC δ decreased Roy-Bz-induced cell death compared to control HCT116 cells. Accordingly, the depletion of PKC δ in HCT116 cells abolished Roy-Bz-induced Annexin V-positive cells (Fig. 3.1.7B), PARP cleavage, and increase of BAX and p53 expression levels (Fig. 3.1.7C).

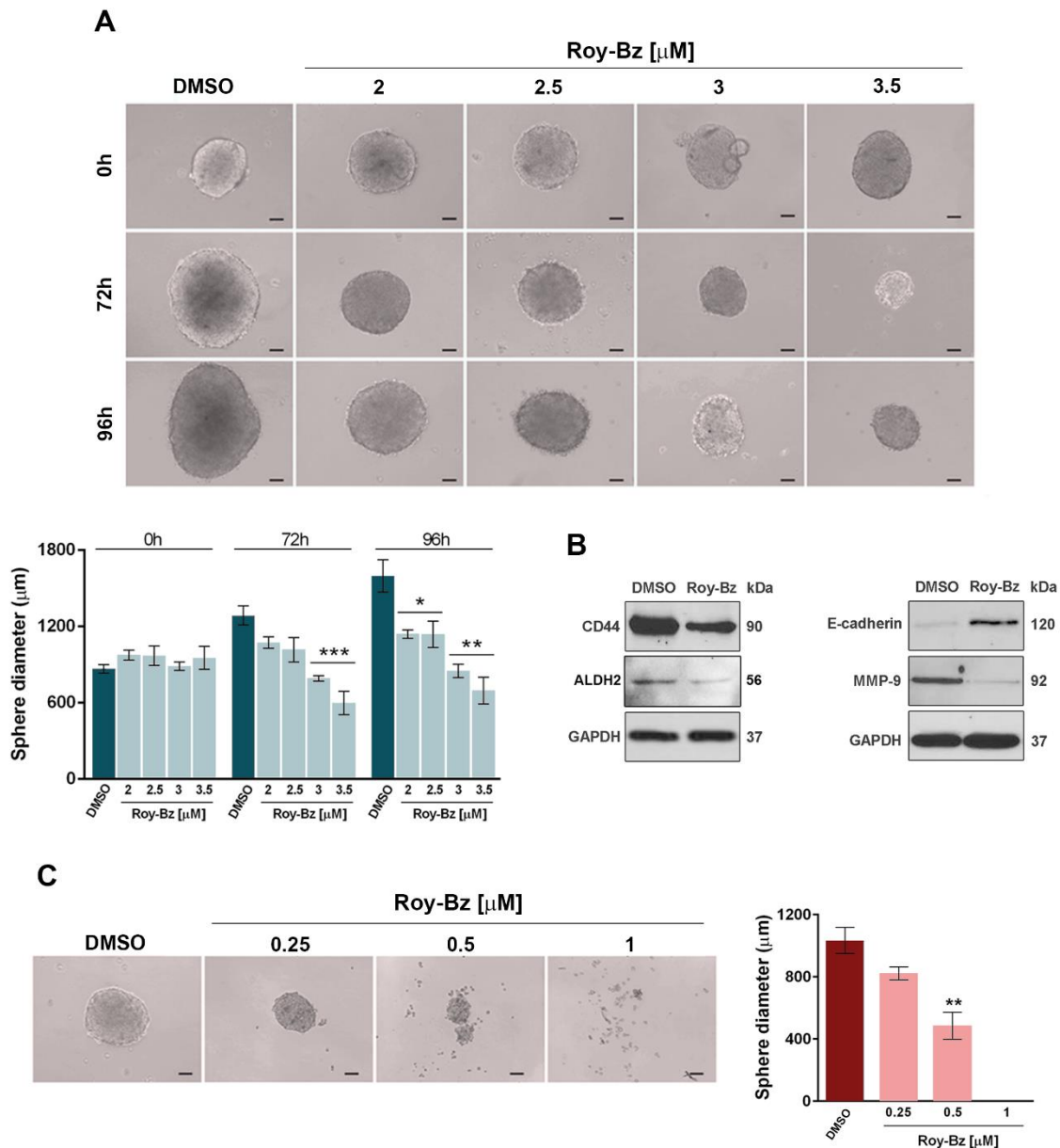


Figure 3.1.6. Roy-Bz inhibits the growth of colonospheres. (A) Evaluation of 3-day-old HCT116 spheroids diameter for 72 and 96 h treatment with Roy-Bz or vehicle. **(B)** CD44, ALDH2, E-cadherin and MMP-9 expression levels for 96 h treatment with 3.5 μ M Roy-Bz. **(C)** Evaluation of spheroids diameter formed after 48 h treatment of seeded HCT116 cells with Roy-Bz or vehicle. In **B** immunoblots represent one of three independent experiments; GAPDH was used as loading control. In **A** and **C**, brightfield imaging of spheroids (scale bar=50 μ m, magnification=100x); graphs

represent mean \pm SEM of four independent experiments; values significantly different from vehicle ($*p < 0.05$, $**p < 0.01$, $***p < 0.001$), unpaired Student's *t*-test.

It has been previously established in certain cellular models that PKC δ undergoes a proteolytic cleavage by caspases that generates a catalytically active fragment, termed PKC δ -CF (116, 306). Interestingly, we found that in HCT116 cells, Roy-Bz caused a time-dependent increase in PKC δ -CF levels, without a visible interference in total PKC δ expression levels (Fig. 3.1.7D). Additionally, since it was previously reported that activation of PKC δ is a required factor for histone H3 phosphorylation on Ser-10 (pSer-10 histone H3), which is a crucial event in apoptosis (307), we next assessed the effect of Roy-Bz on pSer-10 histone H3 levels in HCT116 cells. To this end, HCT116 cells were synchronized in G1-phase by hydroxyurea, in order to exclude mitotic pSer-10 histone H3, followed by treatment with 1 μ M Roy-Bz for up to 8 h. We observed that 1 μ M Roy-Bz caused a pronounced increase of pSer-10 histone H3 levels that was noticeable at 8 h. This effect was abolished by PKC δ -knockdown (Fig. 3.1.7E, F), again reinforcing the concept that Roy-Bz is a potent inducer of apoptotic cancer cell death via activation of PKC δ .

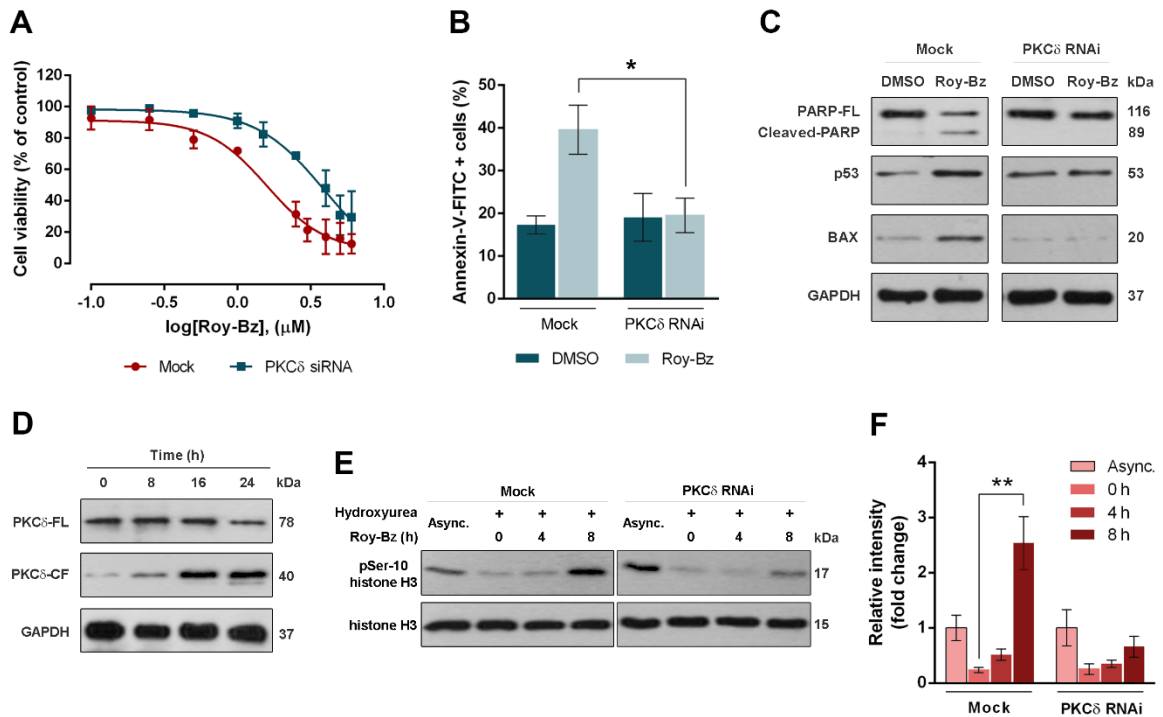


Figure 3.1.7: Roy-Bz pro-apoptotic activity is mediated by PKC δ -selective activation in HCT116 cancer cells. (A) Cell viability dose-response curves were determined by trypan blue assay

for control (Mock) and PKC δ -knockdown (PKC δ RNAi) HCT116 cells treated with 0.1-6 μ M Roy-Bz for 24 h; cell viability of vehicle was set as 100%. **(B)** Annexin V-positive cells were determined in control and PKC δ -knockdown HCT116 cells after 24 h treatment with 1 μ M Roy-Bz or vehicle. **(C)** Western blot analysis of PARP cleavage, p53 and BAX expression levels for 16 h treatment with 1 μ M Roy-Bz or vehicle in control and PKC δ -knockdown HCT116 cells; GAPDH (loading control). **(D)** Western blot analysis of full-length PKC δ (PKC δ -FL) and cleaved PKC δ -CF in HCT116 cells treated with 1 μ M Roy-Bz for up to 24 h; GAPDH (loading control). **(E,F)** Levels of histone H3 phosphorylation on Ser-10 (pSer-10) in control and PKC δ -knockdown HCT116 cells treated with 1 μ M Roy-Bz for up to 8 h; histone H3 (loading control); in **F**, quantification of pSer-10 levels normalized to histone H3, values of asynchronous cells were set as 1. In **C**, **D** and **E**, immunoblots represent one of three independent experiments; in **A**, **B** and **F**, data are mean \pm SEM of three independent experiments; values significantly different are indicated ($*p<0.05$, $**p<0.01$), unpaired Student's *t*-test.

The impact of Roy-Bz on MMP-9 and E-cadherin expression levels in colonosphere cultures led us to further investigate the effect of Roy-Bz on the migration of HCT116 cells and its dependence on PKC δ . Using a wound healing assay, we found that Roy-Bz caused a pronounced inhibition of migration. Notably, the inhibitory effect of Roy-Bz was not observed in HCT116 cells subject to PKC δ -knockdown (Fig. 3.1.8A, B). It is important to note that at the concentration of Roy-Bz used in these assays (0.25 μ M), there were no significant effects on cell viability. These results were also recapitulated using a chemotaxis cell migration assay, in which the anti-migratory effect of Roy-Bz observed in control HCT116 cells was significantly prevented by RNAi silencing of PKC δ expression (Fig. 3.1.8C). Altogether, these results showed that Roy-Bz is a potent pro-apoptotic and anti-migratory agent in human colon cancer cells through PKC δ -selective activation.

3.1.5. Roy-Bz is non-genotoxic in human cancer and normal cells and has *in vivo* PKC δ -dependent antitumor activity with no apparent toxic side effects

The genotoxicity of Roy-Bz in human cancer cells was evaluated by checking comet-positive cells and histone H2AX phosphorylation on Serine-139 (γ H2AX) as markers of DNA damage (single/double-strand breaks). Our results showed that, conversely to 25 μ M ETOP (positive control), 48 h treatment with Roy-Bz failed to induce DNA damage in HCT116 cells, as demonstrated by the negligible number of cells with more than 5% of DNA in tail (Fig. 3.1.9A, B), by the low tail moment (Fig. 3.1.9A, C), as well as by the absence of increased γ H2AX levels compared to vehicle (Fig. 3.1.9D). Additionally, Roy-Bz failed to

increase the number of micronuclei in peripheral lymphocytes of normal individuals, compared to vehicle (Fig. 3.1.9E).

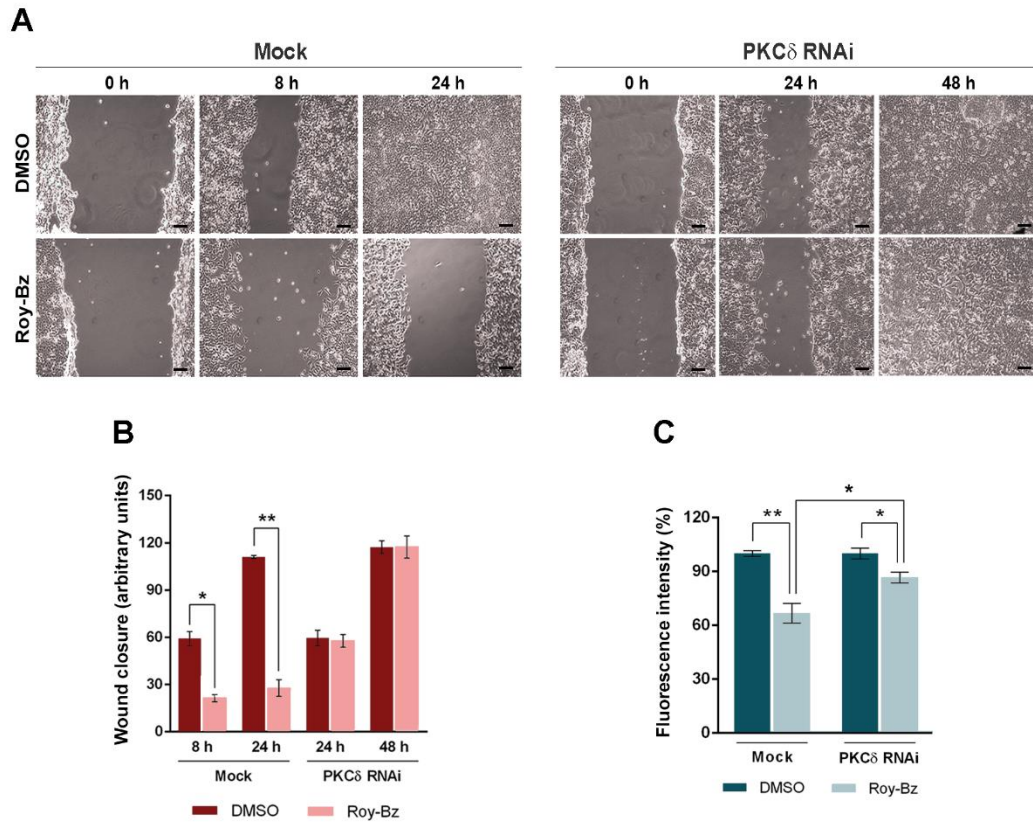


Figure 3.1.8: Roy-Bz anti-migratory activity is mediated by PKC δ -selective activation in HCT116 cancer cells. (A,B) Wound healing assay for control and PKC δ -knockdown HCT116 confluent cells treated with 0.25 μ M Roy-Bz or vehicle, at different time-points; in **A**, scale bar=50 μ m and magnification=100 \times ; in **B**, quantification of wound closure in five randomly selected microscopic fields. **(C)** Chemotaxis migration assay for control and PKC δ -knockdown HCT116 cells for 24 h treatment with 0.25 μ M Roy-Bz; migratory cells were quantified by fluorescence intensity, which was set as 100% for untreated cells. In **B** and **C**, data are mean \pm SEM of three independent experiments; values significantly different are indicated (* p <0.05, ** p <0.01), unpaired Student's t -test.

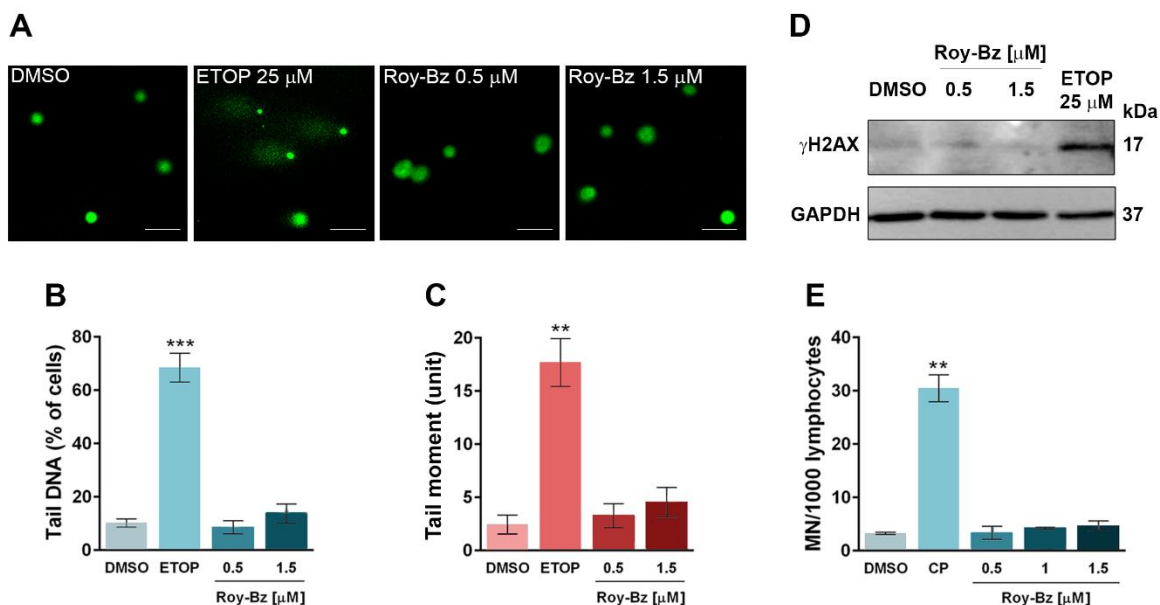


Figure 3.1.9: Roy-Bz is non-genotoxic in human cancer and normal cells. (A-D) Analysis of DNA damage was performed for 48 h treatment with ETOP, Roy-Bz or vehicle; in **(A-C)**, comet assay in HCT116 cells; in **A**, scale bar=20 μm; magnification=200x; in **B** and **C**, one hundred cells were analyzed in each group; in **D**, western blot analysis of γH2AX levels; immunoblots are representative of three independent experiments; GAPDH (loading control). **(E)** Genotoxicity of Roy-Bz evaluated by cytokinesis-block micronucleus (MN) assay for 72 h treatment, in human lymphocyte cells; 5 μg/mL CP (positive control); the number of MN per 1000 binucleated lymphocytes was recorded. In **B**, **C**, and **E**, data are mean ± SEM of three independent experiments, values significantly different from vehicle (** $p < 0.01$, *** $p < 0.001$), unpaired Student's t -test.

We next examined potential primary toxicity signs induced by Roy-Bz treatment *in vivo*. To this end, Wistar rats were treated with 10 mg/kg Roy-Bz, vehicle, or saline solution (control) by intraperitoneal injection, twice a week during two weeks, followed by analysis of organs relative weight, biochemical and hematological data (Table 3.1.2). No differences in the relative weight of liver, kidneys, heart and spleen were observed among the three groups. Regarding biochemical data, despite the slight increase in uric acid and total proteins, compared to control groups, caused by Roy-Bz, the values of both parameters are in accordance with reference database (308, 309). These results indicated no apparent liver or kidney toxicity. Additionally, no differences in hematological data were observed between the three groups. Overall, no apparent toxic side effects were observed for Roy-Bz on the tissues most commonly affected by conventional chemotherapeutics.

Table 3.1.2. Toxicity studies of Roy-Bz in Wistar rats.

	Saline	Vehicle	Treated
Body weight and relative tissue weight (trophism)			
BW (g)	340.30 ± 13.45	361.80 ± 0.01	308.25 ± 10.51
Heart/BW (g/kg)	3.03 ± 0.03	3.01 ± 0.09	3.33 ± 0.21
Liver/BW (g/kg)	38.71 ± 2,36	38.52 ± 0.89	42.06 ± 0.98
Kidney/BW (g/kg)	7.08 ± 0.40	6.81 ± 0.27	8.07 ± 0.31
Spleen (g/kg)	2.10 ± 0.20	2.15 ± 0.12	2.93 ± 0.14
Biochemical data			
Blood glucose (mg/dL)	188.00 ± 7.51	207.20 ± 7.00	155.00 ± 22.67
Urea (mg/dL)	20.67 ± 0.77	18.34 ± 0.24*	17.95 ± 0.59
Uric acid (mg/dL)	1.07 ± 0.07	0.82 ± 0.10	2.08 ± 0.45#
Creatinine (mg/dL)	0.30 ± 0.00	0.30 ± 0.01	0.29 ± 0.01
Total Proteins (g/dL)	5.50 ± 0.00	5.35 ± 0.17	6.30 ± 0.11#
Albumin (g/dL)	3.03 ± 0.03	2.90 ± 0.05	3.13 ± 0.10
ALT (U/L)	36.00 ± 2.89	30.75 ± 3.30	45.75 ± 10.29
AST (U/L)	95.33 ± 25.36	56.25 ± 4.60	125.67 ± 41.79
Total Chol (mg/dL)	44.33 ± 1.76	52.40 ± 3.54	67.00 ± 6.10
Triglycerides (mg/dL)	107.00 ± 16.29	161.40 ± 17.55	137.00 ± 0.07
Hematological data			
RBC count (x10 ⁶ /μL)	7.10 ± 0.15	7.41 ± 0.28	7.84 ± 0.30
HGB (g/dL)	13.97 ± 0.18	13.95 ± 0.46	13.48 ± 0.54
HCT (%)	40.50 ± 0.82	42.28 ± 2.03	43.33 ± 1.89
WBC counts (x10 ³ /μL)	1.93 ± 0.68	2.15 ± 0.88	1.55 ± 0.49
PLT counts (x10 ³ /μL)	811.00 ± 29.61	793.80 ± 28.35	913.25 ± 81.96
RET counts (%)	2.80 ± 0.12	3.56 ± 0.23	4.65 ± 0.33

Data were analyzed for saline, vehicle and 10 mg/kg Roy-Bz (treated) rat groups, after four intraperitoneal administrations (twice a week). Results are mean ± SEM of four independent experiments; **p*<0.05 (comparison between saline and vehicle groups; control groups); #*p*<0.05 (comparison between Roy-Bz and control groups), and between vehicle and treated groups). *ALT*, alanine aminotransferase; *AST*, aspartate aminotransferase; *BW*, body weight; *CK*, Creatine Kinase; *HCT*, hematocrit; *HGB*, Hemoglobin concentration; *PCT*, plateletcrit; *PLT*, platelet; *RBC*, red blood cell count; *RET*, reticulocytes; *WBC*, white blood cells.

The *in vivo* antitumor potential of Roy-Bz was thereafter evaluated using human tumor xenograft mouse models of control and PKC δ -knockdown HCT116 cells, following the same administration procedure conducted in the toxicological studies. A significant inhibition in the growth of control HCT116 tumors was observed after administration of Roy-Bz (10 mg/kg) compared to vehicle (Fig. 3.1.10A, left panel). Notably, the antitumor activity of Roy-Bz was lost when mice were inoculated with PKC δ -depleted HCT116 cells (Fig. 3.1.10A, right panel), further reinforcing the concept that the antitumor activity of Roy-Bz was mediated by PKC δ . Of note, no significant body weight loss or morbidity signs were observed in Roy-Bz-treated mice compared to vehicle (Fig. 3.1.10B).

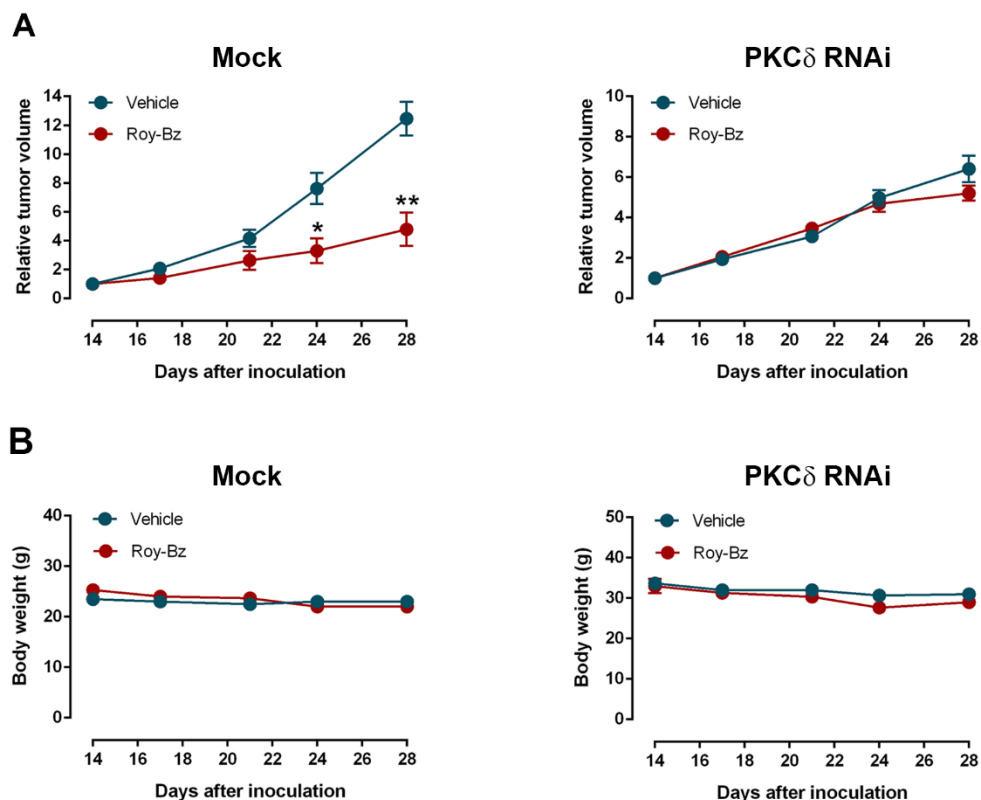


Figure 3.1.10: Roy-Bz has *in vivo* PKC δ -dependent antitumor activity with no apparent toxic side effects. (A) Growth curves for relative tumor volume of BALB/c nude mice carrying control (Mock) and PKC δ -knockdown (PKC δ RNAi) HCT116 xenografts treated with vehicle or 10 mg/kg Roy-Bz; data are mean \pm SEM of tumor volume fold change to the start of treatment, values significantly different from vehicle (* p <0.05, ** p <0.01), unpaired Student's t -test. **(B)** BALB/c nude mice body weight during vehicle or Roy-Bz treatment; no significant differences between vehicle- and Roy-Bz-treated mice: p >0.05, unpaired Student's t -test.

Lastly, proliferation, apoptosis and angiogenesis markers were checked in tumor samples from control and PKC δ -knockdown HCT116 xenografts obtained at the end of *in vivo* antitumor assays (Fig. 3.1.11A-D). In PKC δ -expressing tumor samples, Roy-Bz reduced proliferation (decrease in Ki-67-positive staining, Fig. 3.1.11A, B) and stimulated apoptosis (increase in BAX expression, caspase-3 cleavage and DNA fragmentation as demonstrated by TUNEL-positive staining, Fig. 3.1.11A, C-D), when compared to vehicle. The expression levels of VEGF were also analyzed as a readout of angiogenesis. Data showed a marked reduction in VEGF expression in samples from tumors treated with Roy-Bz relative to vehicle (Fig. 3.1.11A, C). On the other hand, no apparent differences in these markers were observed between Roy-Bz and vehicle in PKC δ -knockdown tumor samples (Fig. 3.1.11A-D). Altogether, these results demonstrated that Roy-Bz has strong *in vivo* PKC δ -dependent antitumor activity, through inhibition of proliferation and angiogenesis, and stimulation of apoptosis.

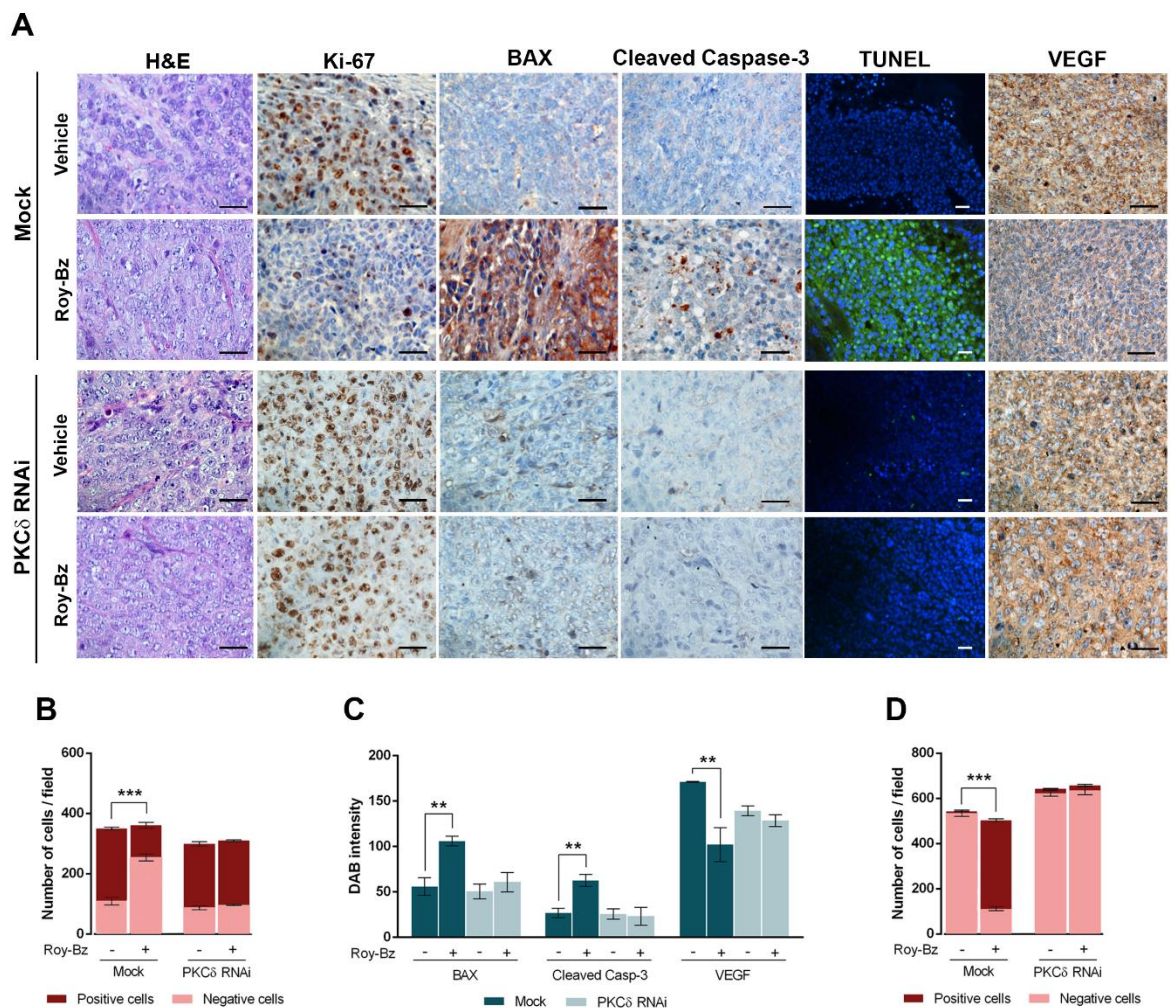


Figure 3.1.11: Roy-Bz inhibits proliferation and angiogenesis, and induces apoptosis in tumor tissues of human HCT116 xenograft mouse models. (A) Representative images of Ki-67, BAX, cleaved caspase-3, DNA fragmentation (TUNEL) and VEGF detection in tumor tissues of control and PKC δ -knockdown HCT116 xenografts treated with Roy-Bz or vehicle, collected at the end of treatment (scale bar=5 μ m; magnification=400 \times , 200 \times for TUNEL). **(B-D)** Quantification of immunohistochemistry of HCT116 xenograft tumor tissues of Mock and PKC δ RNAi treated with Roy-Bz or vehicle; in **B**, quantification of the number of positive and negative Ki-67 cells; in **C**, BAX, cleaved caspase-3 and VEGF staining quantification by evaluation of 3,3'-diaminobenzidine (DAB) intensity; in **D**, quantification of the number of positive and negative TUNEL cells. In **B**, **C** and **D**, data are mean \pm SEM of three independent experiments, values significantly different from vehicle (* p <0.05, ** p <0.01, *** p <0.001), unpaired Student's t -test.

3.1.6. Discussion

Despite the critical role of PKCs in numerous human diseases, the understanding of the function of specific isozymes in a given disease remains under intense controversy due to the lack of PKC isozyme-selective modulators (76, 212). Herein, the compound Roy-Bz was identified as a potent and selective activator of PKC δ that, like phorbol esters, has the C1-domain as binding site. Additionally, it was shown that Roy-Bz has potent anticancer properties against colon cancer. Accordingly, it strongly inhibited the proliferation of colon cancer cells by triggering a PKC δ -dependent apoptotic pathway involving caspase-3 activation. The selectivity of Roy-Bz towards PKC δ in human colon cancer cells is further reinforced by the observation of the specific translocation of PKC δ , without any noticeable effect on the relocalization of other phorbol ester responsive PKC isozymes. Activation of PKC δ was also associated with the generation of a constitutive active PKC δ catalytic fragment, an effect observed in other models (116, 306), and the phosphorylation of histone H3 on Ser-10, a PKC δ -dependent event crucial in chromatin condensation during apoptosis (307).

Despite the positive role of PKC δ in migration and invasiveness in some cellular models (310, 311), it was also disclosed that PKC δ suppressed migration and the secretion of MMP-9 in highly motility breast cancer cells (153, 154). Supporting this anti-migratory activity of PKC δ , we found that Roy-Bz inhibited the migration of colon cancer cells in a PKC δ -dependent manner, with a reduction of MMP-9 and up-regulation of E-cadherin expression levels in colonospheres.

Recent studies have also demonstrated the relevant role of PKC isozymes in controlling cellular signaling of CSCs, which are critical in drug resistance, metastasis and

relapse of cancer (312). However, further studies are required since scarce data are available on this subject. Our results support a negative regulation of stemness of colon cancer cells by PKC δ . Additionally, they indicate that Roy-Bz may also target drug resistant CSCs, preventing tumor dissemination and recurrence, as evidenced by the pronounced reduction of colonosphere growth and formation, and by the depletion of the CD44 stemness marker. Interestingly, CD44 is a known downstream target of the Wnt/ β -catenin pathway (313, 314), which is intricately involved in the growth and maintenance of colonospheres (315). Accordingly, our results are in line with the recently reported inhibition of the Wnt/ β -catenin pathway by PKC δ to suppress proliferation of colon cancer cells (150).

Notably, a PKC δ -dependent antitumor effect of Roy-Bz, associated with anti-proliferative, pro-apoptotic, and anti-angiogenic activities, was demonstrated in xenograft mouse models. The great potential of Roy-Bz as an anticancer agent in colon cancer treatment was reinforced by the absence of genotoxicity in normal and tumor cells, as well as the lack of *in vivo* apparent toxic side effects.

PKC δ has been generally assumed as an anti-proliferative and pro-apoptotic kinase, and subsequently as a crucial death mediator of chemotherapeutic agents and radiotherapy (76, 116, 306, 316). Our experimental results with Roy-Bz in colon cancer cells are consistent with the notion that PKC δ preferentially acts as a tumor suppressor in intestinal carcinogenesis (146-150). In fact, numerous studies have shown that PKC δ inhibits cell proliferation as well as anchorage-dependent and -independent growth, and in addition it enhances differentiation of colon cancer cells (146-150). PKC δ has also been implicated in growth inhibition and apoptosis of several other cancer types, including prostate and glioma (133, 144). However, anti-apoptotic and pro-survival roles of PKC δ have also been reported in other cancer types, particularly in breast cancer (317, 318), suggesting notable differences depending on the cellular context. It has been also reported that the tumor promoting properties of PKC δ after PMA treatment may result from the loss of PKC (down-regulation) due to its chronic application, rather than to its acute activation (319). Interestingly, as observed with the PKC activator prostratin (320), Roy-Bz did not significantly affect the PKC δ stability, what may explain the tumor suppression rather than tumor promoting activity of PKC δ associated with Roy-Bz.

In conclusion, in this work Roy-Bz was identified as the first small-molecule PKC δ -selective activator, with encouraging clinical application in colon cancer therapy. Moreover, the elucidation of the structural requirements underlying its selectivity for PKC δ will be crucial to the structure-based design of other PKC isozyme-selective agents. In turn, these new agents will help in the elucidation of the specific functions of PKC isozymes in human diseases.

CHAPTER 3.2

**Roy-Bz: a potential dual inhibitor of
glycolysis and oxidative phosphorylation in
colon cancer**

In the present chapter, it was studied the impact of Roy-Bz on mitochondrial respiration and glycolysis of colon cancer.

3.2.1. Roy-Bz induces mitochondrial dysfunction with inhibition of cellular respiration in colon cancer cells

The cytotoxic effect of Roy-Bz was evaluated both in terms of cell mass and metabolic activity, using the SRB and resazurin reduction assays, respectively, as described (321). The results showed that the treatment of HCT116 cells with increasing doses of Roy-Bz induced a concomitant decrease of cell mass (Fig. 3.2.1A) and metabolic activity (Fig. 3.2.1B), for all concentrations tested when compared to vehicle.

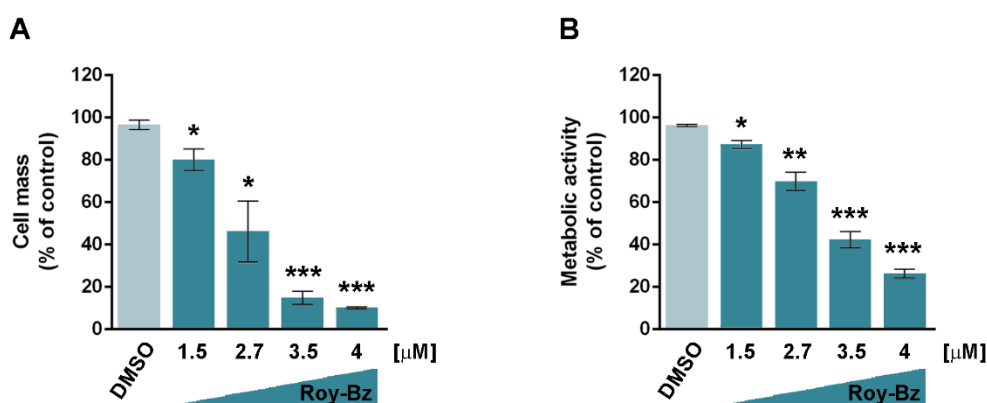


Figure 3.2.1: Roy-Bz has cytotoxic effect in colon cancer cells. (A, B) HCT116 cells were treated with 1.5 to 4 μM Roy-Bz for 48 h. In **A**, cell mass was determined using SRB assay. In **B**, metabolic activity was determined by resorufin fluorescence measurement after 6 h incubation using resazurin assay. In **A** and **B**, data are expressed as percentage of vehicle and are mean ± SEM of five independent experiments; values significantly different from vehicle: * $p < 0.05$, ** $p < 0.01$, *** $p < 0.001$, unpaired Student's *t*-test.

Afterwards, the involvement of the mitochondrial pathway in Roy-Bz-induced growth inhibition was studied in HCT116 cells. In these cells, Roy-Bz increased the production of mitochondrial ROS and caused $\Delta\psi_m$ dissipation (Fig. 3.2.2A). Additionally, it increased the release of cyt *c* to cytosol (Fig. 3.2.2B).

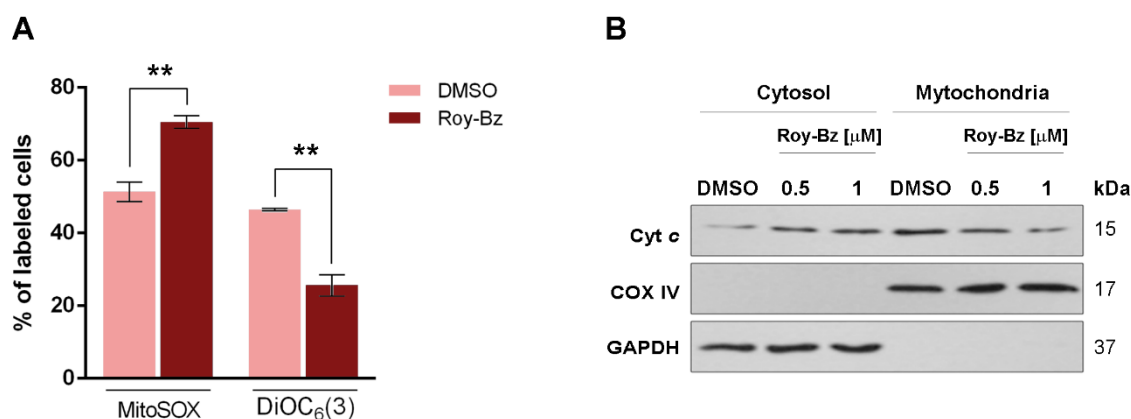


Figure 3.2.2: Roy-Bz induces mitochondrial dysfunction in colon cancer cells. (A) Mitochondrial ROS generation (MitoSOX labeled cells) and $\Delta\psi_m$ dissipation (DiOC₆(3) labeled cells), after 24 h and 16 h, respectively, treatment with 0.5 μ M Roy-Bz, in HCT116 cells; data are mean \pm SEM of four independent experiments. **(B)** Mitochondrial cyt c release in HCT116 cells after 24 h treatment with Roy-Bz; immunoblots represent one of three independent experiments; loading control of cytosolic (GAPDH) and mitochondrial (COX IV) fractions. In **A**, values significantly different from vehicle (** p <0.01), unpaired Student's t -test.

Based on these data, it was hypothesized that Roy-Bz may directly interfere with mitochondrial activity. As such, we next investigated the effect of Roy-Bz on mitochondrial respiration using a Seahorse Bioanalyzer to measure the OCR, a surrogate readout of mitochondrial function. As shown in Fig. 3.2.3A, increasing doses of Roy-Bz (from 1.5 to 4 μ M) resulted in a dose-dependent decrease in OCR. Thereafter, different parameters associated with mitochondrial respiration were real-time assessed in cells treated with Roy-Bz, through sequential administration of complex inhibitors (Fig. 3.2.3B). Particularly, it was used oligomycin (complex V inhibitor) to determine the amount of ATP production linked to respiration, FCCP (mitochondrial uncoupler) to measure the maximal respiratory capacity, and a combination of rotenone (complex I inhibitor) and antimycin A (complex III inhibitor) to determine the reserved respiratory capacity. Impressively, with exception of non-mitochondrial respiration, Roy-Bz impaired all the parameters evaluated, including maximal respiration, spare respiratory capacity and ATP production, when compared to vehicle (Fig. 3.2.3C).

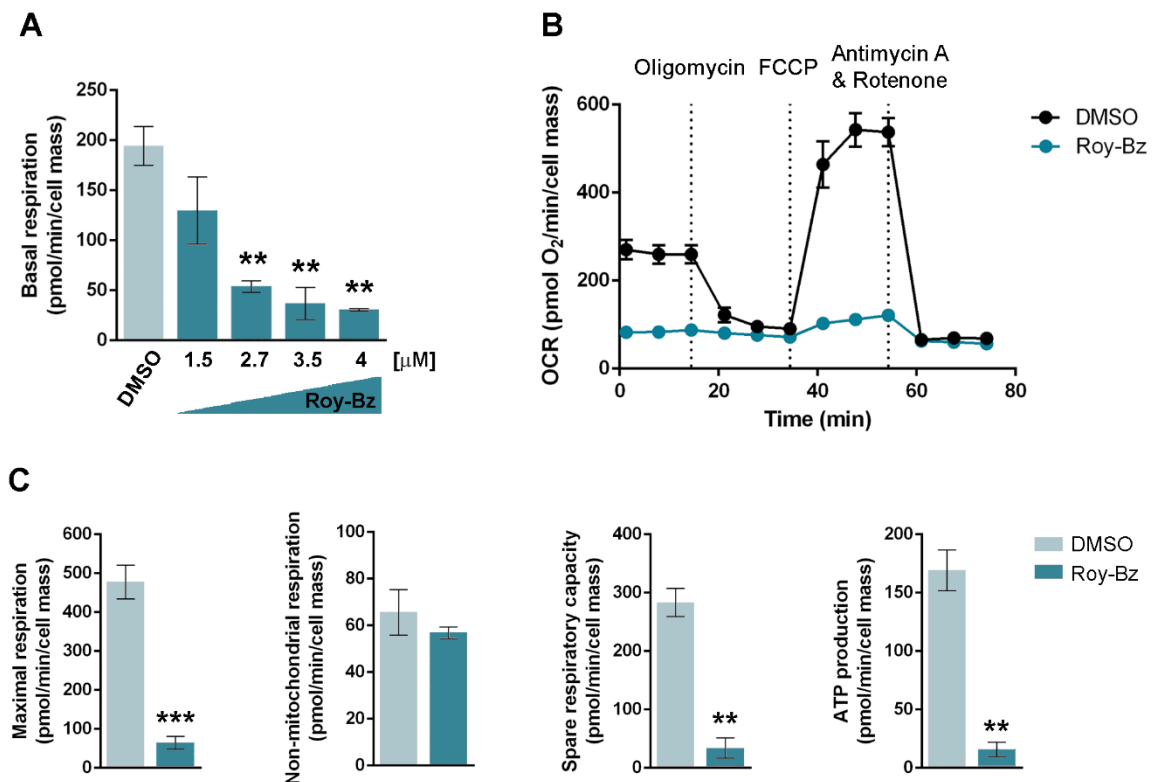


Figure 3.2.3: Roy-Bz inhibits cellular respiration in colon cancer cells. (A-C) The Seahorse XFe96 Extracellular Flux Analyzer was used to measure OCR. In **A**, measurement of basal cell respiration (prior to oligomycin addition minus non-mitochondria-derived OCR) after treatment with 1.5 to 4 μM Roy-Bz (or DMSO only) for 48 h. In **B**, baseline measurements of OCRs prior to sequential administration of oligomycin, FCCP, and a combination of rotenone and antimycin A; data correspond to treatments with 4 μM Roy-Bz (or DMSO only) for 48 h. In **C**, measurement of several OCR parameters: maximal respiration (maximal measurement after FCCP addition minus non-mitochondria-derived OCR), non-mitochondrial respiration (minimal measurement after rotenone and antimycin A addition), spare respiratory capacity (maximal respiration minus basal respiration), and ATP production (basal respiration minus proton leak); data correspond to treatments with 4 μM Roy-Bz (or DMSO only) for 48 h. In **A** and **C**, data are mean \pm SEM of three independent experiments; values significantly different from vehicle: * $p < 0.05$, ** $p < 0.01$, *** $p < 0.001$, unpaired Student's *t*-test.

3.2.2. Roy-Bz inhibits glycolysis in tumor tissues of human HCT116 xenografts

The anti-glycolytic potential of Roy-Bz was studied in tumor tissues of HCT116 xenografts, obtained at the end of the *in vivo* antitumor assays described in Chapter 3.1. To this end, the expression of some glycolytic markers was assessed by immunohistochemistry (Fig. 3.2.4). Consistently with an inhibition of glycolysis, Roy-Bz significantly reduced the expression levels of GLUT1, hexokinase 2 (HK2) and

monocarboxylate transporter 4 (MCT4), and increased *TP53*-induced glycolysis and apoptosis regulator (TIGAR) levels, when compared to vehicle (Fig. 3.2.4A and B). The results obtained showed that Roy-Bz had *in vivo* anti-glycolytic activity.

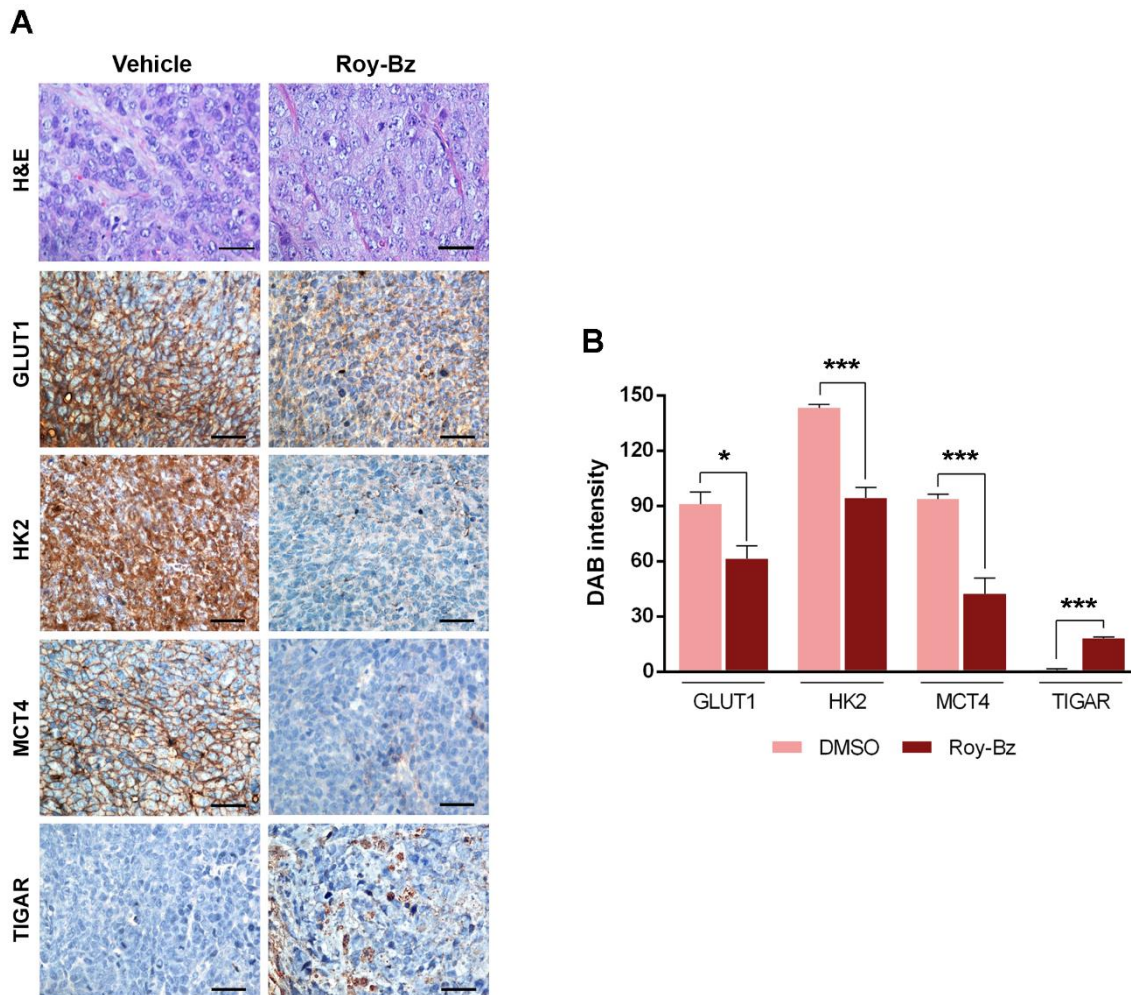


Figure 3.2.4: Roy-Bz has anti-glycolytic activity in tumor tissues of human HCT116 xenograft mouse models. (A) Representative images of GLUT1, HK2, MCT4 and TIGAR detection in tumor tissues of HCT116 xenografts treated with 10 mg/kg Roy-Bz or vehicle, collected at the end of the treatment (scale bar=5 μ m; magnification=400 \times). (B) Quantification of immunohistochemistry of HCT116 xenograft tumor tissues by evaluation of DAB intensity; data are mean \pm SEM of three independent experiments, values significantly different from vehicle (* p <0.01, *** p <0.001), unpaired Student's *t*-test.

3.2.3. Discussion

In this chapter, it was shown that Roy-Bz stimulated a mitochondrial pathway in colon cancer cells, increasing mitochondrial ROS production, depolarization of $\Delta\psi_m$, and release of cyt c to cytosol. Moreover, Roy-Bz greatly decreased the OCR of colon cancer cells, with simultaneous reduction of ATP synthesis and maximal respiration. These results strongly supported an inhibition of mitochondrial respiration by Roy-Bz. It is possible to hypothesize that the mechanism of action of Roy-Bz may involve the inhibition of the ETC, particularly complexes I/III and/or V, which are directly related with alterations in mitochondrial parameters measured. Being Roy-Bz a PKC δ -selective activator, these results also supported an involvement of PKC δ in the impairment of mitochondrial activity. This is in accordance with a previous work, which reported the PKC δ interaction with mitochondria, thereby regulating mitochondrial metabolism (322).

Interestingly, *in vivo*, Roy-Bz also inhibited glycolysis, inducing the downregulation of enzymes directly implicated in glucose metabolism, including GLUT1 (involved in the uptake of glucose into the cell), HK2 (that catalyzes the first committed step of the glycolytic flux with phosphorylation of glucose to glucose-6-phosphate), and MCT4 (that mediates the export of lactate). Additionally, Roy-Bz upregulated TIGAR, which is a negative regulator of the glycolytic flux through inhibition of phosphofructose kinase 1 (PFK1) and subsequent accumulation of glucose-6-phosphate, a substrate of glucose-6-phosphate dehydrogenase (G6PDH), thereby redirecting the glucose to nucleic acid synthesis.

Although further studies are still required to validate the results obtained in the present chapter, they strongly support the ability of Roy-Bz to target both ATP producing pathways of glucose metabolism. In fact, this dual-inhibitory effect on glucose metabolism was already described for metformin (as described in introductory section).

As a whole, with this work, the anticancer potential of Roy-Bz was further reinforced by showing its ability to also target the glucose metabolism of cancer cells. The exploitation of its potential as dual inhibitor of glycolysis and OXPHOS in combination therapy with other metabolic drugs or chemotherapeutic agents holds great promise in cancer therapy.

CHAPTER 3.3

Exploring the anticancer potential of *Plectranthus* genus

Part of this work was submitted for publication:

***Plectranthus* genus as a source of bioactive compounds: unveil the antimicrobial and cytotoxic activity of the *P. strigosus* acetonc extract**

Garcia, C., Roque, L., Rebelo, A., Borozan, A., Ntungwe, E., Andrade, J.M., **Bessa, C.**, Saraiva, L., Lanza, A.D., Reis, C.P., Stankovic, T., Dinic, J., Roberto, A., Pesic, M., Duarte, N., Rijo, P.

Abietane diterpenoids are the major constituents of some species of the *Plectranthus* genus, and the main responsible for the therapeutic value of these plants (323, 324). In fact, these natural occurring compounds exhibit a plethora of biological activities, including cytotoxic and anti-proliferative effects in human cancer cells (323, 324). This has encouraged the exploitation of *Plectranthus* species as a source of potential anticancer agents. In addition, the discovery of the semi-synthetic derivative Roy-Bz, obtained from a natural diterpenoid isolated from *P. grandidentatus*, with potent anticancer activity, led us to search for new anticancer agents in *Plectranthus* species. Particularly, it was evaluated the *in vitro* anti-proliferative activity of the abietane diterpenoid 6,7-dehydroroyleanone (DeRoy; Fig. 3.3.1), obtained from the *P. madagascariensis*, and of their synthetic derivatives, 6,7-dehydro-12-O-pro-2-yn-1-yloxy-royleanone (FRP19) and 6,7-dehydro-12-O-(1*R*,2*S*,5*R*)-2-isopropyl-5-methylcyclohexyl)oxy)-royleanone (FRP20), in a panel of human cancer cell lines. Additionally, it was evaluated the anti-proliferative activity of other extracts obtained from *Plectranthus* spp. plants.

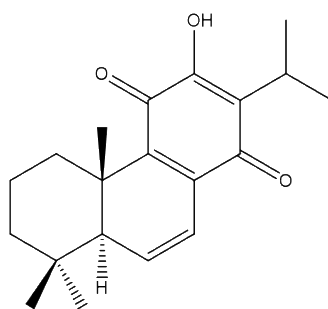


Figure 3.3.1: Chemical structure of abietane diterpenoid 6,7-dehydroroyleanone.

3.3.1. Anti-proliferative activity of DeRoy and synthetic derivatives in human cancer cells

Human colon adenocarcinoma HCT116, breast adenocarcinoma MCF-7, and NSCLC NCI-H460 cells were treated with 1.56 - 50 μ M DeRoy, FRP19 or FRP20 for 48 h, and the tumor growth inhibitory activity was evaluated by SRB assay. The IC₅₀ values obtained showed that DeRoy was an inhibitor of the growth of the three cancer cell lines (Table 3.3.1). These results led us to test two derivatives of DeRoy (FRP19 and FRP20), with different alkyl substituents based on the C-12 hydroxyl group of the starting material, as described (292). However, contrary to what was expected, the obtained derivatives did not show

improved *in vitro* anticancer activity, being less potent than the starting natural material, in all tested cancer cell lines.

Table 3.3.1. IC₅₀ values of DeRoy and derivative compounds in human cancer cells.

Compound	IC ₅₀ [μM]		
	HCT116	MCF-7	NCI-H460
DeRoy	6.68 ± 1,37	6.12 ± 1,62	3.23 ± 0.11
FRP19	9.72 ± 0,39	10.51 ± 0,41	10.91 ± 0.05
FRP20	≥ 50	≥ 50	≥ 50

Results were obtained by SRB assay after 48 h treatment. Data are mean ± SEM of four independent experiments.

3.3.2. Anti-proliferative activity of *Plectranthus* spp. extracts in human cancer cells

The anti-proliferative activity of 16 extracts, obtained from different *Plectranthus* spp. plants, was studied in human HCT116, MCF-7 and NCI-H460 cells. These human cancer cells were treated with 1.56 – 50 μg/mL plant extracts for 48 h, and the tumor growth inhibitory activity was evaluated by SRB assay. The IC₅₀ values obtained for each extract (Table 3.3.2), showed that the majority of the extracts tested were able to inhibit the growth of the three human cancer cells (Table 3.3.2). In fact, only the extract P.R-A. was ineffective in all tested cancer cells. P.M.L-A. and P.ST-A. were the extracts with the highest anti-proliferative activity (IC₅₀ values lower than 10 μg/mL), followed by extracts P.S-A., P.HE-A., P.HA-A., P.A-A., and P.AB-A. (IC₅₀ values lower than 20 μg/mL), in all tested cancer cells. Interestingly, while HCT116 cells showed to be quite sensible, MCF-7 cells proved to be rather resistant to *Plectranthus* spp. extracts. Particularly, P.Z-A. was quite effective against HCT116 and NCI-H460 cells, while presenting low anti-proliferative activity against MCF-7 cells. An interesting exception occurred with the P.E.A. extract, which was ineffective against NCI-H460 cells and presented a high anti-proliferative activity against HCT116 and MCF-7 cells.

Table 3.3.2. IC₅₀ values of *Plectranthus* spp. extracts in human cancer cells.

Extract	IC ₅₀ [µg/mL]		
	HCT116	MCF-7	NCI-H460
P.M.L-A.	5.72 ± 0.59	3.47 ± 0.15	5.39 ± 0.48
P.ST-A.	3.78 ± 0.49	8.35 ± 0.57	8.75 ± 0.70
P.S-A.	6.64 ± 0.12	15.13 ± 0.85	17.43 ± 0.89
P.HE-A.	10.72 ± 0.86	14.14 ± 0.07	15.53 ± 1.74
P.HA-A.	13.41 ± 0.46	16.57 ± 1.20	16.09 ± 2.10
P.A-A.	16.67 ± 0.10	14.59 ± 1.70	15.45 ± 0.41
P.AB-A.	11.74 ± 1.78	13.38 ± 2.56	18.27 ± 0.84
P.J-A.	4.99 ± 0.20	12.85 ± 1.76	22.56 ± 0.46
P.O-A.	18.25 ± 2.65	16.55 ± 0.19	27.52 ± 2.11
P.MV-A.	17.23 ± 1.87	13.37 ± 1.49	41.22 ± 0.18
P.M-A.	24.29 ± 1.00	27.23 ± 1.27	25.90 ± 2.26
P.E-A.	4.35 ± 0.08	12.23 ± 0.90	≥ 50
P.Z-A.	8.08 ± 0.19	≥ 50	10.76 ± 2.03
P.BA-A.	10.58 ± 1.01	≥ 50	31.79 ± 0.31
P.F-A.	29.05 ± 0.63	≥ 50	34.88 ± 1.06
P.R-A.	≥ 50	≥ 50	≥ 50

IC₅₀ values were determined after 48 h treatment using the SRB assay. Data are mean ± SEM of four independent experiments.

3.3.3. Discussion

For many years, *Plectranthus* species have been recognized by their medicinal relevance in the treatment of diverse diseases (282). In a previous work, the phytochemical analysis of *P. madagascariensis* identified the abietane diterpenoid DeRoy as the main component of the essential oil of this species (291). Previous studies with this natural occurring compound demonstrated its potent cytotoxic and antioxidant activity (325).

In the present work, it is evidenced its anti-proliferative activity against human cancer cells. Further studies are still required to elucidate the molecular mechanism of action underlying its tumor growth inhibitory activity. Despite this, DeRoy revealed to be a

promising starting material for the development of a library of new compounds with improved *in vitro* antitumor activity. However, the strategy used to modify the DeRoy scaffold was not well-succeeded, since all the synthesized derivatives exhibited lower antiproliferative activity against human cancer cells than the starting material.

Regarding to *Plectranthus* spp. extracts, the majority of the extracts tested in this work revealed growth inhibitory effect against human cancer cells. Particularly, P.M.L-A. and P.ST-A. showed to be promising sources of new potential anticancer drug candidates. Consequently, further studies will be performed with these extracts in order to identify the bioactive compounds.

As a whole, the results herein obtained reinforced the therapeutic value of *Plectranthus* genus as an attractive source of new anticancer agents, and identified new compounds and raw materials that may conduct to the discovery of new effective anticancer agents.

CHAPTER 4

General Discussion

Final conclusions and Future perspectives

Despite an evident progress in diagnosis and treatment, the worldwide cancer mortality is increasing every year (1). Great efforts have been made to improve the efficacy of anticancer drugs in clinical use. However, this has shown to be a challenge, as demonstrated by the disappointing results achieved in the clinical translation of an impressive number of new drugs.

As a critical player in carcinogenesis, PKC early became an attractive therapeutic target in cancer (68, 212). For long, PKC-targeting drugs were developed based on the assumption that PKC positively contributes to cancer development and progression. Therefore, many PKC inhibitors were tested in clinical trials with no success (212). More recently, cumulating data have supported that PKC primarily function as tumor suppressor, indicating that PKC-targeting strategies should be focused on restoring, rather than inhibiting, PKC activity (77). On the basis of all controversy, it is the inability of addressing the isozyme-specific function in the different cancer subsets due to the reduced specificity of available pharmacological PKC modulators.

With this thesis, great advances were reached concerning the PKC pharmacology and cancer therapy with the discovery of a new:

i) PKC isozyme-selective agent

The identification of isozyme-selective PKC modulators has been the main determining factor for the success of PKC-targeting therapy. In this thesis, a previously developed yeast-based PKC screening assay (275) was used to analyze the effect of a small chemical library of royleanone derivatives on PKC activity (Chapter 3.1). Using this approach, the compound Roy-Bz was identified as a potential PKC δ -selective activator. The selective activation of PKC δ by Roy-Bz was thereafter confirmed in an *in vitro* kinase assay using recombinant PKC isozymes and in human colon cancer cell lines (Chapter 3.1). Additionally, molecular docking studies supported the binding of Roy-Bz to the PKC δ -C1-domain (Chapter 3.1).

ii) Anticancer drug candidate by targeting PKC

The anticancer potential of the PKC δ -selective activator Roy-Bz was also validated in the present thesis (Chapter 3.1 and 3.2). In colon cancer cells, Roy-Bz potently inhibited the proliferation by inducing an apoptotic cell death (Fig. 5.1) and presented an anti-migratory effect, in a PKC δ -dependent manner. It also impaired the colonosphere growth and formation with depletion of stemness markers. Notably, *in vivo*, Roy-Bz showed a PKC δ -dependent antitumor activity, with no apparent toxic side effects. Beyond these results, it was demonstrated that Roy-Bz potentially targets tumor glucose metabolism by

dual inhibition of glycolysis and OXPHOS (Chapter 3.2). Altogether, these data demonstrated that Roy-Bz was a promising anticancer drug candidate.

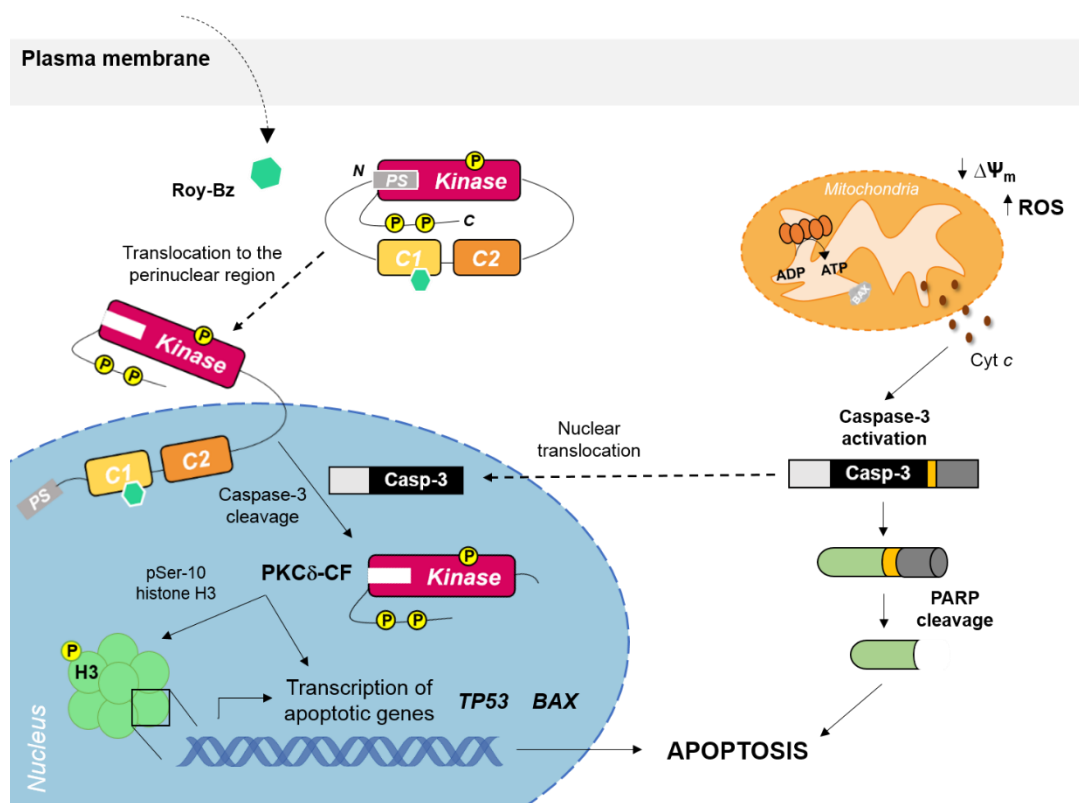


Figure 5.1: Putative molecular mechanism of action of Roy-Bz-induced apoptosis. Roy-Bz binds to the PKC δ -C1 domain, inducing its translocation to the perinuclear region. In the nucleus, PKC δ is cleaved by caspase-3, resulting in the generation of the PKC δ -CF, which in turn phosphorylates nuclear substrates, such as of histone H3 on Ser-10, that promotes apoptosis. Additionally, the transcription of apoptotic genes, namely *TP53* and *BAX*, activates a mitochondrial apoptotic pathway, with subsequent cyt c release, activation of caspase-3, PARP cleavage, and subsequent apoptosis induction.

Final conclusions and future perspectives

The establishment of Roy-Bz as the first small-molecule selective activator of PKC δ may contribute to unravel fundamental aspects of the pharmacology of PKC δ . In fact, besides the elucidation of the structural requirements underlying the selectivity of compounds to PKC δ , Roy-Bz will improve the structure-based design of new PKC isozyme-selective agents. Roy-Bz may also provide relevant insights concerning the PKC δ biology

in human diseases, including cancer. Most importantly, encouraging applications can be envisaged for Roy-Bz in cancer therapy, particularly in the treatment of CRC that is a leading cause of cancer incidence and death worldwide (3). Actually, cumulated data have shown reduced PKC δ levels in colon cancer tissues, compared to normal ones (146), and have demonstrated a tumor suppressive role of PKC δ in colon cancer (146-150). The therapeutic value of Roy-Bz in CRC is further emphasized by the limited therapeutic options available for the treatment of patients with advanced or metastatic CRC. Currently, the first-line treatment for metastatic CRC is still based on conventional chemotherapeutic agents, such as irinotecan or oxaliplatin combined with a fluoropyrimidine and leucovorin (FOLFIRI or FOLFOX regimens), with modest therapeutic efficacy (326-328). The PKC δ -targeting therapy with Roy-Bz, alone or in combination with other therapeutic agents, may represent a new hope in CRC treatment. However, besides CRC, other types of cancer in which PKC δ has been implicated in growth inhibition and apoptosis induction, such as prostate and glioma, may also benefit from Roy-Bz therapy (133, 144).

Finally, in this thesis it is reinforced the potential of *Plectranthus* genus as a promising source of new compounds with anticancer activity (Chapter 3.3). In particular, it was identified one abietane diterpenoid (DeRoy) and two extracts (P.M.L-A. and P.ST-A.) with anti-proliferative activity in distinct cancer cell lines. These data may give rise to additional works with the subsequent identification of more effective anticancer drugs.

In conclusion, with the discovery of Roy-Bz, it is possible to open the way to a new era on PKC biology and pharmacology. Notably, Roy-Bz will contribute to the redefinition of PKC isozymes as feasible therapeutic targets in precision medicine. Besides this, the work carried out under this thesis gives rise to new therapeutic opportunities in cancer treatment by providing a new effective anticancer drug candidate.

CHAPTER 5

References

1. Ferlay J, Soerjomataram I, Dikshit R, Eser S, Mathers C, Rebelo M, et al. Cancer incidence and mortality worldwide: sources, methods and major patterns in GLOBOCAN 2012. *Int J Cancer* 2015 Mar; 136 (5): E359-86.
2. Ferlay J, Steliarova-Foucher E, Lortet-Tieulent J, Rosso S, Coebergh JW, Comber H, et al. Cancer incidence and mortality patterns in Europe: estimates for 40 countries in 2012. *Eur J Cancer* 2013 Apr; 49 (6): 1374-403.
3. Arnold M, Sierra MS, Laversanne M, Soerjomataram I, Jemal A, Bray F. Global patterns and trends in colorectal cancer incidence and mortality. *Gut* 2017 Apr; 66 (4): 683-91.
4. Hanahan D, Weinberg RA. Hallmarks of cancer: the next generation. *Cell* 2011 Mar; 144 (5): 646-74.
5. Hanahan D, Weinberg RA. The hallmarks of cancer. *Cell* 2000 Jan; 100 (1): 57-70.
6. Adams JM, Cory S. The Bcl-2 apoptotic switch in cancer development and therapy. *Oncogene* 2007 Feb; 26 (9): 1324-37.
7. Lowe SW, Cepero E, Evan G. Intrinsic tumour suppression. *Nature* 2004 Nov; 432 (7015): 307-15.
8. Raica M, Cimpean AM, Ribatti D. Angiogenesis in pre-malignant conditions. *Eur J Cancer* 2009 Jul; 45 (11): 1924-34.
9. Hanahan D, Folkman J. Patterns and emerging mechanisms of the angiogenic switch during tumorigenesis. *Cell* 1996 Aug; 86 (3): 353-64.
10. Hay M, Thomas DW, Craighead JL, Economides C, Rosenthal J. Clinical development success rates for investigational drugs. *Nat Biotechnol* 2014 Jan; 32 (1): 40-51.
11. Venkatakrishnan K, Zhou X, Ecsedy J, Mould DR, Liu H, Danaee H, et al. Dose selection for the investigational anticancer agent alisertib (MLN8237): Pharmacokinetics, pharmacodynamics, and exposure-safety relationships. *J Clin Pharmacol* 2015 Mar; 55 (3): 336-47.
12. Ewer MS, Ewer SM. Cardiotoxicity of anticancer treatments. *Nat Rev Cardiol* 2015 Nov; 12 (11): 620.
13. Cheung-Ong K, Giaever G, Nislow C. DNA-damaging agents in cancer chemotherapy: serendipity and chemical biology. *Chem Biol* 2013 May; 20 (5): 648-59.

14. Urruticoechea A, Alemany R, Balart J, Villanueva A, Vinals F, Capella G. Recent advances in cancer therapy: an overview. *Curr Pharm Des* 2010 Jan; 16 (1): 3-10.
15. Chessum N, Jones K, Pasqua E, Tucker M. Recent advances in cancer therapeutics. *Prog Med Chem* 2015 Jan; 54:1-63.
16. Liu Z, Delavan B, Roberts R, Tong W. Lessons Learned from Two Decades of Anticancer Drugs. *Trends Pharmacol Sci* 2017 Oct; 38 (10): 852-72.
17. Shekhar MP. Drug resistance: challenges to effective therapy. *Curr Cancer Drug Targets* 2011 Jun; 11 (5): 613-23.
18. Stratton MR, Campbell PJ, Futreal PA. The cancer genome. *Nature* 2009 Apr; 458 (7239): 719-24.
19. Reya T, Morrison SJ, Clarke MF, Weissman IL. Stem cells, cancer, and cancer stem cells. *Nature* 2001 Nov; 414 (6859): 105-11.
20. Bonnet D, Dick JE. Human acute myeloid leukemia is organized as a hierarchy that originates from a primitive hematopoietic cell. *Nat Med* 1997 Jul; 3 (7): 730-7.
21. Bruce WR, Van Der Gaag H. A Quantitative Assay for the Number of Murine Lymphoma Cells Capable of Proliferation in Vivo. *Nature* 1963 Jul; 199: 79-80.
22. Kreso A, Dick JE. Evolution of the cancer stem cell model. *Cell Stem Cell* 2014 Mar; 14 (3): 275-91.
23. Malanchi I, Peinado H, Kassen D, Hussenet T, Metzger D, Chambon P, et al. Cutaneous cancer stem cell maintenance is dependent on beta-catenin signalling. *Nature* 2008 Apr; 452 (7187): 650-3.
24. Ito K, Suda T. Metabolic requirements for the maintenance of self-renewing stem cells. *Nat Rev Mol Cell Biol* 2014 Apr; 15 (4): 243-56.
25. Li S, Li Q. Cancer stem cells and tumor metastasis (Review). *Int J Oncol* 2014 Jun; 44 (6): 1806-12.
26. Dave B, Mittal V, Tan NM, Chang JC. Epithelial-mesenchymal transition, cancer stem cells and treatment resistance. *Breast Cancer Res* 2012 Jan; 14 (1): 202.
27. Flemming A. Cancer stem cells: Targeting the root of cancer relapse. *Nat Rev Drug Discov* 2015 Mar; 14 (3): 165.

28. Merlos-Suarez A, Barriga FM, Jung P, Iglesias M, Cespedes MV, Rossell D, et al. The intestinal stem cell signature identifies colorectal cancer stem cells and predicts disease relapse. *Cell Stem Cell* 2011 May; 8 (5): 511-24.
29. Bao S, Wu Q, McLendon RE, Hao Y, Shi Q, Hjelmeland AB, et al. Glioma stem cells promote radioresistance by preferential activation of the DNA damage response. *Nature* 2006 Dec; 444 (7120): 756-60.
30. Li X, Lewis MT, Huang J, Gutierrez C, Osborne CK, Wu MF, et al. Intrinsic resistance of tumorigenic breast cancer cells to chemotherapy. *J Natl Cancer Inst* 2008 May; 100 (9): 672-9.
31. Diehn M, Cho RW, Lobo NA, Kalisky T, Dorie MJ, Kulp AN, et al. Association of reactive oxygen species levels and radioresistance in cancer stem cells. *Nature* 2009 Apr; 458 (7239): 780-3.
32. Fang H, Declerck YA. Targeting the tumor microenvironment: from understanding pathways to effective clinical trials. *Cancer Res* 2013 Aug; 73 (16): 4965-77.
33. Ingber DE. Can cancer be reversed by engineering the tumor microenvironment? *Semin Cancer Biol* 2008 Oct; 18 (5): 356-64.
34. Casey SC, Amedei A, Aquilano K, Azmi AS, Benencia F, Bhakta D, et al. Cancer prevention and therapy through the modulation of the tumor microenvironment. *Semin Cancer Biol* 2015 Dec; 35 Suppl: S199-S223.
35. Carmeliet P, Jain RK. Molecular mechanisms and clinical applications of angiogenesis. *Nature* 2011 May; 473 (7347): 298-307.
36. Ricciuti B, Foglietta J, Bianconi V, Sahebkar A, Pirro M. Enzymes involved in tumor-driven angiogenesis: A valuable target for anticancer therapy. *Semin Cancer Biol* 2017 Nov; pii: S1044-579X(17)30043-3
37. Warburg O. On the origin of cancer cells. *Science* 1956 Feb; 123 (3191): 309-14.
38. Martinez-Outschoorn UE, Peiris-Pages M, Pestell RG, Sotgia F, Lisanti MP. Cancer metabolism: a therapeutic perspective. *Nat Rev Clin Oncol* 2017 Jan; 14 (1): 11-31.
39. Gomes AS, Ramos H, Soares J, Saraiva L. p53 and glucose metabolism: an orchestra to be directed in cancer therapy. *Pharmacol Res* 2018 (accepted for publication).

40. Salani B, Marini C, Rio AD, Ravera S, Massollo M, Orengo AM, et al. Metformin impairs glucose consumption and survival in Calu-1 cells by direct inhibition of hexokinase-II. *Sci Rep* 2013; 3:2070.
41. Wheaton WW, Weinberg SE, Hamanaka RB, Soberanes S, Sullivan LB, Anso E, et al. Metformin inhibits mitochondrial complex I of cancer cells to reduce tumorigenesis. *Elife* 2014 May; 3: e02242.
42. Ben Sahra I, Laurent K, Giuliano S, Larbret F, Ponzio G, Gounon P, et al. Targeting cancer cell metabolism: the combination of metformin and 2-deoxyglucose induces p53-dependent apoptosis in prostate cancer cells. *Cancer Res* 2010 Mar; 70 (6): 2465-75.
43. Ben Sahra I, Tanti JF, Bost F. The combination of metformin and 2 deoxyglucose inhibits autophagy and induces AMPK-dependent apoptosis in prostate cancer cells. *Autophagy* 2010 Jul; 6 (5): 670-1.
44. Miskimins WK, Ahn HJ, Kim JY, Ryu S, Jung YS, Choi JY. Synergistic anti-cancer effect of phenformin and oxamate. *PLoS One* 2014 Jan; 9 (1): e85576.
45. Sun H, Zhu A, Zhou X, Wang F. Suppression of pyruvate dehydrogenase kinase-2 re-sensitizes paclitaxel-resistant human lung cancer cells to paclitaxel. *Oncotarget* 2017 Aug; 8 (32): 52642-50.
46. Xie Q, Zhang HF, Guo YZ, Wang PY, Liu ZS, Gao HD, et al. Combination of Taxol(R) and dichloroacetate results in synergistically inhibitory effects on Taxol-resistant oral cancer cells under hypoxia. *Mol Med Rep* 2015 Apr; 11 (4): 2935-40.
47. De Palma M, Hanahan D. The biology of personalized cancer medicine: facing individual complexities underlying hallmark capabilities. *Mol Oncol* 2012 Apr; 6 (2): 111-27.
48. Takai Y, Yamamoto M, Inoue M, Kishimoto A, Nishizuka Y. A proenzyme of cyclic nucleotide-independent protein kinase and its activation by calcium-dependent neutral protease from rat liver. *Biochem Biophys Res Commun* 1977 Jul; 77 (2): 542-50.
49. Takai Y, Kishimoto A, Inoue M, Nishizuka Y. Studies on a cyclic nucleotide-independent protein kinase and its proenzyme in mammalian tissues. I. Purification and characterization of an active enzyme from bovine cerebellum. *J Biol Chem* 1977 Nov; 252 (21): 7603-9.
50. Inoue M, Kishimoto A, Takai Y, Nishizuka Y. Studies on a cyclic nucleotide-independent protein kinase and its proenzyme in mammalian tissues. II. Proenzyme and its

activation by calcium-dependent protease from rat brain. *J Biol Chem* 1977 Nov; 252 (21): 7610-6.

51. Takai Y, Kishimoto A, Iwasa Y, Kawahara Y, Mori T, Nishizuka Y, et al. A role of membranes in the activation of a new multifunctional protein kinase system. *J Biochem* 1979 Aug; 86 (2): 575-8.

52. Takai Y, Kishimoto A, Kikkawa U, Mori T, Nishizuka Y. Unsaturated diacylglycerol as a possible messenger for the activation of calcium-activated, phospholipid-dependent protein kinase system. *Biochem Biophys Res Commun* 1979 Dec; 91 (4): 1218-24.

53. Kishimoto A, Takai Y, Mori T, Kikkawa U, Nishizuka Y. Activation of calcium and phospholipid-dependent protein kinase by diacylglycerol, its possible relation to phosphatidylinositol turnover. *J Biol Chem* 1980 Mar; 255 (6): 2273-6.

54. Castagna M, Takai Y, Kaibuchi K, Sano K, Kikkawa U, Nishizuka Y. Direct activation of calcium-activated, phospholipid-dependent protein kinase by tumor-promoting phorbol esters. *J Biol Chem* 1982 Jul; 257 (13): 7847-51.

55. Konig B, Di Nitto PA, Blumberg PM. Phospholipid and Ca⁺⁺ dependency of phorbol ester receptors. *J Cell Biochem* 1985; 27 (3): 255-65.

56. Sharkey NA, Leach KL, Blumberg PM. Competitive inhibition by diacylglycerol of specific phorbol ester binding. *Proc Natl Acad Sci U S A* 1984 Jan; 81 (2): 607-10.

57. Griner EM, Kazanietz MG. Protein kinase C and other diacylglycerol effectors in cancer. *Nat Rev Cancer* 2007 Apr; 7 (4): 281-94.

58. Gerald P, King GL. Activation of protein kinase C isoforms and its impact on diabetic complications. *Circ Res* 2010 Apr; 106 (8): 1319-31.

59. Das Evcimen N, King GL. The role of protein kinase C activation and the vascular complications of diabetes. *Pharmacol Res* 2007 Jun; 55 (6): 498-510.

60. Inagaki K, Churchill E, Mochly-Rosen D. Epsilon protein kinase C as a potential therapeutic target for the ischemic heart. *Cardiovasc Res* 2006 May; 70 (2): 222-30.

61. Ferreira JC, Brum PC, Mochly-Rosen D. beta1IPKC and epsilonPKC isozymes as potential pharmacological targets in cardiac hypertrophy and heart failure. *J Mol Cell Cardiol* 2011 Oct; 51 (4): 479-84.

62. Garrido JL, Godoy JA, Alvarez A, Bronfman M, Inestrosa NC. Protein kinase C inhibits amyloid beta peptide neurotoxicity by acting on members of the Wnt pathway. *FASEB J* 2002 Dec; 16 (14): 1982-4.
63. Zhang D, Anantharam V, Kanthasamy A, Kanthasamy AG. Neuroprotective effect of protein kinase C delta inhibitor rottlerin in cell culture and animal models of Parkinson's disease. *J Pharmacol Exp Ther* 2007 Sep; 322 (3): 913-22.
64. Maioli E, Valacchi G. Rottlerin: bases for a possible usage in psoriasis. *Curr Drug Metab* 2010 Jun; 11 (5): 425-30.
65. Cirillo N, Lanza A, Prime SS. Induction of hyper-adhesion attenuates autoimmune-induced keratinocyte cell-cell detachment and processing of adhesion molecules via mechanisms that involve PKC. *Exp Cell Res* 2010 Feb; 316 (4): 580-92.
66. Isakov N, Altman A. Protein kinase C(theta) in T cell activation. *Annu Rev Immunol* 2002; 20: 761-94.
67. Altman A, Kong KF. Protein Kinase C Enzymes in the Hematopoietic and Immune Systems. *Annu Rev Immunol* 2016 May; 34: 511-38.
68. Garg R, Benedetti LG, Abera MB, Wang H, Abba M, Kazanietz MG. Protein kinase C and cancer: what we know and what we do not. *Oncogene* 2014 Nov; 33 (45): 5225-37.
69. Newton AC. Protein kinase C: poised to signal. *Am J Physiol Endocrinol Metab* 2010 Mar; 298 (3): E395-402.
70. Levin DE, Fields FO, Kunisawa R, Bishop JM, Thorner J. A candidate protein kinase C gene, PKC1, is required for the *S. cerevisiae* cell cycle. *Cell* 1990 Jul; 62 (2): 213-24.
71. Watanabe M, Chen CY, Levin DE. *Saccharomyces cerevisiae* PKC1 encodes a protein kinase C (PKC) homolog with a substrate specificity similar to that of mammalian PKC. *J Biol Chem* 1994 Jun; 269 (24): 16829-36.
72. Hernandez AI, Blace N, Crary JF, Serrano PA, Leitges M, Libien JM, et al. Protein kinase M zeta synthesis from a brain mRNA encoding an independent protein kinase C zeta catalytic domain. Implications for the molecular mechanism of memory. *J Biol Chem* 2003 Oct; 278 (41): 40305-16.
73. Jiang K, Apostolatos AH, Ghansah T, Watson JE, Vickers T, Cooper DR, et al. Identification of a novel antiapoptotic human protein kinase C delta isoform, PKCdeltaVIII in NT2 cells. *Biochemistry* 2008 Jan; 47 (2): 787-97.

74. Ueyama T, Ren Y, Ohmori S, Sakai K, Tamaki N, Saito N. cDNA cloning of an alternative splicing variant of protein kinase C delta (PKC deltaIII), a new truncated form of PKCdelta, in rats. *Biochem Biophys Res Commun* 2000 Mar; 269 (2): 557-63.
75. Kim JD, Seo KW, Lee EA, Quang NN, Cho HR, Kwon B. A novel mouse PKCdelta splice variant, PKCdeltaIX, inhibits etoposide-induced apoptosis. *Biochem Biophys Res Commun* 2011 Jul; 410 (2): 177-82.
76. Cooke M, Magimaidas A, Casado-Medrano V, Kazanietz MG. Protein kinase C in cancer: The top five unanswered questions. *Mol Carcinog* 2017 Jun; 56 (6): 1531-42.
77. Newton AC. Protein kinase C as a tumor suppressor. *Semin Cancer Biol* 2018 Feb; 48: 18-26.
78. Puls A, Schmidt S, Grawe F, Stabel S. Interaction of protein kinase C zeta with ZIP, a novel protein kinase C-binding protein. *Proc Natl Acad Sci U S A* 1997 Jun; 94 (12): 6191-6.
79. Sanchez P, De Carcer G, Sandoval IV, Moscat J, Diaz-Meco MT. Localization of atypical protein kinase C isoforms into lysosome-targeted endosomes through interaction with p62. *Mol Cell Biol* 1998 May; 18 (5): 3069-80.
80. Joberty G, Petersen C, Gao L, Macara IG. The cell-polarity protein Par6 links Par3 and atypical protein kinase C to Cdc42. *Nat Cell Biol* 2000 Aug; 2 (8): 531-9.
81. Lin D, Edwards AS, Fawcett JP, Mbamalu G, Scott JD, Pawson T. A mammalian PAR-3-PAR-6 complex implicated in Cdc42/Rac1 and aPKC signalling and cell polarity. *Nat Cell Biol* 2000 Aug; 2 (8): 540-7.
82. Qiu RG, Abo A, Steven Martin G. A human homolog of the *C. elegans* polarity determinant Par-6 links Rac and Cdc42 to PKCzeta signaling and cell transformation. *Curr Biol* 2000 Jun; 10 (12): 697-707.
83. Mochly-Rosen D. Localization of protein kinases by anchoring proteins: a theme in signal transduction. *Science* 1995 Apr; 268 (5208): 247-51.
84. Budas GR, Churchill EN, Disatnik MH, Sun L, Mochly-Rosen D. Mitochondrial import of PKCepsilon is mediated by HSP90: a role in cardioprotection from ischaemia and reperfusion injury. *Cardiovasc Res* 2010 Oct; 88 (1): 83-92.
85. Antal CE, Newton AC. Tuning the signalling output of protein kinase C. *Biochem Soc Trans* 2014 Dec; 42 (6): 1477-83.

86. Antal CE, Callender JA, Kornev AP, Taylor SS, Newton AC. Intramolecular C2 Domain-Mediated Autoinhibition of Protein Kinase C betaII. *Cell Rep* 2015 Aug; 12 (8): 1252-60.
87. Gould CM, Kannan N, Taylor SS, Newton AC. The chaperones Hsp90 and Cdc37 mediate the maturation and stabilization of protein kinase C through a conserved PXXP motif in the C-terminal tail. *J Biol Chem* 2009 Feb; 284 (8): 4921-35.
88. Corbalan-Garcia S, Garcia-Garcia J, Rodriguez-Alfaro JA, Gomez-Fernandez JC. A new phosphatidylinositol 4,5-bisphosphate-binding site located in the C2 domain of protein kinase C alpha. *J Biol Chem* 2003 Feb; 278 (7): 4972-80.
89. Evans JH, Murray D, Leslie CC, Falke JJ. Specific translocation of protein kinase C alpha to the plasma membrane requires both Ca²⁺ and PIP₂ recognition by its C2 domain. *Mol Biol Cell* 2006 Jan; 17 (1): 56-66.
90. Giorgione JR, Lin JH, McCammon JA, Newton AC. Increased membrane affinity of the C1 domain of protein kinase C delta compensates for the lack of involvement of its C2 domain in membrane recruitment. *J Biol Chem* 2006 Jan; 281 (3): 1660-9.
91. Dries DR, Gallegos LL, Newton AC. A single residue in the C1 domain sensitizes novel protein kinase C isoforms to cellular diacylglycerol production. *J Biol Chem* 2007 Jan; 282 (2): 826-30.
92. Gallegos LL, Kunkel MT, Newton AC. Targeting protein kinase C activity reporter to discrete intracellular regions reveals spatiotemporal differences in agonist-dependent signaling. *J Biol Chem* 2006 Oct; 281 (41): 30947-56.
93. Jaken S, Tashjian AH, Jr., Blumberg PM. Characterization of phorbol ester receptors and their down-modulation in GH4C1 rat pituitary cells. *Cancer Res* 1981 Jun; 41 (6): 2175-81.
94. Dutil EM, Keranen LM, DePaoli-Roach AA, Newton AC. In vivo regulation of protein kinase C by trans-phosphorylation followed by autophosphorylation. *J Biol Chem* 1994 Nov; 269 (47): 29359-62.
95. Gao T, Brognard J, Newton AC. The phosphatase PHLPP controls the cellular levels of protein kinase C. *J Biol Chem* 2008 Mar; 283 (10): 6300-11.
96. Hansra G, Garcia-Paramio P, Prevostel C, Whelan RD, Bornancin F, Parker PJ. Multisite dephosphorylation and desensitization of conventional protein kinase C isotypes. *Biochem J* 1999 Sep; 342 (Pt 2): 337-44.

97. Leontieva OV, Black JD. Identification of two distinct pathways of protein kinase Calpha down-regulation in intestinal epithelial cells. *J Biol Chem* 2004 Feb; 279 (7): 5788-801.
98. Reyland ME, Jones DN. Multifunctional roles of PKCdelta: Opportunities for targeted therapy in human disease. *Pharmacol Ther* 2016 Sep; 165: 1-13.
99. Reyland ME. Protein kinase C isoforms: Multi-functional regulators of cell life and death. *Front Biosci (Landmark Ed)* 2009 Jan; 14: 2386-99.
100. Antal CE, Hudson AM, Kang E, Zanca C, Wirth C, Stephenson NL, et al. Cancer-associated protein kinase C mutations reveal kinase's role as tumor suppressor. *Cell* 2015 Jan; 160 (3): 489-502.
101. Hata AN, Engelman JA, Faber AC. The BCL2 Family: Key Mediators of the Apoptotic Response to Targeted Anticancer Therapeutics. *Cancer Discov* 2015 May; 5 (5): 475-87.
102. Mukhopadhyay S, Panda PK, Sinha N, Das DN, Bhutia SK. Autophagy and apoptosis: where do they meet? *Apoptosis* 2014 Apr; 19 (4): 555-66.
103. Dillon CP, Green DR. Molecular Cell Biology of Apoptosis and Necroptosis in Cancer. *Adv Exp Med Biol* 2016; 930: 1-23.
104. Galluzzi L, Kepp O, Kroemer G. Mitochondria: master regulators of danger signalling. *Nat Rev Mol Cell Biol* 2012 Dec; 13 (12): 780-8.
105. Tait SW, Green DR. Mitochondria and cell death: outer membrane permeabilization and beyond. *Nat Rev Mol Cell Biol* 2010 Sep; 11 (9): 621-32.
106. Illera VA, Perandones CE, Stunz LL, Mower DA, Jr., Ashman RF. Apoptosis in splenic B lymphocytes. Regulation by protein kinase C and IL-4. *J Immunol* 1993 Sep; 151 (6): 2965-73.
107. Lucas M, Sanchez-Margalet V. Protein kinase C involvement in apoptosis. *Gen Pharmacol* 1995 Sep; 26 (5): 881-7.
108. Brodie C, Blumberg PM. Regulation of cell apoptosis by protein kinase c delta. *Apoptosis* 2003 Jan; 8 (1): 19-27.
109. Majumder PK, Mishra NC, Sun X, Bharti A, Kharbanda S, Saxena S, et al. Targeting of protein kinase C delta to mitochondria in the oxidative stress response. *Cell Growth Differ* 2001 Sep; 12 (9): 465-70.

110. Matassa AA, Carpenter L, Biden TJ, Humphries MJ, Reyland ME. PKCdelta is required for mitochondrial-dependent apoptosis in salivary epithelial cells. *J Biol Chem* 2001 Aug; 276 (32): 29719-28.

111. Basu A, Pal D. Two faces of protein kinase Cdelta: the contrasting roles of PKCdelta in cell survival and cell death. *ScientificWorldJournal* 2010 Nov; 10: 2272-84.

112. Leitges M, Mayr M, Braun U, Mayr U, Li C, Pfister G, et al. Exacerbated vein graft arteriosclerosis in protein kinase Cdelta-null mice. *J Clin Invest* 2001 Nov; 108 (10): 1505-12.

113. Humphries MJ, Limesand KH, Schneider JC, Nakayama KI, Anderson SM, Reyland ME. Suppression of apoptosis in the protein kinase Cdelta null mouse in vivo. *J Biol Chem* 2006 Apr; 281 (14): 9728-37.

114. DeVries TA, Neville MC, Reyland ME. Nuclear import of PKCdelta is required for apoptosis: identification of a novel nuclear import sequence. *EMBO J* 2002 Nov; 21 (22): 6050-60.

115. Ghayur T, Hugunin M, Talanian RV, Ratnofsky S, Quinlan C, Emoto Y, et al. Proteolytic activation of protein kinase C delta by an ICE/CED 3-like protease induces characteristics of apoptosis. *J Exp Med* 1996 Dec; 184 (6): 2399-404.

116. DeVries-Seimon TA, Ohm AM, Humphries MJ, Reyland ME. Induction of apoptosis is driven by nuclear retention of protein kinase C delta. *J Biol Chem* 2007 Aug; 282 (31): 22307-14.

117. Bharti A, Kraeft SK, Gounder M, Pandey P, Jin S, Yuan ZM, et al. Inactivation of DNA-dependent protein kinase by protein kinase Cdelta: implications for apoptosis. *Mol Cell Biol* 1998 Nov; 18 (11): 6719-28.

118. Majumder PK, Pandey P, Sun X, Cheng K, Datta R, Saxena S, et al. Mitochondrial translocation of protein kinase C delta in phorbol ester-induced cytochrome c release and apoptosis. *J Biol Chem* 2000 Jul; 275 (29): 21793-6.

119. Murriel CL, Churchill E, Inagaki K, Szweda LI, Mochly-Rosen D. Protein kinase Cdelta activation induces apoptosis in response to cardiac ischemia and reperfusion damage: a mechanism involving BAD and the mitochondria. *J Biol Chem* 2004 Nov; 279 (46): 47985-91.

120. Choi SY, Kim MJ, Kang CM, Bae S, Cho CK, Soh JW, et al. Activation of Bak and Bax through c-abl-protein kinase Cdelta-p38 MAPK signaling in response to ionizing

radiation in human non-small cell lung cancer cells. *J Biol Chem* 2006 Mar; 281 (11): 7049-59.

121. Abbas T, White D, Hui L, Yoshida K, Foster DA, Bargonetti J. Inhibition of human p53 basal transcription by down-regulation of protein kinase Cdelta. *J Biol Chem*. 2004;279(11):9970-7.

122. Yoshida K, Liu H, Miki Y. Protein kinase C delta regulates Ser46 phosphorylation of p53 tumor suppressor in the apoptotic response to DNA damage. *J Biol Chem* 2006 Mar; 281 (9): 5734-40.

123. Hecker E. Cocarcinogenic principles from the seed oil of *Croton tiglium* and from other Euphorbiaceae. *Cancer Res* 1968 Nov; 28 (11): 2338-49.

124. Ewing MW, Conti CJ, Kruszewski FH, Slaga TJ, DiGiovanni J. Tumor progression in Sencar mouse skin as a function of initiator dose and promoter dose, duration, and type. *Cancer Res* 1988 Dec; 48 (24 Pt 1): 7048-54.

125. Yuspa SH. Mechanisms of initiation and promotion in mouse epidermis. *IARC Sci Publ* 1984 (56): 191-204.

126. Ono Y, Fujii T, Igarashi K, Kuno T, Tanaka C, Kikkawa U, et al. Phorbol ester binding to protein kinase C requires a cysteine-rich zinc-finger-like sequence. *Proc Natl Acad Sci U S A* 1989 Jul; 86 (13): 4868-71.

127. Zhang G, Kazanietz MG, Blumberg PM, Hurley JH. Crystal structure of the cys2 activator-binding domain of protein kinase C delta in complex with phorbol ester. *Cell* 1995 Jun; 81 (6): 917-24.

128. Dries DR, Newton AC. Kinetic analysis of the interaction of the C1 domain of protein kinase C with lipid membranes by stopped-flow spectroscopy. *J Biol Chem* 2008 Mar; 283 (12): 7885-93.

129. Cameron AJ, Procyk KJ, Leitges M, Parker PJ. PKC alpha protein but not kinase activity is critical for glioma cell proliferation and survival. *Int J Cancer* 2008Aug; 123 (4): 769-79.

130. Haughian JM, Bradford AP. Protein kinase C alpha (PKCalpha) regulates growth and invasion of endometrial cancer cells. *J Cell Physiol* 2009 Jul; 220 (1): 112-8.

131. Nakagawa S, Fujii T, Yokoyama G, Kazanietz MG, Yamana H, Shirouzu K. Cell growth inhibition by all-trans retinoic acid in SKBR-3 breast cancer cells: involvement of

protein kinase Calpha and extracellular signal-regulated kinase mitogen-activated protein kinase. *Mol Carcinog* 2003 Nov; 38 (3): 106-16.

132. Kong C, Zhu Y, Liu D, Yu M, Li S, Li Z, et al. Role of protein kinase C-alpha in superficial bladder carcinoma recurrence. *Urology* 2005 Jun; 65 (6): 1228-32.

133. Mandil R, Ashkenazi E, Blass M, Kronfeld I, Kazimirsky G, Rosenthal G, et al. Protein kinase Calpha and protein kinase Cdelta play opposite roles in the proliferation and apoptosis of glioma cells. *Cancer Res* 2001 Jun; 61 (11): 4612-9.

134. Blackburn RV, Galoforo SS, Berns CM, Motwani NM, Corry PM, Lee YJ. Differential induction of cell death in human glioma cell lines by sodium nitroprusside. *Cancer* 1998 Mar; 82 (6): 1137-45.

135. Ways DK, Kukoly CA, deVente J, Hooker JL, Bryant WO, Posekany KJ, et al. MCF-7 breast cancer cells transfected with protein kinase C-alpha exhibit altered expression of other protein kinase C isoforms and display a more aggressive neoplastic phenotype. *J Clin Invest* 1995 Apr; 95 (4): 1906-15.

136. Tanaka Y, Gavrielides MV, Mitsuuchi Y, Fujii T, Kazanietz MG. Protein kinase C promotes apoptosis in LNCaP prostate cancer cells through activation of p38 MAPK and inhibition of the Akt survival pathway. *J Biol Chem* 2003 Sep; 278 (36): 33753-62.

137. Oliva JL, Caino MC, Senderowicz AM, Kazanietz MG. S-Phase-specific activation of PKC alpha induces senescence in non-small cell lung cancer cells. *J Biol Chem* 2008 Feb; 283 (9): 5466-76.

138. Tan M, Li P, Sun M, Yin G, Yu D. Upregulation and activation of PKC alpha by ErbB2 through Src promotes breast cancer cell invasion that can be blocked by combined treatment with PKC alpha and Src inhibitors. *Oncogene* 2006 Jun; 25 (23): 3286-95.

139. Kim S, Han J, Lee SK, Choi MY, Kim J, Lee J, et al. Berberine suppresses the TPA-induced MMP-1 and MMP-9 expressions through the inhibition of PKC-alpha in breast cancer cells. *J Surg Res* 2012 Jul; 176 (1): e21-9.

140. Lahn M, Kohler G, Sundell K, Su C, Li S, Paterson BM, et al. Protein kinase C alpha expression in breast and ovarian cancer. *Oncology* 2004; 67 (1): 1-10.

141. Kim J, Thorne SH, Sun L, Huang B, Mochly-Rosen D. Sustained inhibition of PKCalpha reduces intravasation and lung seeding during mammary tumor metastasis in an in vivo mouse model. *Oncogene* 2011 Jan; 30 (3): 323-33.

142. Watanabe T, Ono Y, Taniyama Y, Hazama K, Igarashi K, Ogita K, et al. Cell division arrest induced by phorbol ester in CHO cells overexpressing protein kinase C-delta subspecies. *Proc Natl Acad Sci U S A* 1992 Nov; 89 (21): 10159-63.
143. Nakagawa M, Oliva JL, Kothapalli D, Fournier A, Assoian RK, Kazanietz MG. Phorbol ester-induced G1 phase arrest selectively mediated by protein kinase Cdelta-dependent induction of p21. *J Biol Chem* 2005 Oct; 280 (40): 33926-34.
144. Fujii T, Garcia-Bermejo ML, Bernabo JL, Caamano J, Ohba M, Kuroki T, et al. Involvement of protein kinase C delta (PKCdelta) in phorbol ester-induced apoptosis in LNCaP prostate cancer cells. Lack of proteolytic cleavage of PKCdelta. *J Biol Chem* 2000 Mar; 275 (11): 7574-82.
145. Reddig PJ, Dreckschmidt NE, Ahrens H, Simsiman R, Tseng CP, Zou J, et al. Transgenic mice overexpressing protein kinase Cdelta in the epidermis are resistant to skin tumor promotion by 12-O-tetradecanoylphorbol-13-acetate. *Cancer Res* 1999 Nov; 59 (22): 5710-8.
146. Cerda SR, Bissonnette M, Scaglione-Sewell B, Lyons MR, Khare S, Mustafi R, et al. PKC-delta inhibits anchorage-dependent and -independent growth, enhances differentiation, and increases apoptosis in CaCo-2 cells. *Gastroenterology* 2001 Jun; 120 (7): 1700-12.
147. Perletti GP, Marras E, Concaro P, Piccinini F, Tashjian AH, Jr. PKCdelta acts as a growth and tumor suppressor in rat colonic epithelial cells. *Oncogene* 1999 Feb; 18 (5): 1251-6.
148. Perletti G, Marras E, Osti D, Felici L, Zaro S, de Eguileor M. PKCdelta requires p53 for suppression of the transformed phenotype in human colon cancer cells. *J Cell Mol Med* 2004 Oct-Dec; 8 (4): 563-9.
149. Cerda SR, Mustafi R, Little H, Cohen G, Khare S, Moore C, et al. Protein kinase C delta inhibits Caco-2 cell proliferation by selective changes in cell cycle and cell death regulators. *Oncogene* 2006 May; 25 (22): 3123-38.
150. Hernandez-Maqueda JG, Luna-Ulloa LB, Santoyo-Ramos P, Castaneda-Patlan MC, Robles-Flores M. Protein kinase C delta negatively modulates canonical Wnt pathway and cell proliferation in colon tumor cell lines. *PLoS One* 2013 Mar; 8 (3): e58540.
151. Grosioni VC, Falbo KB, Kazanietz MG, de Kier Joffe ED, Urtreger AJ. Protein kinase C delta enhances proliferation and survival of murine mammary cells. *Mol Carcinog* 2007 May; 46 (5): 381-90.

152. Kim J, Koyanagi T, Mochly-Rosen D. PKCdelta activation mediates angiogenesis via NADPH oxidase activity in PC-3 prostate cancer cells. *Prostate* 2011 Jun; 71 (9): 946-54.
153. Jackson D, Zheng Y, Lyo D, Shen Y, Nakayama K, Nakayama KI, et al. Suppression of cell migration by protein kinase Cdelta. *Oncogene* 2005 Apr; 24 (18): 3067-72.
154. Kiley SC, Clark KJ, Goodnough M, Welch DR, Jaken S. Protein kinase C delta involvement in mammary tumor cell metastasis. *Cancer Res* 1999 Jul; 59 (13): 3230-8.
155. Li N, Du ZX, Zong ZH, Liu BQ, Li C, Zhang Q, et al. PKCdelta-mediated phosphorylation of BAG3 at Ser187 site induces epithelial-mesenchymal transition and enhances invasiveness in thyroid cancer FRO cells. *Oncogene* 2013 Sep; 32 (38): 4539-48.
156. Mischak H, Goodnight JA, Kolch W, Martiny-Baron G, Schaechtle C, Kazanietz MG, et al. Overexpression of protein kinase C-delta and -epsilon in NIH 3T3 cells induces opposite effects on growth, morphology, anchorage dependence, and tumorigenicity. *J Biol Chem* 1993 Mar; 268 (9): 6090-6.
157. Cacace AM, Guadagno SN, Krauss RS, Fabbro D, Weinstein IB. The epsilon isoform of protein kinase C is an oncogene when overexpressed in rat fibroblasts. *Oncogene* 1993 Aug; 8 (8): 2095-104.
158. Perletti GP, Folini M, Lin HC, Mischak H, Piccinini F, Tashjian AH, Jr. Overexpression of protein kinase C epsilon is oncogenic in rat colonic epithelial cells. *Oncogene* 1996 Feb; 12 (4): 847-54.
159. Lu D, Sivaprasad U, Huang J, Shankar E, Morrow S, Basu A. Protein kinase C-epsilon protects MCF-7 cells from TNF-mediated cell death by inhibiting Bax translocation. *Apoptosis* 2007 Oct; 12 (10): 1893-900.
160. Pan Q, Bao LW, Kleer CG, Sabel MS, Griffith KA, Teknos TN, et al. Protein kinase C epsilon is a predictive biomarker of aggressive breast cancer and a validated target for RNA interference anticancer therapy. *Cancer Res* 2005 Sep; 65 (18): 8366-71.
161. Gorin MA, Pan Q. Protein kinase C epsilon: an oncogene and emerging tumor biomarker. *Mol Cancer* 2009 Feb; 8: 9.
162. Huang B, Cao K, Li X, Guo S, Mao X, Wang Z, et al. The expression and role of protein kinase C (PKC) epsilon in clear cell renal cell carcinoma. *J Exp Clin Cancer Res* 2011 Sep; 30: 88.

163. Bae KM, Wang H, Jiang G, Chen MG, Lu L, Xiao L. Protein kinase C epsilon is overexpressed in primary human non-small cell lung cancers and functionally required for proliferation of non-small cell lung cancer cells in a p21/Cip1-dependent manner. *Cancer Res* 2007 Jul; 67 (13): 6053-63.
164. Baxter G, Oto E, Daniel-Issakani S, Strulovici B. Constitutive presence of a catalytic fragment of protein kinase C epsilon in a small cell lung carcinoma cell line. *J Biol Chem* 1992 Jan; 267 (3): 1910-7.
165. Nazarenko I, Jenny M, Keil J, Gieseler C, Weisshaupt K, Sehouli J, et al. Atypical protein kinase C zeta exhibits a proapoptotic function in ovarian cancer. *Mol Cancer Res* 2010 Jun; 8 (6): 919-34.
166. Ma L, Tao Y, Duran A, Llado V, Galvez A, Barger JF, et al. Control of nutrient stress-induced metabolic reprogramming by PKCzeta in tumorigenesis. *Cell* 2013 Jan; 152 (3): 599-611.
167. Xin M, Gao F, May WS, Flagg T, Deng X. Protein kinase Czeta abrogates the proapoptotic function of Bax through phosphorylation. *J Biol Chem* 2007 Jul; 282 (29): 21268-77.
168. Rimessi A, Zecchini E, Siviero R, Giorgi C, Leo S, Rizzuto R, et al. The selective inhibition of nuclear PKCzeta restores the effectiveness of chemotherapeutic agents in chemoresistant cells. *Cell Cycle* 2012 Mar; 11 (5): 1040-8.
169. Regala RP, Weems C, Jamieson L, Copland JA, Thompson EA, Fields AP. Atypical protein kinase Ciota plays a critical role in human lung cancer cell growth and tumorigenicity. *J Biol Chem* 2005 Sep; 280 (35): 31109-15.
170. Regala RP, Weems C, Jamieson L, Khor A, Edell ES, Lohse CM, et al. Atypical protein kinase C iota is an oncogene in human non-small cell lung cancer. *Cancer Res* 2005 Jul; 65 (19): 8905-11.
171. Scotti ML, Smith KE, Butler AM, Calcagno SR, Crawford HC, Leitges M, et al. Protein kinase C iota regulates pancreatic acinar-to-ductal metaplasia. *PLoS One* 2012 Feb; 7 (2): e30509.
172. Wang Y, Hill KS, Fields AP. PKCiota maintains a tumor-initiating cell phenotype that is required for ovarian tumorigenesis. *Mol Cancer Res* 2013 Dec; 11 (12): 1624-35.

173. Gao J, Aksoy BA, Dogrusoz U, Dresdner G, Gross B, Sumer SO, et al. Integrative analysis of complex cancer genomics and clinical profiles using the cBioPortal. *Sci Signal* 2013 Apr; 6 (269): pl1.

174. Meharena HS, Chang P, Keshwani MM, Oruganty K, Nene AK, Kannan N, et al. Deciphering the structural basis of eukaryotic protein kinase regulation. *PLoS Biol* 2013 Oct; 11 (10): e1001680.

175. Garcia-Paramio P, Cabrerizo Y, Bornancin F, Parker PJ. The broad specificity of dominant inhibitory protein kinase C mutants infers a common step in phosphorylation. *Biochem J* 1998 Aug; 333 (Pt 3): 631-6.

176. Newton AC, Brognard J. Reversing the Paradigm: Protein Kinase C as a Tumor Suppressor. *Trends Pharmacol Sci* 2017 May; 38 (5): 438-47.

177. Hunter T, Ling N, Cooper JA. Protein kinase C phosphorylation of the EGF receptor at a threonine residue close to the cytoplasmic face of the plasma membrane. *Nature* 1984 Oct; 311 (5985): 480-3.

178. Livneh E, Dull TJ, Berent E, Prywes R, Ullrich A, Schlessinger J. Release of a phorbol ester-induced mitogenic block by mutation at Thr-654 of the epidermal growth factor receptor. *Mol Cell Biol* 1988 Jun; 8 (6): 2302-8.

179. Livneh E, Reiss N, Berent E, Ullrich A, Schlessinger J. An insertional mutant of epidermal growth factor receptor allows dissection of diverse receptor functions. *EMBO J* 1987 Sep; 6 (9): 2669-76.

180. Santiskulvong C, Rozengurt E. Protein kinase C α mediates feedback inhibition of EGF receptor transactivation induced by Gq-coupled receptor agonists. *Cell Signal* 2007 Jun; 19 (6): 1348-57.

181. Wang MT, Holderfield M, Galeas J, Delrosario R, To MD, Balmain A, et al. K-Ras Promotes Tumorigenicity through Suppression of Non-canonical Wnt Signaling. *Cell* 2015 Nov; 163 (5): 1237-51.

182. Isakov N. Protein kinase C (PKC) isoforms in cancer, tumor promotion and tumor suppression. *Semin Cancer Biol* 2018 Feb; 48: 36-52.

183. Karaman MW, Herrgard S, Treiber DK, Gallant P, Atteridge CE, Campbell BT, et al. A quantitative analysis of kinase inhibitor selectivity. *Nat Biotechnol* 2008 Jan; 26 (1): 127-32.

184. Davis MI, Hunt JP, Herrgard S, Ciceri P, Wodicka LM, Pallares G, et al. Comprehensive analysis of kinase inhibitor selectivity. *Nat Biotechnol* 2011 Oct; 29 (11): 1046-51.
185. Anastassiadis T, Deacon SW, Devarajan K, Ma H, Peterson JR. Comprehensive assay of kinase catalytic activity reveals features of kinase inhibitor selectivity. *Nat Biotechnol* 2011 Oct; 29 (11): 1039-45.
186. Wilkinson SE, Parker PJ, Nixon JS. Isoenzyme specificity of bisindolylmaleimides, selective inhibitors of protein kinase C. *Biochem J* 1993 Sep; 294 (Pt 2): 335-7.
187. Propper DJ, McDonald AC, Man A, Thavasu P, Balkwill F, Braybrooke JP, et al. Phase I and pharmacokinetic study of PKC412, an inhibitor of protein kinase C. *J Clin Oncol* 2001 Mar; 19 (5): 1485-92.
188. Monnerat C, Henriksson R, Le Chevalier T, Novello S, Berthaud P, Faivre S, et al. Phase I study of PKC412 (N-benzoyl-staurosporine), a novel oral protein kinase C inhibitor, combined with gemcitabine and cisplatin in patients with non-small-cell lung cancer. *Ann Oncol* 2004 Feb; 15 (2): 316-23.
189. Chandesris MO, Damaj G, Canioni D, Brouzes C, Lhermitte L, Hanssens K, et al. Midostaurin in Advanced Systemic Mastocytosis. *N Engl J Med* 2016 Jun; 374 (26): 2605-7.
190. Gallogly MM, Lazarus HM. Midostaurin: an emerging treatment for acute myeloid leukemia patients. *J Blood Med* 2016 Apr; 7: 73-83.
191. Graff JR, McNulty AM, Hanna KR, Konicek BW, Lynch RL, Bailey SN, et al. The protein kinase C β -selective inhibitor, Enzastaurin (LY317615.HCl), suppresses signaling through the AKT pathway, induces apoptosis, and suppresses growth of human colon cancer and glioblastoma xenografts. *Cancer Res* 2005 Aug; 65 (16): 7462-9.
192. Crump M, Leppa S, Fayad L, Lee JJ, Di Rocco A, Ogura M, et al. Randomized, Double-Blind, Phase III Trial of Enzastaurin Versus Placebo in Patients Achieving Remission After First-Line Therapy for High-Risk Diffuse Large B-Cell Lymphoma. *J Clin Oncol* 2016 Jul; 34 (21): 2484-92.
193. Kilburn LB, Kocak M, Decker RL, Wetmore C, Chintagumpala M, Su J, et al. A phase 1 and pharmacokinetic study of enzastaurin in pediatric patients with refractory primary central nervous system tumors: a pediatric brain tumor consortium study. *Neuro Oncol* 2015 Feb; 17 (2): 303-11.

194. Oda Y, Iwamoto FM, Moustakas A, Fraum TJ, Salgado CA, Li A, et al. A phase II trial of enzastaurin (LY317615) in combination with bevacizumab in adults with recurrent malignant gliomas. *J Neurooncol* 2016 Mar; 127 (1): 127-35.
195. Gschwendt M, Muller HJ, Kielbassa K, Zang R, Kittstein W, Rincke G, et al. Rottlerin, a novel protein kinase inhibitor. *Biochem Biophys Res Commun* 1994 Feb; 199 (1): 93-8.
196. Soltoff SP. Rottlerin is a mitochondrial uncoupler that decreases cellular ATP levels and indirectly blocks protein kinase Cdelta tyrosine phosphorylation. *J Biol Chem* 2001 Oct; 276 (41): 37986-92.
197. Takashima A, English B, Chen Z, Cao J, Cui R, Williams RM, et al. Protein kinase Cdelta is a therapeutic target in malignant melanoma with NRAS mutation. *ACS Chem Biol* 2014 Apr; 9 (4): 1003-14.
198. Berkow RL, Kraft AS. Bryostatin, a non-phorbol macrocyclic lactone, activates intact human polymorphonuclear leukocytes and binds to the phorbol ester receptor. *Biochem Biophys Res Commun* 1985 Sep; 131 (3): 1109-16.
199. Hennings H, Blumberg PM, Pettit GR, Herald CL, Shores R, Yuspa SH. Bryostatin 1, an activator of protein kinase C, inhibits tumor promotion by phorbol esters in SENCAR mouse skin. *Carcinogenesis* 1987 Sep; 8 (9): 1343-6.
200. Szallasi Z, Denning MF, Smith CB, Dlugosz AA, Yuspa SH, Pettit GR, et al. Bryostatin 1 protects protein kinase C-delta from down-regulation in mouse keratinocytes in parallel with its inhibition of phorbol ester-induced differentiation. *Mol Pharmacol* 1994 Nov; 46 (5): 840-50.
201. Propper DJ, Macaulay V, O'Byrne KJ, Braybrooke JP, Wilner SM, Ganesan TS, et al. A phase II study of bryostatin 1 in metastatic malignant melanoma. *Br J Cancer* 1998 Nov; 78 (10): 1337-41.
202. Zonder JA, Shields AF, Zalupski M, Chaplen R, Heilbrun LK, Arlauskas P, et al. A phase II trial of bryostatin 1 in the treatment of metastatic colorectal cancer. *Clin Cancer Res* 2001 Jan; 7 (1): 38-42.
203. Ajani JA, Jiang Y, Faust J, Chang BB, Ho L, Yao JC, et al. A multi-center phase II study of sequential paclitaxel and bryostatin-1 (NSC 339555) in patients with untreated, advanced gastric or gastroesophageal junction adenocarcinoma. *Invest New Drugs* 2006 Jul; 24 (4): 353-7.

204. Ku GY, Ilson DH, Schwartz LH, Capanu M, O'Reilly E, Shah MA, et al. Phase II trial of sequential paclitaxel and 1 h infusion of bryostatin-1 in patients with advanced esophageal cancer. *Cancer Chemother Pharmacol* 2008 Oct; 62 (5): 875-80.
205. Barr PM, Lazarus HM, Cooper BW, Schluchter MD, Panneerselvam A, Jacobberger JW, et al. Phase II study of bryostatin 1 and vincristine for aggressive non-Hodgkin lymphoma relapsing after an autologous stem cell transplant. *Am J Hematol* 2009 Aug; 84 (8): 484-7.
206. Wender PA, Baryza JL, Brenner SE, DeChristopher BA, Loy BA, Schrier AJ, et al. Design, synthesis, and evaluation of potent bryostatin analogs that modulate PKC translocation selectivity. *Proc Natl Acad Sci U S A* 2011 Apr; 108 (17): 6721-6.
207. DeChristopher BA, Fan AC, Felsher DW, Wender PA. "Picolog," a synthetically-available bryostatin analog, inhibits growth of MYC-induced lymphoma in vivo. *Oncotarget* 2012 Jan; 3 (1): 58-66.
208. Lopez-Campistrous A, Song X, Schrier AJ, Wender PA, Dower NA, Stone JC. Bryostatin analogue-induced apoptosis in mantle cell lymphoma cell lines. *Exp Hematol* 2012 Aug; 40 (8): 646-56 e2.
209. Garcia-Bermejo ML, Leskow FC, Fujii T, Wang Q, Blumberg PM, Ohba M, et al. Diacylglycerol (DAG)-lactones, a new class of protein kinase C (PKC) agonists, induce apoptosis in LNCaP prostate cancer cells by selective activation of PKC α . *J Biol Chem* 2002 Jan; 277 (1): 645-55.
210. Kedei N, Lundberg DJ, Toth A, Welburn P, Garfield SH, Blumberg PM. Characterization of the interaction of ingenol 3-angelate with protein kinase C. *Cancer Res* 2004 May; 64 (9): 3243-55.
211. Bettencourt MS. Treatment of superficial basal cell carcinoma with ingenol mebutate gel, 0.05%. *Clin Cosmet Investig Dermatol* 2016 Aug; 9: 205-9.
212. Mochly-Rosen D, Das K, Grimes KV. Protein kinase C, an elusive therapeutic target? *Nat Rev Drug Discov* 2012 Dec; 11 (12): 937-57.
213. Budas GR, Koyanagi T, Churchill EN, Mochly-Rosen D. Competitive inhibitors and allosteric activators of protein kinase C isoenzymes: a personal account and progress report on transferring academic discoveries to the clinic. *Biochem Soc Trans* 2007 Nov; 35 (Pt 5): 1021-6.

214. Brandman R, Disatnik MH, Churchill E, Mochly-Rosen D. Peptides derived from the C2 domain of protein kinase C epsilon (epsilon PKC) modulate epsilon PKC activity and identify potential protein-protein interaction surfaces. *J Biol Chem* 2007 Feb; 282 (6): 4113-23.

215. Caino MC, Lopez-Haber C, Kim J, Mochly-Rosen D, Kazanietz MG. Protein kinase C ϵ is required for non-small cell lung carcinoma growth and regulates the expression of apoptotic genes. *Oncogene* 2012 May; 31 (20): 2593-600.

216. Caino MC, Lopez-Haber C, Kissil JL, Kazanietz MG. Non-small cell lung carcinoma cell motility, Rac activation and metastatic dissemination are mediated by protein kinase C epsilon. *PLoS One*. 2012;7(2):e31714.

217. Erdogan E, Lamark T, Stallings-Mann M, Lee J, Pellecchia M, Thompson EA, et al. Aurothiomalate inhibits transformed growth by targeting the PB1 domain of protein kinase C ι . *J Biol Chem* 2006 Sep; 281 (38): 28450-9.

218. Regala RP, Thompson EA, Fields AP. Atypical protein kinase C iota expression and aurothiomalate sensitivity in human lung cancer cells. *Cancer Res* 2008 Jul; 68 (14): 5888-95.

219. Dean N, McKay R, Miraglia L, Howard R, Cooper S, Giddings J, et al. Inhibition of growth of human tumor cell lines in nude mice by an antisense oligonucleotide inhibitor of protein kinase C α expression. *Cancer Res* 1996 Aug; 56 (15): 3499-507.

220. Tortora G, Ciardiello F. Antisense strategies targeting protein kinase C: preclinical and clinical development. *Semin Oncol* 2003 Aug; 30 (4 Suppl 10): 26-31.

221. Martiny-Baron G, Fabbro D. Classical PKC isoforms in cancer. *Pharmacol Res* 2007 Jun; 55 (6): 477-86.

222. Ma CX, Ellis MJ, Petroni GR, Guo Z, Cai SR, Ryan CE, et al. A phase II study of UCN-01 in combination with irinotecan in patients with metastatic triple negative breast cancer. *Breast Cancer Res Treat* 2013 Jan; 137 (2): 483-92.

223. Li T, Christensen SD, Frankel PH, Margolin KA, Agarwala SS, Luu T, et al. A phase II study of cell cycle inhibitor UCN-01 in patients with metastatic melanoma: a California Cancer Consortium trial. *Invest New Drugs* 2012 Apr; 30 (2): 741-8.

224. Welch S, Hirte HW, Carey MS, Hotte SJ, Tsao MS, Brown S, et al. UCN-01 in combination with topotecan in patients with advanced recurrent ovarian cancer: a study of

the Princess Margaret Hospital Phase II consortium. *Gynecol Oncol* 2007 Aug; 106 (2): 305-10.

225. Stone RM, Mandrekar SJ, Sanford BL, Laumann K, Geyer S, Bloomfield CD, et al. Midostaurin plus Chemotherapy for Acute Myeloid Leukemia with a FLT3 Mutation. *N Engl J Med* 2017 Aug; 377 (5): 454-64.

226. Millward MJ, House C, Bowtell D, Webster L, Olver IN, Gore M, et al. The multikinase inhibitor midostaurin (PKC412A) lacks activity in metastatic melanoma: a phase IIA clinical and biologic study. *Br J Cancer* 2006 Oct; 95 (7): 829-34.

227. El-Gamal D, Williams K, LaFollette TD, Cannon M, Blachly JS, Zhong Y, et al. PKC-beta as a therapeutic target in CLL: PKC inhibitor AEB071 demonstrates preclinical activity in CLL. *Blood* 2014 Aug; 124 (9): 1481-91.

228. Richards DA, Kuefler PR, Becerra C, Wilfong LS, Gersh RH, Boehm KA, et al. Gemcitabine plus enzastaurin or single-agent gemcitabine in locally advanced or metastatic pancreatic cancer: results of a phase II, randomized, noncomparative study. *Invest New Drugs* 2011 Feb; 29 (1): 144-53.

229. Gray JE, Altiock S, Alexandrow MG, Walsh FW, Chen J, Schell MJ, et al. Phase 2 randomized study of enzastaurin (LY317615) for lung cancer prevention in former smokers. *Cancer* 2013 Mar; 119 (5): 1023-32.

230. Morgan RJ, Jr., Leong L, Chow W, Gandara D, Frankel P, Garcia A, et al. Phase II trial of bryostatin-1 in combination with cisplatin in patients with recurrent or persistent epithelial ovarian cancer: a California cancer consortium study. *Invest New Drugs* 2012 Apr; 30 (2): 723-8.

231. Lam AP, Sparano JA, Vinciguerra V, Ocean AJ, Christos P, Hochster H, et al. Phase II study of paclitaxel plus the protein kinase C inhibitor bryostatin-1 in advanced pancreatic carcinoma. *Am J Clin Oncol* 2010 Apr; 33 (2): 121-4.

232. Haas NB, Smith M, Lewis N, Littman L, Yeslow G, Joshi ID, et al. Weekly bryostatin-1 in metastatic renal cell carcinoma: a phase II study. *Clin Cancer Res* 2003 Jan; 9 (1): 109-14.

233. Siller G, Gebauer K, Welburn P, Katsamas J, Ogbourne SM. PEP005 (ingenol mebutate) gel, a novel agent for the treatment of actinic keratosis: results of a randomized, double-blind, vehicle-controlled, multicentre, phase IIa study. *Australas J Dermatol* 2009 Feb; 50 (1): 16-22.

234. Anderson L, Schmieder GJ, Werschler WP, Tschen EH, Ling MR, Stough DB, et al. Randomized, double-blind, double-dummy, vehicle-controlled study of ingenol mebutate gel 0.025% and 0.05% for actinic keratosis. *J Am Acad Dermatol* 2009 Jun; 60 (6): 934-43.

235. Lebwohl M, Swanson N, Anderson LL, Melgaard A, Xu Z, Berman B. Ingenol mebutate gel for actinic keratosis. *N Engl J Med* 2012 Mar; 366 (11): 1010-9.

236. Berman B, Goldenberg G, Hanke CW, Tying SK, Werschler WP, Knudsen KM, et al. Efficacy and safety of ingenol mebutate 0.015% gel after cryosurgery of actinic keratosis: 12-month results. *J Drugs Dermatol* 2014 Jun; 13 (6): 741-7.

237. Ramsay JR, Suhrbier A, Aylward JH, Ogbourne S, Cozzi SJ, Poulsen MG, et al. The sap from *Euphorbia peplus* is effective against human nonmelanoma skin cancers. *Br J Dermatol* 2011 Mar; 164 (3): 633-6.

238. Mansfield AS, Fields AP, Jatoi A, Qi Y, Adjei AA, Erlichman C, et al. Phase I dose escalation study of the PKC α inhibitor aurothiomalate for advanced non-small-cell lung cancer, ovarian cancer, and pancreatic cancer. *Anticancer Drugs* 2013 Nov; 24 (10): 1079-83.

239. Advani R, Peethambaram P, Lum BL, Fisher GA, Hartmann L, Long HJ, et al. A Phase II trial of aprinocarsen, an antisense oligonucleotide inhibitor of protein kinase C α , administered as a 21-day infusion to patients with advanced ovarian carcinoma. *Cancer* 2004 Jan; 100 (2): 321-6.

240. Grossman SA, Alavi JB, Supko JG, Carson KA, Priet R, Dorr FA, et al. Efficacy and toxicity of the antisense oligonucleotide aprinocarsen directed against protein kinase C- α delivered as a 21-day continuous intravenous infusion in patients with recurrent high-grade astrocytomas. *Neuro Oncol* 2005 Jan; 7 (1): 32-40.

241. Vansteenkiste J, Canon JL, Riska H, Pirker R, Peterson P, John W, et al. Randomized phase II evaluation of aprinocarsen in combination with gemcitabine and cisplatin for patients with advanced/metastatic non-small cell lung cancer. *Invest New Drugs* 2005 Jun; 23 (3): 263-9.

242. Ritch P, Rudin CM, Bitran JD, Edelman MJ, Makalinao A, Irwin D, et al. Phase II study of PKC- α antisense oligonucleotide aprinocarsen in combination with gemcitabine and carboplatin in patients with advanced non-small cell lung cancer. *Lung Cancer* 2006 May; 52 (2): 173-80.

243. Paz-Ares L, Douillard JY, Koralewski P, Manegold C, Smit EF, Reyes JM, et al. Phase III study of gemcitabine and cisplatin with or without aprinocarsen, a protein kinase

C-alpha antisense oligonucleotide, in patients with advanced-stage non-small-cell lung cancer. *J Clin Oncol* 2006 Mar; 24 (9): 1428-34.

244. Rao S, Watkins D, Cunningham D, Dunlop D, Johnson P, Selby P, et al. Phase II study of ISIS 3521, an antisense oligodeoxynucleotide to protein kinase C alpha, in patients with previously treated low-grade non-Hodgkin's lymphoma. *Ann Oncol* 2004 Sep; 15 (9): 1413-8.

245. Cripps MC, Figueredo AT, Oza AM, Taylor MJ, Fields AL, Holmlund JT, et al. Phase II randomized study of ISIS 3521 and ISIS 5132 in patients with locally advanced or metastatic colorectal cancer: a National Cancer Institute of Canada clinical trials group study. *Clin Cancer Res* 2002 Jul; 8 (7): 2188-92.

246. Marshall JL, Eisenberg SG, Johnson MD, Hanfelt J, Dorr FA, El-Ashry D, et al. A phase II trial of ISIS 3521 in patients with metastatic colorectal cancer. *Clin Colorectal Cancer* 2004 Nov; 4 (4): 268-74.

247. Mattingly RR. Mitogen-activated protein kinase signaling in drug-resistant neuroblastoma cells. *Methods Mol Biol.* 2003; 218: 71-83.

248. Pan TT, Neo KL, Hu LF, Yong QC, Bian JS. H₂S preconditioning-induced PKC activation regulates intracellular calcium handling in rat cardiomyocytes. *Am J Physiol Cell Physiol* 2008 Jan; 294 (1): C169-77.

249. Hosoda K, Saito N, Kose A, Ito A, Tsujino T, Ogita K, et al. Immunocytochemical localization of the beta I subspecies of protein kinase C in rat brain. *Proc Natl Acad Sci U S A* 1989 Feb; 86 (4): 1393-7.

250. Saito N, Kose A, Ito A, Hosoda K, Mori M, Hirata M, et al. Immunocytochemical localization of beta II subspecies of protein kinase C in rat brain. *Proc Natl Acad Sci U S A* 1989 May; 86 (9): 3409-13.

251. Violin JD, Newton AC. Pathway illuminated: visualizing protein kinase C signaling. *IUBMB Life* 2003 Dec; 55 (12): 653-60.

252. Sakai N, Sasaki K, Ikegaki N, Shirai Y, Ono Y, Saito N. Direct visualization of the translocation of the gamma-subspecies of protein kinase C in living cells using fusion proteins with green fluorescent protein. *J Cell Biol* 1997 Dec; 139 (6): 1465-76.

253. Oancea E, Meyer T. Protein kinase C as a molecular machine for decoding calcium and diacylglycerol signals. *Cell* 1998 Oct; 95 (3): 307-18.

254. Wang QJ, Bhattacharyya D, Garfield S, Nacro K, Marquez VE, Blumberg PM. Differential localization of protein kinase C delta by phorbol esters and related compounds using a fusion protein with green fluorescent protein. *J Biol Chem* 1999 Dec; 274 (52): 37233-9.
255. Stryer L, Haugland RP. Energy transfer: a spectroscopic ruler. *Proc Natl Acad Sci U S A* 1967 Aug; 58 (2): 719-26.
256. Stryer L. Exploring light and life. *J Biol Chem* 2012 May; 287 (19): 15164-73.
257. Antal CE, Violin JD, Kunkel MT, Skovso S, Newton AC. Intramolecular conformational changes optimize protein kinase C signaling. *Chem Biol* 2014 Apr; 21 (4): 459-69.
258. Kumar S, Kellish P, Robinson WE, Jr., Wang D, Appella DH, Arya DP. Click dimers to target HIV TAR RNA conformation. *Biochemistry* 2012 Mar; 51 (11): 2331-47.
259. Zwier JM, Roux T, Cottet M, Durroux T, Douzon S, Bdioui S, et al. A fluorescent ligand-binding alternative using Tag-lite(R) technology. *J Biomol Screen* 2010 Dec; 15 (10): 1248-59.
260. Nomura W, Tanabe Y, Tsutsumi H, Tanaka T, Ohba K, Yamamoto N, et al. Fluorophore labeling enables imaging and evaluation of specific CXCR4-ligand interaction at the cell membrane for fluorescence-based screening. *Bioconjug Chem* 2008 Sep; 19 (9): 1917-20.
261. Nomura W, Ohashi N, Okuda Y, Narumi T, Ikura T, Ito N, et al. Fluorescence-quenching screening of protein kinase C ligands with an environmentally sensitive fluorophore. *Bioconjug Chem* 2011 May; 22 (5): 923-30.
262. Ting AY, Kain KH, Klemke RL, Tsien RY. Genetically encoded fluorescent reporters of protein tyrosine kinase activities in living cells. *Proc Natl Acad Sci U S A* 2001 Dec; 98 (26): 15003-8.
263. Zhang J, Ma Y, Taylor SS, Tsien RY. Genetically encoded reporters of protein kinase A activity reveal impact of substrate tethering. *Proc Natl Acad Sci U S A* 2001 Dec; 98 (26): 14997-5002.
264. Riedel H, Hansen H, Parissenti AM, Su L, Shieh HL, Zhu J. Phorbol ester activation of functional rat protein kinase C beta-1 causes phenotype in yeast. *J Cell Biochem* 1993Jul; 52 (3): 320-9.

265. Riedel H, Su L, Hansen H. Yeast phenotype classifies mammalian protein kinase C cDNA mutants. *Mol Cell Biol* 1993 Aug; 13 (8): 4728-35.
266. Keenan C, Goode N, Pears C. Isoform specificity of activators and inhibitors of protein kinase C gamma and delta. *FEBS Lett* 1997 Sep; 415 (1): 101-8.
267. Silva RD, Saraiva L, Coutinho I, Goncalves J, Corte-Real M. Yeast as a powerful model system for the study of apoptosis regulation by protein kinase C isoforms. *Curr Pharm Des* 2012; 18 (17): 2492-500.
268. Parissenti AM, Su L, Riedel H. Reconstitution of protein kinase C alpha function by the protein kinase C beta-I carboxy terminus. *Mol Cell Endocrinol* 1993 Dec; 98 (1): 9-16.
269. Rotenberg SA, Zhu J, Hansen H, Li XD, Sun XG, Michels CA, et al. Deletion analysis of protein kinase C alpha reveals a novel regulatory segment. *J Biochem* 1998 Oct; 124 (4): 756-63.
270. Kirwan AF, Bibby AC, Mvilongo T, Riedel H, Burke T, Millis SZ, et al. Inhibition of protein kinase C catalytic activity by additional regions within the human protein kinase C alpha-regulatory domain lying outside of the pseudosubstrate sequence. *Biochem J* 2003 Jul; 373 (Pt 2): 571-81.
271. Saraiva L, Fresco P, Pinto E, Kijjoa A, Gonzalez MJ, Goncalves J. Differential activation of protein kinase C isoforms by euxanthone, revealed by an in vivo yeast phenotypic assay. *Planta Med* 2002 Nov; 68 (11): 1039-41.
272. Saraiva L, Fresco P, Pinto E, Sousa E, Pinto M, Goncalves J. Synthesis and in vivo modulatory activity of protein kinase C of xanthone derivatives. *Bioorg Med Chem* 2002 Oct; 10 (10): 3219-27.
273. Saraiva L, Fresco P, Pinto E, Sousa E, Pinto M, Goncalves J. Inhibition of alpha, beta, delta, eta, and zeta protein kinase C isoforms by xanthonolignoids. *J Enzyme Inhib Med Chem* 2003 Aug; 18 (4): 357-70.
274. Saraiva L, Fresco P, Pinto E, Sousa E, Pinto M, Goncalves J. Inhibition of protein kinase C by synthetic xanthone derivatives. *Bioorg Med Chem* 2003 Apr; 11 (7): 1215-25.
275. Coutinho I, Pereira G, Simoes MF, Corte-Real M, Goncalves J, Saraiva L. Selective activation of protein kinase C-delta and -epsilon by 6,11,12,14-tetrahydro-abieta-5,8,11,13-tetraene-7-one (coleon U). *Biochem Pharmacol* 2009 Sep; 78 (5): 449-59.
276. Wang QJ, Lu G, Schlapkohl WA, Goerke A, Larsson C, Mischak H, et al. The V5 domain of protein kinase C plays a critical role in determining the isoform-specific

localization, translocation, and biological function of protein kinase C-delta and -epsilon. *Mol Cancer Res* 2004 Feb; 2 (2): 129-40.

277. Pereira C, Coutinho I, Soares J, Bessa C, Leao M, Saraiva L. New insights into cancer-related proteins provided by the yeast model. *FEBS J* 2012 Mar; 279 (5): 697-712.

278. Pereira C, Leao M, Soares J, Bessa C, Saraiva L. New therapeutic strategies for cancer and neurodegeneration emerging from yeast cell-based systems. *Curr Pharm Des* 2012; 18 (27): 4223-35.

279. Atanasov AG, Waltenberger B, Pferschy-Wenzig EM, Linder T, Wawrosch C, Uhrin P, et al. Discovery and resupply of pharmacologically active plant-derived natural products: A review. *Biotechnol Adv* 2015 Aug.

280. Newman DJ, Cragg GM. Natural products as sources of new drugs over the 30 years from 1981 to 2010. *J Nat Prod* 2012 Mar; 75 (3): 311-35.

281. Brusotti G, Cesari I, Dentamaro A, Caccialanza G, Massolini G. Isolation and characterization of bioactive compounds from plant resources: the role of analysis in the ethnopharmacological approach. *J Pharm Biomed Anal* 2014 Jan; 87: 218-28.

282. Lukhoba CW, Simmonds MS, Paton AJ. *Plectranthus*: a review of ethnobotanical uses. *J Ethnopharmacol* 2006 Jan; 103 (1): 1-24.

283. Marques CG, Pedro M, Simoes MF, Nascimento MS, Pinto MM, Rodriguez B. Effect of abietane diterpenes from *Plectranthus grandidentatus* on the growth of human cancer cell lines. *Planta Med* 2002 Sep; 68 (9): 839-40.

284. Burmistrova O, Simoes MF, Rijo P, Quintana J, Bermejo J, Estevez F. Antiproliferative activity of abietane diterpenoids against human tumor cells. *J Nat Prod* 2013 Aug; 76 (8): 1413-23.

285. Burmistrova O, Perdomo J, Simoes MF, Rijo P, Quintana J, Estevez F. The abietane diterpenoid parvifloron D from *Plectranthus ecklonii* is a potent apoptotic inducer in human leukemia cells. *Phytomedicine* 2015 Oct; 22 (11): 1009-16.

286. Gaspar-Marques C, Rijo P, Simoes MF, Duarte MA, Rodriguez B. Abietanes from *Plectranthus grandidentatus* and *P. hereroensis* against methicillin- and vancomycin-resistant bacteria. *Phytomedicine* 2006 Mar; 13 (4): 267-71.

287. Grayer RJ, Eckert MR, Veitch NC, Kite GC, Marin PD, Kokubun T, et al. The chemotaxonomic significance of two bioactive caffeic acid esters, nepetoidins A and B, in the Lamiaceae. *Phytochemistry* 2003 Sep; 64 (2): 519-28.

288. Lin LG, Ung CO, Feng ZL, Huang L, Hu H. Naturally Occurring Diterpenoid Dimers: Source, Biosynthesis, Chemistry and Bioactivities. *Planta Med* 2016 Oct; 82 (15): 1309-28.
289. Rijo P, Simoes MF, Francisco AP, Rojas R, Gilman RH, Vaisberg AJ, et al. Antimycobacterial metabolites from *Plectranthus*: royleanone derivatives against *Mycobacterium tuberculosis* strains. *Chem Biodivers* 2010 Apr; 7 (4): 922-32.
290. Cragg GM, Newman DJ. Natural products: a continuing source of novel drug leads. *Biochim Biophys Acta* 2013 Jun; 1830 (6): 3670-95.
291. Garcia C, Silva CO, Monteiro CM, Nicolai M, Viana A, Andrade JM, et al. Anticancer properties of the abietane diterpene 6,7-dehydroroyleanone obtained by optimized extraction. *Future Med Chem* 2018 May, 10:1177-89.
292. Poerwono H, Sasaki S, Hattori Y, Higashiyama K. Efficient microwave-assisted prenylation of pinostrobin and biological evaluation of its derivatives as antitumor agents. *Bioorg Med Chem Lett* 2010 Apr; 20 (7): 2086-9.
293. Garcia C, Roque L, Borozan A, Ntungwe E, Nicolai M, Andrade JM, et al. *Plectranthus* genus as a source of bioactive compounds: unveil the antimicrobial and cytotoxic activity of the *P. strigosus* acetonic extract. 2018 (Submitted for publication).
294. Ho SN, Hunt HD, Horton RM, Pullen JK, Pease LR. Site-directed mutagenesis by overlap extension using the polymerase chain reaction. *Gene* 1989 Apr; 77 (1): 51-9.
295. Gietz RD, Schiestl RH. High-efficiency yeast transformation using the LiAc/SS carrier DNA/PEG method. *Nat Protoc* 2007 Feb; 2 (1): 31-4.
296. Storz P, Doppler H, Toker A. Protein kinase Cdelta selectively regulates protein kinase D-dependent activation of NF-kappaB in oxidative stress signaling. *Mol Cell Biol* 2004 Apr; 24 (7): 2614-26.
297. Labelle-Cote M, Dusseault J, Ismail S, Picard-Cloutier A, Siegel PM, Larose L. Nck2 promotes human melanoma cell proliferation, migration and invasion in vitro and primary melanoma-derived tumor growth in vivo. *BMC Cancer* 2011 Oct; 11:443.
298. Fernandes JC, Borges M, Nascimento H, Bronze-da-Rocha E, Ramos OS, Pintado ME, et al. Cytotoxicity and genotoxicity of chitooligosaccharides upon lymphocytes. *Int J Biol Macromol* 2011 Oct; 49 (3): 433-8.

299. Silva FS, Starostina IG, Ivanova VV, Rizvanov AA, Oliveira PJ, Pereira SP. Determination of Metabolic Viability and Cell Mass Using a Tandem Resazurin/Sulforhodamine B Assay. *Curr Protoc Toxicol* 2016 May; 68: 2 24 1-2 15.
300. von Burstin VA, Xiao L, Kazanietz MG. Bryostatins 1 inhibits phorbol ester-induced apoptosis in prostate cancer cells by differentially modulating protein kinase C (PKC) delta translocation and preventing PKCdelta-mediated release of tumor necrosis factor-alpha. *Mol Pharmacol* 2010 Sep; 78 (3): 325-32.
301. Shaheen S, Ahmed M, Lorenzi F, Nateri AS. Spheroid-Formation (Colonosphere) Assay for in Vitro Assessment and Expansion of Stem Cells in Colon Cancer. *Stem Cell Rev* 2016 Aug; 12 (4): 492-9.
302. Dalerba P, Dylla SJ, Park IK, Liu R, Wang X, Cho RW, et al. Phenotypic characterization of human colorectal cancer stem cells. *Proc Natl Acad Sci U S A* 2007 Jun; 104 (24): 10158-63.
303. Chu P, Clanton DJ, Snipas TS, Lee J, Mitchell E, Nguyen ML, et al. Characterization of a subpopulation of colon cancer cells with stem cell-like properties. *Int J Cancer* 2009 Mar; 124 (6): 1312-21.
304. Palagani V, El Khatib M, Krech T, Manns MP, Malek NP, Plentz RR. Decrease of CD44-positive cells correlates with tumor response to chemotherapy in patients with gastrointestinal cancer. *Anticancer Res* 2012 May; 32 (5): 1747-55.
305. Zhou JY, Chen M, Ma L, Wang X, Chen YG, Liu SL. Role of CD44(high)/CD133(high) HCT-116 cells in the tumorigenesis of colon cancer. *Oncotarget* 2016 Feb; 7 (7): 7657-66.
306. Clavijo C, Chen JL, Kim KJ, Reyland ME, Ann DK. Protein kinase Cdelta-dependent and -independent signaling in genotoxic response to treatment of desferrioxamine, a hypoxia-mimetic agent. *Am J Physiol Cell Physiol* 2007 Jun; 292 (6): C2150-60.
307. Park CH, Kim KT. Apoptotic phosphorylation of histone H3 on Ser-10 by protein kinase Cdelta. *PLoS One* 2012 Sep; 7 (9): e44307.
308. Boehm O, Zur B, Koch A, Tran N, Freyenhagen R, Hartmann M, et al. Clinical chemistry reference database for Wistar rats and C57/BL6 mice. *Biol Chem* 2007 May; 388 (5): 547-54.

309. Teixeira MA, Chaguri L, Carissimi AS, Souza NL, Mori C, Gomes V, et al. Hematological and biochemical profiles of rats (*Rattus norvegicus*) kept under microenvironmental ventilation system. *Braz J Vet Res Anim Sci* 2000; 37: 341–7.
310. Miyazawa Y, Uekita T, Hiraoka N, Fujii S, Kosuge T, Kanai Y, et al. CUB domain-containing protein 1, a prognostic factor for human pancreatic cancers, promotes cell migration and extracellular matrix degradation. *Cancer Res* 2010 Jun; 70 (12): 5136-46.
311. Sarkar S, Yong VW. Reduction of protein kinase C delta attenuates tenascin-C stimulated glioma invasion in three-dimensional matrix. *Carcinogenesis* 2010 Feb; 31 (2): 311-7.
312. Kang, J. Protein Kinase C (PKC) Isozymes and Cancer. *New J Sci* 2014; 36. Article ID231418.
313. Naor D, Sionov RV, Ish-Shalom D. CD44: structure, function, and association with the malignant process. *Adv Cancer Res* 1997; 71: 241-319.
314. Marhaba R, Zoller M. CD44 in cancer progression: adhesion, migration and growth regulation. *J Mol Histol* 2004 Mar; 35 (3): 211-31.
315. Kanwar SS, Yu Y, Nautiyal J, Patel BB, Majumdar AP. The Wnt/beta-catenin pathway regulates growth and maintenance of colonospheres. *Mol Cancer* 2010 Aug; 9: 212.
316. Zhao M, Xia L, Chen GQ. Protein kinase cdelta in apoptosis: a brief overview. *Arch Immunol Ther Exp (Warsz)* 2012 Oct; 60 (5): 361-72.
317. Allen-Petersen BL, Carter CJ, Ohm AM, Reyland ME. Protein kinase Cdelta is required for ErbB2-driven mammary gland tumorigenesis and negatively correlates with prognosis in human breast cancer. *Oncogene* 2014 Mar; 33 (10): 1306-15.
318. Chen Z, Forman LW, Williams RM, Faller DV. Protein kinase C-delta inactivation inhibits the proliferation and survival of cancer stem cells in culture and in vivo. *BMC Cancer* 2014 Feb; 14:90.
319. Lu Z, Hornia A, Jiang YW, Zang Q, Ohno S, Foster DA. Tumor promotion by depleting cells of protein kinase C delta. *Mol Cell Biol* 1997 Jun; 17 (6): 3418-28.
320. Szallasi Z, Blumberg PM. Prostratin, a nonpromoting phorbol ester, inhibits induction by phorbol 12-myristate 13-acetate of ornithine decarboxylase, edema, and hyperplasia in CD-1 mouse skin. *Cancer Res* 1991 Oct; 51 (19): 5355-60.

321. Teixeira J, Amorim R, Santos K, Soares P, Datta S, Cortopassi GA, et al. Disruption of mitochondrial function as mechanism for anti-cancer activity of a novel mitochondriotropic menadione derivative. *Toxicology* 2018 Jan; 393: 123-39.

322. Wu-Zhang AX, Murphy AN, Bachman M, Newton AC. Isozyme-specific interaction of protein kinase Cdelta with mitochondria dissected using live cell fluorescence imaging. *J Biol Chem* 2012 Nov; 287 (45): 37891-906.

323. Wang X, Morris-Natschke SL, Lee KH. New developments in the chemistry and biology of the bioactive constituents of Tanshen. *Med Res Rev* 2007 Jan; 27 (1): 133-48.

324. Fronza M, Lamy E, Gunther S, Heinzmann B, Laufer S, Merfort I. Abietane diterpenes induce cytotoxic effects in human pancreatic cancer cell line MIA PaCa-2 through different modes of action. *Phytochemistry* 2012 Jun; 78: 107-19.

325. Gazim ZC, Rodrigues F, Amarin AC, de Rezende CM, Sokovic M, Tesevic V, et al. New natural diterpene-type abietane from *Tetradenia riparia* essential oil with cytotoxic and antioxidant activities. *Molecules* 2014 Jan; 19 (1): 514-24.

326. Goldberg RM, Sargent DJ, Morton RF, Fuchs CS, Ramanathan RK, Williamson SK, et al. A randomized controlled trial of fluorouracil plus leucovorin, irinotecan, and oxaliplatin combinations in patients with previously untreated metastatic colorectal cancer. *J Clin Oncol* 2004 Jan; 22 (1): 23-30.

327. Meyerhardt JA, Mayer RJ. Systemic therapy for colorectal cancer. *N Engl J Med* 2005 Feb; 352 (5): 476-87.

328. Tournigand C, Andre T, Achille E, Lledo G, Flesh M, Mery-Mignard D, et al. FOLFIRI followed by FOLFOX6 or the reverse sequence in advanced colorectal cancer: a randomized GERCOR study. *J Clin Oncol* 2004 Jan; 22 (2): 229-37.

Causes of death in Portugal. Available in <https://www.ine.pt> [accessed in 10/11/2017]

GLOBOCAN 2012: Estimated cancer Incidence Mortality and Prevalence Worldwide in 2012. Available in <http://globocan.iarc.fr/Default.aspx> [accessed in 10/11/2017]

Toxic side effects of conventional chemotherapy. Available in www.cancer.org [accessed in 25/11/2017]

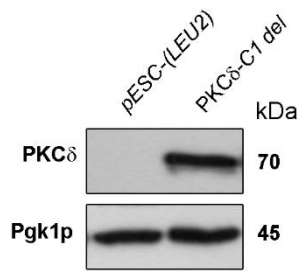
Clinical trials with midostaurin. Available in <https://clinicaltrials.gov/ct2/results?term=Midostaurin> [accessed in 5/12/2017]

Clinical trials with enzastaurin. Available in
<https://clinicaltrials.gov/ct2/results?term=LY317615> [accessed in 5/12/2017]

Clinical trials with bryostatin. Available in
<https://clinicaltrials.gov/ct2/results?term=bryostatin> [accessed in 5/12/2017]

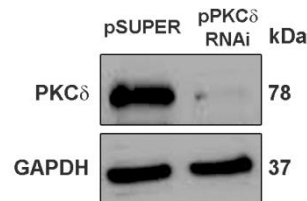
Appendix

Fig. 1. PKC δ expression levels in yeast cells



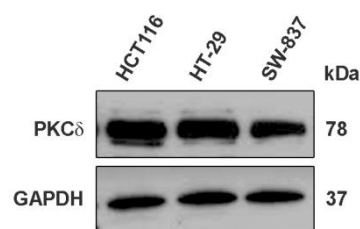
Western blot analysis of PKC δ expression levels in yeast cells transformed with pESC-(*LEU2*) (empty vector) or pESC-PKC δ Δ C1 cells after 48 h incubation in selective induction medium. Immunoblot represents one of three independent experiments; Pgk1p was used as loading control.

Fig. 2. PKC δ -knockdown in HCT116 colon cancer cells



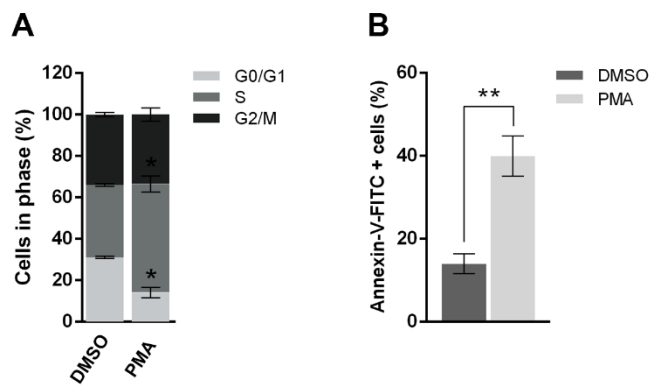
Efficiency of PKC δ -knockdown was assessed by Western blot analysis after 24 h post-transfection with control plasmid (pSUPER) or pSuperPKC δ .RNAi. Immunoblots represent one of three independent experiments; GAPDH was used as loading control.

Fig. 3. PKC δ expression levels in colorectal cancer cells



Western blot analysis of PKC δ expression levels assessed in HCT116, HT-29 and SW-837 cells after 48 h incubation. Immunoblots represent one of three independent experiments; GAPDH was used as loading control.

Fig. 4. PKC δ expression levels in colorectal cancer cells



(A) Cell cycle (B) and apoptosis were analyzed after 24 h treatment with 8 μ M PMA or vehicle in HCT116 cells. Data are mean \pm SEM of four independent experiments; values significantly different from vehicle: (* p <0.05, ** p <0.01), unpaired Student's t -test.

Table 1: Antibodies used in Western blot.

Antigen	Final Dilution	Supplier	
Primary antibodies			
Caspase-3 (#9662) (rabbit polyclonal)	1:300	Cell Signaling Technology (Werfen/IZASA, Carnaxide, Portugal)	
Phospho-Histone H3 (Ser10) (#9701) (rabbit polyclonal)	1:100		
Histone H3 (#9715) (rabbit polyclonal)	1:1000		
PKC δ (G-9) (mouse monoclonal)	1:300	Santa Cruz Biotechnology (Firilabo)	
PARP (C2-10) (mouse monoclonal)	1:1000		
p53 (DO-1) (mouse monoclonal)	1:5000		
BAX (2D2) (mouse monoclonal)	1:100		
Bcl-2 (C-2) (mouse monoclonal)	1:200		
Cytochrome <i>c</i> (A-8) (mouse monoclonal)	1:50		
HCAM (CD44) (F-4) (mouse monoclonal)	1:200		
COX IV (F-8) (mouse monoclonal)	1:500		
GAPDH (6C5) (mouse monoclonal)	1:10000		
Survivin (ab76424) (rabbit monoclonal)	1:10000		Abcam (Cambridge, United Kingdom)
ALDH2 (ab108306) (rabbit monoclonal)	1:1000		
MMP-9 (ab38898) (rabbit polyclonal)	1:200		
Histone γ H2AX (phospho-Ser139) (rabbit monoclonal)	1:50		
Secondary antibodies			
Anti-mouse horseradish-peroxidase (HRP)-conjugated	1:5000	Santa Cruz Biotechnology	
Anti-rabbit horseradish-peroxidase (HRP)-conjugated	1:5000		

Table 2: Antibodies used in immunohistochemistry.

Antigen	Final Dilution	Supplier
Primary antibodies		
Caspase-3 (AB3623) (rabbit polyclonal)	1:100	Merck Millipore
HK2 (MABN702) (mouse monoclonal)	1:50	
TIGAR (AB10545) (rabbit polyclonal)	1:200	
Ki-67 (SP6) (rabbit monoclonal)	1:200	Pierce Thermo Scientific
BAX (6A7) (mouse monoclonal)	1:200	
VEGF (VG1) (mouse monoclonal)	1:200	
GLUT1 (ab652) (rabbit polyclonal)	1:200	Abcam
MCT4 (H-90) (rabbit polyclonal)	1:50	Santa Cruz Biotechnology